Genetic and Biochemical Characterization of COP1/SPA Function in *Arabidopsis* Photomorphogenesis

Inaugural-Dissertation

zur

Erlangung des Doktorgrades

der Mathematisch-Naturwissenschaftlichen Fakultät

der Universität zu Köln

vorgelegt von

Alexander Maier

aus Krefeld-Hüls

Köln, 2011

Berichterstatter:	Prof. Dr. Ute Höcker Prof. Dr. Martin Hülskamp
Prüfungsvorsitzender:	Prof. Dr. Wolfgang Werr
Tag der mündlichen Prüfung:	25.05.2011

Contents:

Contents: I
Abbreviations V
Abstract IX
Zusammenfassung XI
I. Introduction 1
I.1 Light signal transduction in higher plants 1
I.2 Repressor proteins of light signaling 4
I.3 COP1 as part of protein complexes 13
I.4 Regulation of anthocyanin biosynthesis in *Arabidopsis thaliana* 14
I.6 Light-mediated regulation of anthocyanin biosynthesis 19
I.7 Aims of this PhD thesis 22
II. Results 23
II.1 Analysis of SPA-SPA protein interactions 23
II.1.1 SPA proteins interact with each other *in vitro* 23
II.1.2 The N-terminus of SPA1 mediates SPA1 self-association and SPA1-SPA2 interaction 24
II.1.3 SPA proteins interact *in planta* 26
II.1.4 SPA proteins co-localize in nuclear speckles 28
II.2 Production of COP1-, SPA1- and SPA2- antibodies 29
II.2.1 Production of anti-COP1 antibodies 29
II.2.1.1 Purification and processing of COP1-915 protein 29
II.2.1.2 Detection of native COP1 protein 30
II.2.2 Production of anti-SPA1 antibodies 34
II.2.2.1 Purification of SPA1 recombinant protein 34
II.2.2.1 Detection of native SPA1 protein in *Arabidopsis* plant extracts 35
II.2.3 Production of anti-SPA2 antibodies 37
II.2.4 *in vivo* CoIP of SPA1-HA and native COP1 protein using COP1-specific antibodies 40
II.2.5 Endogenous SPA1 and SPA2 protein levels are reduced under far-red light 41
II.3 New target proteins for the COP1/SPA complex involved in anthocyanin biosynthesis 44
II.3.1 *cop1-* and *spa-* mutants exhibit increased amounts of anthocyanin in darkness and white light 44

II.3.2 *PAP* proteins interact with COP1 and SPA proteins in Yeast Two-Hybrid analysis 45
II.3.3 Overexpression of *PAP1* and *PAP2* results in increased anthocyanin contents in darkness and white light 47
II.3.4 PAP1 and PAP2 proteins accumulate in white-light-grown seedlings....48
II.3.5 PAP1 and PAP2 proteins are regulated over time 50
II.3.6 Anthocyanin levels in *cop1-4* mutants are dependent on PAP function....53
II.3.7 Overexpression of PAP1 and PAP2 in *cop1-4* mutant background results in increased anthocyanin content in darkness and light....54
II.3.8 HA-PAP2 protein accumulates in the *cop1-4* mutant background 56
II.3.9 Production of anti-PAP1 antibodies....56
III. Discussion....61
III.1 SPA proteins interact with each other *in vitro* and *in planta* 61
III.2 Inactivation of COP1/SPA complexes by light....64
III.3 PAP proteins, potential targets of COP1/SPA complexes....67
III.4 Regulation of PAP-dependent anthocyanin biosynthesis in light and darkness 68
III.5 COP1/SPA-dependent regulation of PAP1 and PAP2 function....70
III.6 PAP protein regulation during *Arabidopsis* plant development 74
IV Materials and Methods....76
IV.1 Materials....76
IV.1.1 Plant materials 76
IV.1.2. Bacterial and Yeast Strains....78
IV.1.2.1 *Escherichia coli* (*E.coli*) strains....78
IV.1.2.2 *Agrobacterium tumefaciens* strains 78
IV.1.2.3 *Saccharomyces cerevisiae* strains 78
IV.1.3 Vectors....79
IV.1.3.1 Gateway™ Entry vectors....79
IV.1.3.2 Vectors used in *in vitro* CoIP studies....80
IV.1.3.3 Vectors used for Bimolecular Fluorescence Complementation assay studies....81
IV.1.3.4 Vectors employed in Co-localization experiments....82
IV.1.3.5 Vectors used for antibody production 83
IV.1.3.6 Vectors used for Yeast Two-Hybrid analysis....84
IV.1.3.7 Vectors used for generation of transgenic *Arabidopsis* plants 85

IV.1.4 Oligonucleotides....86
IV.1.5 Enzymes....87
IV.1.5.1 Restriction endonucleases....87
IV.1.5.2 Nucleic acid modifying enzymes....87
IV.1.5.3 Restriction proteases....88
IV.1.6 Chemicals....88
IV.1.7 Media....88
IV.1.8 Radioactivity....90
IV.1.9 Antibiotics (stock solutions)....90
IV.1.10 Antibodies....90
IV.1.11 Buffers and solutions....91
IV.2. Methods....93
IV.2.1 Seed sterilization....93
IV.2.2 Plant growth....93
IV.2.3 Measurement of Anthocyanin content....94
IV.3 Methods for molecular biology....94
IV.3.1 General methods in molecular biology....94
IV.3.2 Polymerase chain reaction (PCR)....95
IV.3.3 Isolation of total RNA from seedling tissue....95
IV.3.4 DNase treatment and reverse transcription of total RNA....95
IV.3.5 Real time PCR....96
IV.3.6 Gateway™ cloning....96
IV.3.7 DNA sequencing....96
IV.3.8 DNA sequence analysis....96
IV.3.9 Preparation of chemically competent *E.coli* cells....96
IV.3.10 Transformation of chemically competent *E.coli* cells....97
IV.3.11 Transformation of electro-competent *A.tumefaciens* cells....97
IV.3.12 *Agrobacterium*-mediated stable transformation of *Arabidopsis* (floral dip)....97
IV.3.13 Generation of transgenic *Arabidopsis* plants....97
IV.3.13.1 Selection of *Arabidopsis* transformants....98
IV.3.14 Crossings and selection of crosses....98
IV.4 Biochemical methods....98
IV.4.1 *Arabidopsis* total protein extraction for immunoblot analysis....98
IV.4.2 Amido Black assay....99
IV.4.3 Nuclear fractionation for immunoblot analysis....99

IV.4.4 MG132 treatments 100
IV.4.5 Denaturing SDS-polyacrylamide gel electrophoresis (SDS-PAGE)..... 100
IV.4.6 Immunoblot analysis 101
IV.4.7 Staining of SDS-PAGE gels and polyvinylidene difluoride (PVDF) membranes. 102
IV.4.8 *In vivo* Co-immunoprecipitation (CoIP) from *Arabidopsis* seedling extracts 102
IV.4.9 *In vitro* Co-immunoprecipitation (*in vitro* CoIP) using radioactively labeled methionine 102
IV.4.9.1 Production of recombinant protein using the TnT®-system 103
IV.4.9.2 *In vitro* Co-immunoprecipitation 103
IV.4.10 *In planta* interaction assays 104
IV.4.10.1 Bimolecular Fluorescence Complementation assay (BiFC) 104
IV.4.10.2 Co-localization experiments in *Arabidopsis* leaf cells 105
IV.4.10.3 Preparation of gold particles 105
IV.4.10.4 Coating of gold particles 105
IV.4.10.5 Particle bombardment 106
IV.4.10.6 Fluorescence microscopy 106
IV.4.11 Yeast Two-Hybrid analysis 106
IV.4.11.1 Growth and harvesting of competent yeast cells 106
IV.4.11.2 Co-transformation of yeast cells 107
IV.4.11.3 Selection of co-transformed yeast cells 107
IV.4.12 Antibody production 108
IV.4.12.1 Cloning 108
IV.4.12.2 Expression of recombinant protein in *E.coli*. 108
IV.4.12.3 Purification of His_6-tagged protein from *E.coli* 109
IV.4.12.4 Dialysis and protease digestion 109
IV.4.12.5 Protein immunization 110
IV.4.12.6 Purification of polyclonal antibodies using polyvinylidene difluoride membranes (PVDF) membranes 110
V Supplement 112
VI References 113
VII Danksagung 125
VIII Erklärung 126

Abbreviations

°C	degree Celsius
µl	micro liter
µg	micro gram
AD	GAL4-activation domain
B	blue light
BD	GAL4-binding domain
bp	base pair
bHLH	basic helix-loop-helix
CC	coiled-coil structure
cDNA	complementary DNA
Col	Columbia; ecotype of *Arabidopsis thaliana*
cm	centimeter
D	darkness
Da	Dalton
DNA	desoxyribonucleic acid
DTT	Dithiothreitol
dNTPs	2'-desoxynuceloside-5'triphosphate
EDTA	Ethylenediaminetetraacetic acid
EMS	Ethyl methanesulfonate
FR	far-red light
g	grams
g	gravitation
GAD	GAL4-activation domain
GUS	β-Glucuronidase
h	hour
HA	human influenza hemagglutinin
HRP	horseradish peroxidase
kb	kilo bp
kDa	kilo Dalton
l	liter
LB	T-DNA left border

M	molar; mol/l
mA	milliampere
mg	milligram
min	minute
mM	millimolar
mRNA	messenger-ribonucleic-acid
MS	Murashige and Skoog medium
NLS	nuclear localization signal/sequence
nm	nanometer
No	Nossen; ecotype of *Arabidopsis thaliana*
OD	optical density
ORF	open reading frame
PCR	polymerase chain reaction
Pfr	red light absorbing phytochrome conformation
Phy	phytochrome
PMSF	Phenylmethanesulfonylfluoride
Pr	red light absorbing phytochrome conformation
RB	T-DNA right border
RLD	RLD; ecotype of *Arabidopsis thaliana*
RNA	ribonucleic acid
rpm	rotations per minute
RT-PCR	reverse-transcription-PCR
sec	second
SDS	sodium dodecyl sulfate
Suc	sucrose
T-DNA	Transfer-DNA
Tris	tris(hydroxymethyl)aminomethane
U	Unit
Ubi	Ubiquitin
UV	ultraviolet
V	Volts

v/v	volume per volume
Wc	continious white light
WD	aspartic acid; tryptophan
WT	wild type
w/v	weight per volume

Gene and protein nomenclature:

Plants:

SPA1	gene, locus, wild-type allele
spa1	mutant allele
SPA1	protein

Exception: photoreceptors

PHY	gene, locus, wild-type allele
phy	mutant allele
PHY	apoprotein (without chromophore)
phy	holoprotein (with chromophore)

Bacteria:

lacZ	locus, gene
lacZ$^+$	wild-type allele
LacZ	protein
lacZ-1	mutation and number of the allele

Saccharomyces cerevisea:

LEU2	locus, gene, wild-type allele
leu2::YFG1	insertion
*leu2Δ*1	deletion
Leu2 or Leu2p	protein

Abstract

Plants as sessile organisms are dependent on a complex interaction with their environment. Light is one of the most important factors that affect multiple stages of plant growth and development. In concert with the four SPA proteins (SPA1-SPA4) the E3-ubiquitin ligase COP1 acts as a repressor of light signaling in darkness. COP1 and SPA proteins were also found to regulate processes like determination of leaf size, stomata differentiation and induction of photoperiodic flowering. In this regard, COP1 targets transcription factors like HY5, HFR1 or CO for ubiquitination and subsequent 26S proteasome-dependent degradation. Furthermore, SPA proteins physically interact with the COP1 protein.

In the present study I could show that SPA proteins can interact with each other *in vitro* and *in planta,* building homo- and heterodimers. This indicates the existence of larger COP1/SPA containing complexes in which every combination of SPA dimers is possible. Further, I could show that the N-terminus including the proteins' coiled-coil domain mediates the interactions within the SPAs.

Since SPA proteins carry out overlapping but also distinct functions throughout plant development and this cannot be solely explained by their mRNA and protein expression patterns, there must be other mechanisms regulating COP1/SPA complex assembly and/or activity. Using antibodies against native SPA1 and SPA2 protein generated in this study, I could show that SPA1 and SPA2 protein levels decrease in far-red light compared to darkness, whereas transcript levels remained unchanged, pointing to a post-translational mechanism regulating SPA function. However, whether this is dependent on COP1 needs to be verified.

COP1/SPA complexes most likely are involved in a broad spectrum of developmental processes. Thus, I analyzed the regulation of two new potential targets, PAP1 and PAP2, which are transcription factors involved in the regulation of light-dependent anthocyanin biosynthesis. I could show that PAP1 and PAP2 interact with the members of COP1/SPA complexes in yeast. Further, I could show that PAP1 and PAP2 proteins from overexpressing plants are stabilized by light and accumulate upon treatment with the proteasomal blocker MG132, indicating a post-translational regulation of PAP protein abundance. Analysis of RNAi mutants and *PAP* overexpressing plants in *cop1-4* background revealed an effect of the *cop1* mutation on PAP-dependent anthocyanin biosynthesis. Furthermore, an initial experiment showed, that PAP2 protein in *35S::HA-PAP2 cop1-4* overexpressing plants is further stabilized in darkness and light compared to overexpressing lines in

wild-type background, supporting the hypothesis that COP1/SPA complexes regulate PAP protein levels under both conditions.

Zusammenfassung

Pflanzen sind als sessile Organismen auf eine komplexe Interaktion mit ihrer Umgebung angewiesen. In dieser Hinsicht ist Licht einer der wichtigsten Faktoren, der in viele Stadien des Pflanzenwachstums und der Pflanzenentwicklung eingreift. Die E3-Ubiquitin Ligase COP1 und SPA-Proteine (SPA1-SPA4) repremieren zusammen die Lichtsignaltransduktion im Dunkeln. Zusätzlich wurden COP1 und SPA-Proteine auch im Zusammenhang mit z.B. der Regulation der Blattgröße, der Differenzierung der Spaltöffnungen und der Bestimmung des Blühzeitpunktes identifiziert. Es wurde gezeigt, dass COP1 Transkriptionsfaktoren wie HY5, HFR1 und CO ubiquitiniert und durch den 26S Protasom Proteinkomplex degradiert werden.

In der hier vorliegenden Arbeit konnte gezeigt werden, dass SPA Proteine *in vitro* und *in planta* miteinander in Homo- und Heterodimeren interagieren. Diese Tatsache legt die Existenz von größeren Proteinkomplexen unter der Beteiligung von COP1 und SPA-Proteinen, in denen jede Kombination von SPA-Dimeren vertreten ist, nahe. Ferner konnte gezeigt werden, dass SPA-Proteine über ihren N-Terminus, der zusätzlich die Coiled-Coil-Domäne beinhaltet, miteinander interagieren.

Da SPA-Proteine überlappende, aber auch unterschiedliche Funktionen in der Pflanzenentwicklung ausüben, und dies nicht allein durch mRNA- und Protein-Expressionsmuster erklärt werden kann, muss es andere Mechanismen geben, die die Assemblierung und/oder Aktivität von COP1/SPA-Komplexen regulieren. Durch die Analyse von SPA1- und SPA2-Proteinmengen in dunkelrotem Licht verglichen mit denen aus Dunkelheit unter Zuhilfenahme von in dieser Arbeit hergestellten Antikörpern, konnte gezeigt werden, dass SPA-Proteinmengen im Licht verglichen mit denen in Dunkelheit abnehmen. Unter Beachtung der Transkriptpegel, weist dies auf einen posttranslationalen Mechanismus hin, der die Funktion der SPA-Proteine reguliert. Ob COP1 direkt Einfluss auf die lichtabhängige Akkumulation von SPA-Proteinen Einfluss nimmt, muss noch geklärt werden.

COP1/SPA-Komplexe üben aller Voraussicht nach ihre Regulation in einem breiten Spektrum von Entwicklungsprozessen aus. Aus diesem Grund wurden zwei neue potentielle Zielproteine für den COP1/SPA-Komplex untersucht. PAP1 und PAP2 sind Transkriptionsfaktoren, die in der lichtabhängigen Regulation der Anthozyanbiosynthese involviert sind. In dieser Arbeit konnte gezeigt werden, dass beide Proteine mit den Komponenten des COP1/SPA-Komplexes in Hefe interagieren können. Ferner wurden PAP1 und PAP2 in 35S-Überexressoren durch Licht stabilisiert und konnten durch Zugabe des Proteasominhibitors MG132

angereichert werden, was eine posttranslationale Regulation der PAP-Protein nahelegt. Die Analyse von RNAi-Mutanten und PAP-Überexpressoren im *cop1-4*-mutanten Hintergrund zeigte einen Effekt der *cop1*-Mutation auf PAP-abhängige Anthozyanbiosynthese. Darüber hinaus zeigte ein erstes Experiment in *35S::HA-PAP2 cop1-4*-überexpremierenden Pflanzen, dass das PAP2-Protein im Licht und in Dunkelheit im Vergleich zu Überexpressoren im Wildtyphintergrund stärker stabilisiert wurde. Dies bekräftigt die Hypothese, dass COP1/SPA-Komplexe PAP-Proteinmengen unter beiden Bedingungen regulieren.

I. Introduction

I.1 Light signal transduction in higher plants

As sessile organisms, plants are dependent on the perception of and adaption to their environment, which implies a complex sensory network. One of the major environmental stimuli is light, which, in addition to gaining energy by photosynthesis, is mostly regulating differentiation- and developmental-processes. Germination, seedling de-etiolation, shade avoidance, phototropism, circadian rhythm and the induction of flowering are such processes in plants that are tightly regulated by light.

The fact that plants can sense quality, quantity, direction and periodicity of light points out that there must be factors on the molecular level that can perceive and measure light as well as transfer this information, allowing the plant to adjust to environmental requirements. UV-A, UV-B as well as blue light, red light and far-red light are the light qualities that cause the strongest sensitivity in plants (Fankhauser et al., 1997; Quail, 2002). The proteins that gather information from light could be identified as photoreceptors. In the model organism *Arabidopsis thaliana* there are four main classes of photoreceptors known, the phytochromes, cryptochromes, phototropins and the Zeitlupe protein family. (Briggs and Olney, 2001, Imaizumi et al., 2003).

Blue light is perceived by three different types of photoreceptors: the cryptochromes (cry1- cry3), the phototropins (phot1 and phot2) and the zeitlupe (ztl)/flavin-binding, kelch repeat, f-box 1 (fkf1)/lov-kelch protein 2 (lkp2) proteins (Ahmad and Cashmore, 1993; Lin et al., 1996; Huala et al., 1997; Christie et al., 1998; Mazzella et al., 2001; Kleine et al., 2003). In this regard cry1 was found to be the primary photoreceptor that inhibits hypocotyl elongation in response to high fluence rates of B, whereas cry2 plays a role in seedling development under low fluences of B as well as in the photoperiodic induction of flowering (Ahmad and Cashmore, 1993; Lin et al., 1996; Guo et al., 1998; Lin et al., 1998; Mazzella et al., 2001; Kleine et al., 2003; Mockler et al., 2003). The function of cry3 is so far unknown and needs to be elucidated. Cryptochromes are also able to perceive UV-A irradiation (Briggs and Olney,

2001), whereas the photoreceptor monitoring UV-B irradiation, that also triggers developmental processes, is still unknown.

The second class of blue light photoreceptors, the phototropins phot1 and phot2, promote plant growth and are important for phototropic responses, movement of chloroplasts as well as regulation of stomatal opening (Liscum and Briggs, 1995; Briggs and Olney, 2001; Briggs and Christie, 2002; Sakamoto and Briggs, 2002; Ohgishi et al., 2004; Takemiya et al. 2005). ztl/fkf1/lkp2 photoreceptors are involved in the regulation of the circadian clock and determination of flowering time (Schultz et al., 2001; Imaizumi et al., 2003; Somers et al., 2004).

The most well studied class of photoreceptors is the class of phytochromes that monitor red light and far-red light (Sharrock and Quail, 1989). There are five different genes in *Arabidopsis* that encode for the phytochromes phyA-phyE (Sharrock and Quail, 1989). Among the pytochromes phyA and phyB carry out the most important functions in plants (Briggs and Olney, 2001). Based on their stability in light, two classes of phytochromes are distinguished, the light-unstable phytochromes of type I that accumulate in etiolated seedlings, and the light stable phytochromes of type II. phyA is the only phytochrome of type I, whereas phyB-phyE are of type II. phyA can sense far-red light light but also mediates responses to low fluence rates of red and blue light (Nagatani et al., 1993; Whitelam et al., 1993; Casal et al., 1997). phyB is involved in the regulation of seed germination, de-etiolation, shade avoidance and the determination of flowering time (Schepens et al., 2004). Additionally phyC, phyD and phyE play also an important role in these responses but to a minor extent (Quail, 1997). Phytochromes exist in two photo-convertible forms, the Pr- and Pfr-form. Seedlings grown in darkness accumulate the inactive Pr-form that converts by the absorption of red light to the active Pfr-form. The absorption of far-red light converts the Pfr-form again to the Pr-form (Rockwell et al., 2006).

Although the perception of different light qualities is regulated by different sets of photoreceptors, there is crosstalk between the signaling pathways. Physiological processes like seedling development and floral induction are controlled by both, the phytochrome and cryptochrome signaling networks (Casal, 2000; Mazella et al, 2001; Franklin et al., 2005). Figure 1.1

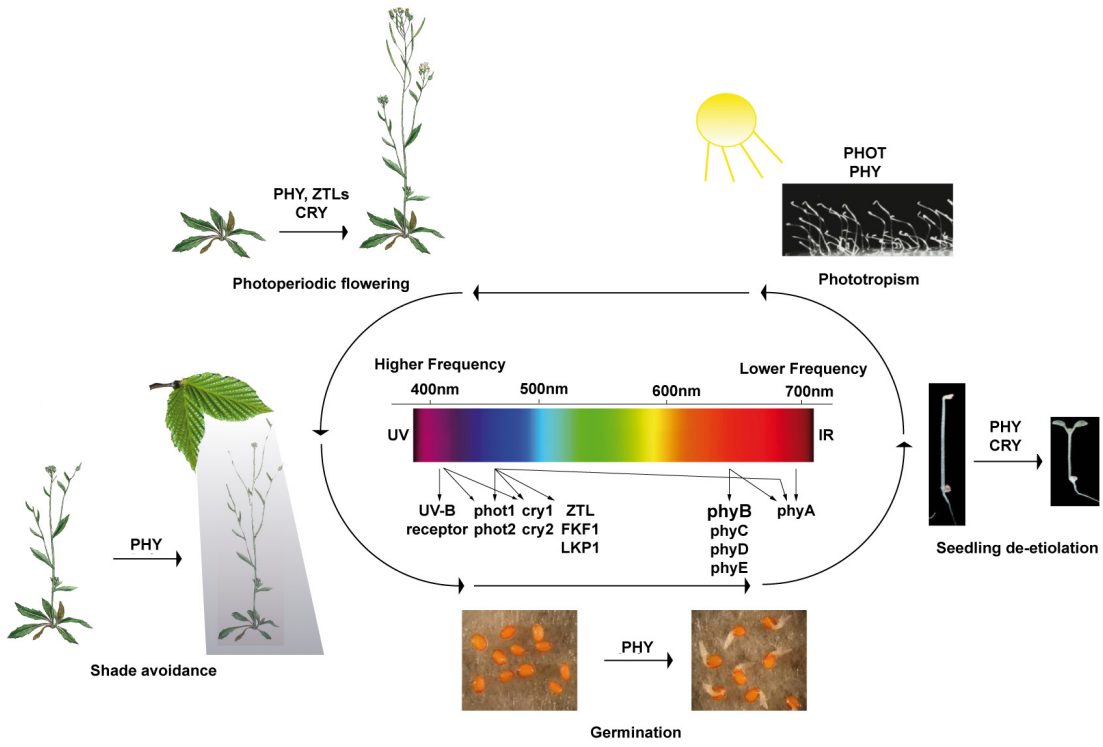

Figure 1.1: Light-dependent regulation of plant growth and development. Different classes of photoreceptors regulate plant growth and developmental processes throughout the whole life cycle of plants. They perceive light of specific wavelengths. Cryptochromes and phototropins as well as the Zeitlupe protein family perceive blue light and UV-A light. The receptor for UV-B light is unknown. phyB mainly responds to red light together with phyA, phyC, phyD and phyE. Far-red light is only sensed by phyA. phyA can also monitor blue light and red light. Germination as well as shade avoidance is regulated by the phytochromes. Cryptochromes and phytochromes together regulate seedling de-etiolation. Phytochromes, cryptochromes and the Zeitlupe protein family regulate photoperiodic flowering. Phototropism is regulated by phototropins and the phytochromes.

shows a summary of the main contributions of photoreceptors to *Arabidopsis* plant development.

After perception of light by the photoreceptors the signal is transferred further downstream in a signal cascade to proteins like transcription factors, that can directly influence the transcription of light-regulated genes by binding to cis-regulatory LIGHT RESPONSIVE ELEMENTS (LREs). Since 10 - 30% of all genes in *Arabidopsis* are light regulated (Ma et al., 2001; Tepperman et al., 2001), this broad and basic mechanism enables plants to react rapidly to environmental changes. This way of transcriptional regulation is well characterized for phytochrome mediated signaling. In darkness, phytochromes are localized in the cytosol and are transported to the nucleus after light absorption (Sakamoto and Nagatani 1996; Kircher et al., 1999;

Nagatani, 2004). There they are interacting with bHLH transcription factors, which belong to the family of PHYTOCHROME INTERACTING FACTORS (PIFs) and PIF-LIKEs (PILs) proteins (Ni et al., 1999; Martinez-Garcia et al., 2000; Duek and Fankhauser, 2005). The PIFs and PILs, which normally act as repressors of light signaling, are phosphorylated by the phytochromes what leads to their degradation (Bauer et al., 2004; Al-Sady et al., 2006; Castillon et al., 2007; Shen et al., 2005; 2007; 2008). Hence, light signaling cannot be repressed any longer. This mechanism was recently also shown for the regulation of flowering time mediated by cry2 and the bHLH transcription factor CIB1 (Liu et al., 2008).

I.2 Repressor proteins of light signaling

One of the most drastic light responses is seedling de-etiolation. When seedlings are grown in darkness they undergo a differentiation process called skotomorphogenesis (in order to reach the surface when grown on soil). Skotomorphogenesis is characterised by an elongated hypocotyl, closed cotyledons, the formation of an apical hook and no chlorophyll biosynthesis. In contrast, seedling that are grown in the light show so called photomorphogenesis, exhibiting a short hypocotyl, expanded cotyledons and accumulation of chlorophyll (McNellis and Deng, 1995; Von Arnim and Deng, 1996; Figure 1.2 A). Several transcription factors are known to promote photomorphogenesis but they do not directly associate with the photoreceptors. The transcription factors LONG HYPOCOTYL 5 (HY5) and HY5 HOMOLOG (HYH) play a role in seedling development in far-red light, red light, blue light and UV-B by binding directly to LREs (Oyama et al., 1997; Chattopadhyay et al., 1998; Osterlund et al., 2000a; Osterlund et al., 2000b; Ulm et al., 2004). The bHLH factor LONG HYPOCOTYL IN FAR-RED1 (HFR1) acts in phyA and cry1 signaling regulating seedling development and shade avoidance (Fairchild et al., 2000; Fankhauser und Chory, 2000; Duek et al., 2003; Sessa et al., 2005). Also, LONG AFTER FAR-RED LIGHT1 (LAF1) is such a transcription factor that regulates gene expression in response to far-red light (Ballesteros et al., 2001). It was shown that the

regulation of protein stability of these promoting factors plays a large role in light signal transduction (Hoecker, 2005; Henriques et al., 2009). HY5, HYH, HFR1 and LAF1 were shown to accumulate in light, whereas they are of low abundance in darkness (Osterlund et al., 2000a; Osterlund et al., 2000b; Seo et al., 2003; Duek et al., 2004; Jang et al., 2005; Yang et al., 2005b).

Downstream of the photoreceptors, a group of genes was identified, the *CONSTITUTIVE PHOTOMORPHOGENISIS (COP)/DE-ETIOLATED/ FUSCA (FUS)* genes, that repress photomorphogenesis in darkness (Chory et al., 1989; Deng et al., 1991). Mutations in these genes lead to constitutive photomorphogenesis. Seedlings grown in darkness display a short hypocotyl, and expanded cotyledons as well as accumulation of anthocyanin, differentiation of etioplasts to chloroplasts and de-regulation of light expressed genes (Chory et al., 1989; Deng et al., 1991). This phenotype was found to be caused by stabilization of transcription factors like HY5 or HFR1 promoting photomorphogenesis in darkness, supporting the notion that *COP/DET/FUS* genes repress the function of HY5 and HFR1 in darkness (Ang und Deng, 1994; Pepper und Chory, 1997; Osterlund et al., 2000a; Osterlund et al., 2000b; Kim et al., 2002; Seo et al., 2003; Duek et al., 2004; Jang et al., 2005; Yang et al., 2005b). Vice versa, the function of the regulators from COP/DET/FUS group needs to be inhibited in the light since transcription factors like HY5 and HFR1 accumulate. This is supported by the observation that the photoreceptors phys and crys are responsible for the stabilization of HY5 in light (Osterlund et al., 2000).

The most well studied gene from the *COP/DET/FUS* group is the *CONSTITUTIVE PHOTOMORPHOGENIC* 1 (*COP1*) gene. The COP1 protein is also found in other higher eukaryotes (Wang et al., 1999). It includes an amino-terminal RING-finger-motif, a coiled-coil domain as well as a carboxy-terminal WD-40-repeat domain (Figure 1.3). All these domains are known to mediate interactions with other proteins (Deng et al., 1992). The RING-finger-motif is found in E3 ubiquitin ligases (Deng et al., 1992) and it was shown that COP1 indeed carries out this function by targeting the transcription factors HY5, HFR1 and LAF1 for degradation via the 26S proteasome pathway (Osterlund et al., 2000a; Saijo et al., 2003; Seo et al., 2003; Figure 1.2 B). For ubiquitination of proteins, the small peptide ubiquitin is ligated to the ubiquitin-

activating enzyme E1. Subsequently, ubiquitin is transferred to an ubiquitin-activating enzyme E2. The ubiquitin from E2 is then transferred to the target protein, which is interacting with the E3 ligase protein. Ubiquitin labeled target proteins are then recognized by the 26S proteasome and degraded (Moon et al., 2004).

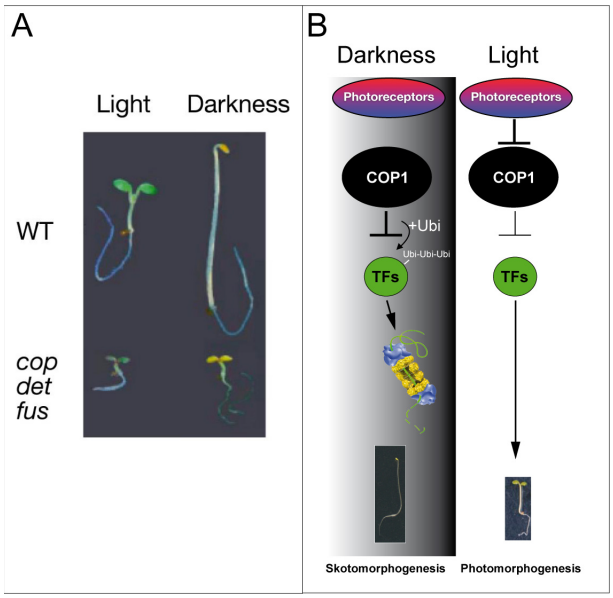

Figure 1.2: *COP/DET/FUS*-dependent repression of photomorphogenesis. (A) Mutants of *COP/DET/FUS* exhibit strong constitutive photomorphogenesis in darkness compared to wild-type, exhibiting a short hypocotyl and expanded cotyledons. (B) Simplified illustration of COP1 function during skotomorphogenesis and photomorphogenesis in darkness and light. In darkness the photoreceptors are inactive and therefore COP1 can suppress the function of transcription factors (TFs) like HY5, HFR1 and LAF1 by ubiquitination. The ubiquitinated proteins are then degraded by the 26S proteasome. In light the photoreceptors can suppress COP1 function thereby leading to the accumulation of TFs that can promote photomorphogenesis.

In darkness, the COP1 protein is localized in the nucleus and transported to the cytosol upon light exposure. This exclusion from the nucleus does not completely suppress COP1 function, pointing to a mechanism that prevents over-stimulation by light (Von Arnim und Deng, 1994; von Arnim et al., 1997; Subramanian et al., 2004). Since this exclusion starts 12 h after light exposure and is finished after 36 h, there must be faster mechanisms in the regulation of COP1 function. Indeed the photoreceptors phyA, phyB, cry1 and cry2 were found to interact with COP1 via the WD40-repeat domain and thus suppress COP1 activity on other factors like HY5, supporting the hypothesis of a faster mechanism in the regulation of COP1 activity (Wang et al., 2001; Yang et al., 2001; Seo et al., 2004). cry1 and cry2

were found to interact with COP1 in light and darkness (Wang et al., 2001). On the other hand, it was shown that COP1 is essential for the degradation of phyA, phyB and cry2, thereby possibly desensitizing light signal transduction to prevent plants from an over-stimulation by light (Shalitin et al., 2002; Jang et al., 2010; Seo et al., 2004; Figure 1.2 B).

In addition to the role as a negative regulator of photomorphogensis, COP1 was also found to act positively in photomorphogenic responses in UV-B light signaling, further underlining the function of COP1 as a central signal integrator in photomorphogenic responses. Flavonoid biosynthesis and hypocotyl elongation in response to UV-B were shown to be impaired in *cop1* mutant plants. Furthermore, it was shown that *HY5* gene expression is positively regulated by COP1 (Favory et al., 2006). In this regard, COP1 interacts with the UV- RESISTANCE LOCUS 8 (UVR8) protein and inhibits a yet unknown factor that represses *HY5* transcription (Favory et al., 2009). Beside the role in repressing or promoting photomorphogenesis, COP1 also acts in many other developmental processes like stomata development (Kang et al. 2009; Ranjan, 2010) or the induction of flowering (Liu et al., 2008; Jang et al., 2008; Yu et al., 2008). In addition, it was recently found to interact genetically with the factor AtBBX21 in suppressing shade avoidance (Crocco et al., 2010). Since HFR1 is a well-known factor regulating shade avoidance (as described above), COP1 is also most likely involved in its regulation here. COP1 plays also a role in blue-light-dependent plant defense (Jeong et al., 2010a; Jeong et al., 2010b).

Another important repressor in light signal transduction is the SUPRESSOR OF PHYTOCHROME A-105 1 (SPA1) protein. Mutants of *spa1* are hypersensitive to far-red, red and blue light (Hoecker et al., 1998; Baumgardt et al., 2002; Fittinghoff et al., 2006). At the seedling stage, they exhibit a short hypocotyl, expanded cotyledons and accumulate increased amounts of anthocyanin, indicating a role of SPA1 similar to that of COP1 in the repression of photomorphogenesis (Hoecker et al., 1998). phyA interacts with SPA1 and is rapidly degraded in the light, a process that is delayed in *spa* and *cop1* mutants (Seo et al., 2004; Saijo et al., 2008). *spa1* mutants grown in darkness cannot be distinguished from wild type implying that SPA1 either functions predominantly in the light or that its function in darkness is

masked by redundantly acting proteins. Since *SPA1* transcript levels are elevated by far-red and red light the function of SPA1 seems to be not exclusively limited to phyA signaling but also to phyB signaling (Hoecker et al., 1999; Fittinghoff et al., 2006).

The SPA1 protein structure shares a high similarity to the COP1 as a carboxy-terminal WD-40-repeat and a coiled-coil domain is present in both proteins. Instead of a RING-finger motif in the amino- terminus of COP1, SPA1 carries a kinase-like domain that exhibits similarity to serin-/threonine-kinases (Hoecker et al., 1999). However, this domain was never shown to have a catalytic function even though deletion of the whole N-terminus of SPA1 results in early flowering under short days (Fittinghoff, 2008). Additionally, *SPA1* contains two nuclear localization sequences (*NLSs*) and the protein is constitutively localized in the nucleus (Hoecker et al. 1999). It could also be shown that SPA1 and COP1 proteins can interact with each other *in vitro* and *in planta* and that the coiled-coil domains of both proteins mediate the association (Hoecker and Quail, 2001; Saijo et al., 2003). Furthermore, *spa1* and *cop1* mutations interact genetically, which suggests that COP1 and SPA1 indeed act together to suppress photomorphogenesis (Saijo et al., 2003). Deletion of the coiled-coil motif in SPA1 leads to a constitutive *spa1* mutant-like phenotype in light grown seedlings, indicating the importance of the coiled-coil interaction motif (Fittinghoff, 2008). Since it was shown that SPA1 modulates COP1 E3-ligase activity *in vitro,* its WD-40-repeat interacts with HY5 and HFR1, and SPA1 is additionally involved in the regulation of their stability, it seems to be clear that SPA1 and COP1 can act together in light-mediated responses (Saijo et al, 2003; Seo et al; 2003; Jang et al; 2005). The interaction of COP1 and SPA1 may indicate that SPA1 is mediating the substrate recognition and/or regulating the E3- ligase activity of COP1.

SPA1 is part of a gene family (*SPA1-SPA4*) (Laubinger and Hoecker, 2003). All SPA proteins exhibit a WD-40-repeat domain, at least one coiled-coil motif and a kinase-like domain (Laubinger and Hoecker, 2003; Figure 1.3). SPA1 is related more closely to SPA2 than to SPA3 and SPA4, which share up to 74% identical amino acids with each other (Laubinger and Hoecker, 2003). Thus, it was shown that SPA1 and SPA2 evolved from

duplication during evolution (Simillion et al., 2002). The N-termini of SPA1 and SPA2 are much longer than those of SPA3 and SPA4 (Laubinger and Hoecker, 2003; Laubinger et al., 2004). Like *spa1* mutants *spa3* and *spa4* single mutant seedlings show enhanced photomorphogenesis in far-red, red and blue light but cannot be distinguished from wild type when grown in the dark (Laubinger and Hoecker, 2003). Since *spa3spa4* double mutants are more hypersensitive to light than the single mutants, one could assume a redundant effect of both proteins (Laubinger and Hoecker, 2003). *spa2* single mutants do not show enhanced photomorphogenesis in light when compared to wild type (Laubinger et al., 2004). Like SPA1, SPA2, SPA3 and SPA4 interact with the COP1 protein supporting the hypothesis of COP1 and different SPA proteins acting together (Laubinger and Hoecker, 2003; Laubinger et al., 2004).

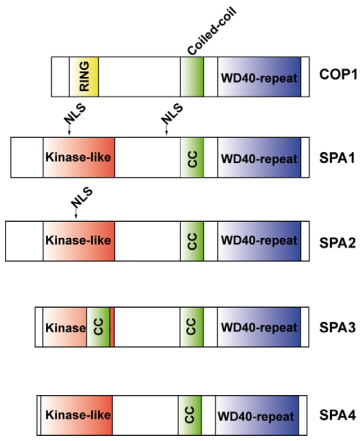

Figure 1.3: Protein structure of COP1 and the SPA protein family. COP1 as well as the SPA proteins contain a WD40-repeat and a coiled-coil (CC) motif. In addition COP1 carries a RING-finger motif in the N-terminus whereas SPA proteins contain a kinase-like domain.

The analysis of *spa1spa2spa3spa4* quadruple mutants revealed, that they undergo strong constitutive photomorphogenesis in darkness similar to *cop1* mutants, indicating a strong redundant effect among the SPA proteins in the reppression of photomorphogenesis in darkness (Laubinger et al., 2004). The analysis of *spa* double- and triple- mutants also revealed that, besides this redundancy, *SPA*s also have distinct functions throughout plant development (Laubinger et al., 2004; Fittinghoff et al., 2006). It was shown that SPA1 is the dominant player in seedlings that represses

photomorphogenesis in light, whereas SPA1 and SPA2 are both sufficient to prevent photomorphogenesis in darkness. In contrast, SPA3 and SPA4 play only a minor role under these conditions (Laubinger et al., 2004; Fittinghoff et al., 2006). SPA3 and SPA4 also contribute to suppression of photomorphogenesis in light, but when compared to SPA1 only to a minor extent (Laubinger et al., 2004; Fittinghoff et al., 2006).

The effect of *spa* mutations could also be observed by looking at the adult stage. *spa3spa4* double mutants exhibit reduced plant size compared to the single mutants or wild type. This phenotype is strongly enhanced in the *spa1spa2spa3spa4* quadruple mutant, which displays dwarfism similar to *cop1* mutant plants (Laubinger et al., 2004). The fact that only slight effects on plant size were detected in *spa3* and *spa4* single mutants, but stronger effects in the double mutant, indicates the role of *SPA3* and *SPA4* as major regulators defining adult plant and leaf size (Laubinger et al., 2004). SPA1 has also a significant function in this developmental process, while SPA2 has very little function in adult plants. Previous studies showed that SPA1 activity in the phloem and mesophyll cells seems to contribute to leaf size and therefore plant size (Ranjan, 2010). Substrates of the SPA proteins for the determination of plant size (transferring the information to the expression level for example) are thus far unknown.

Besides the regulation of seedling development and adult plant size *SPA* genes are also involved in the photoperiodic induction of flowering. *Arabidopsis thaliana* is a facultative long day plant which flowers early in long days and late in short days (Coupland et al., 1998). It was shown that the *spa1* single mutant flowers earlier in short days (Laubinger et al., 2006). In contrast, *spa2spa3spa4* triple mutants flower as late as wild type indicating that SPA1 is the main regulator of flowering time in short days (Laubinger et al., 2006). *spa1spa3spa4* triple mutants, having only functional SPA2 left, show extremely early flowering indicating an additional contribution of *SPA3* and *SPA4* (Laubinger et al., 2006).

The induction of flowering was shown to be mediated by the transcription factor CONSTANS (CO), which activates the expression of *FLOWERING LOCUS T* (*FT*) and its homolog *TWIN-SISTER OF FT* (*TSF*) (Koorneef at al., 1991; Putteril et al., 1995; Yamaguchi et al., 2005). FT

protein moves via the phloem to the shoot apical meristem and regulates the expression of floral genes and therefore induces flowering (Corbesier et al., 2007; Jaeger and Wigge, 2007; Lin et al., 2007a; Mathieu et al., 2007). Since *spa1spa3spa4* triple mutants show increased CO protein levels, and thus increased *FT* expression and since SPA1 and COP1 can physically interact with CO, it is likely that SPA1 and COP1 together regulate flowering time via the stability of CO protein (Ishikawa et al., 2006; Laubinger et al., 2006; Jang et al., 2008). In addition, genetic studies revealed that the early flowering phenotype of the *spa1* mutant is dependent of functional CO and that SPA1 and COP1 indeed act in the phloem where CO is located, to regulate photoperiodic flowering (Laubinger et al., 2006; Jang et al., 2007; Ranjan, 2010).

Recently, SPA proteins were also found to regulate stomata development in the dark, as stomata development of dark grown *spa1spa2spa3* mutant seedlings cannot be distinguished from stomata development of wild-type seedlings grown in the light (Kang et al., 2009; Figure 1.4). In this regard SPA1 was identified to act in the phloem regulating stomata development (Ranjan, 2010).

Taken together, the SPA proteins in concert with COP1 regulate various stages of plant development carrying out redundant and distinct functions (Figure 1.4). SPA1 seems to be important in nearly all stages including seedling development in light and darkness, determination of plant size as well as the regulation of flowering time. SPA2 has its major role in dark grown seedlings, whereas SPA3 and SPA4 are essential for adult plant size. SPAs contribute to stomata development, although the contribution of each single *SPA* gene is not clear. Interestingly, a very recent analysis of promoter swap lines using chimeric constructs of *SPA1* and *SPA2* promoters and cDNAs showed that the protein sequence, rather than the light-dependent expression of *SPA* genes, seems to determine the characteristic SPA function (Balcerowicz et al., 2011).

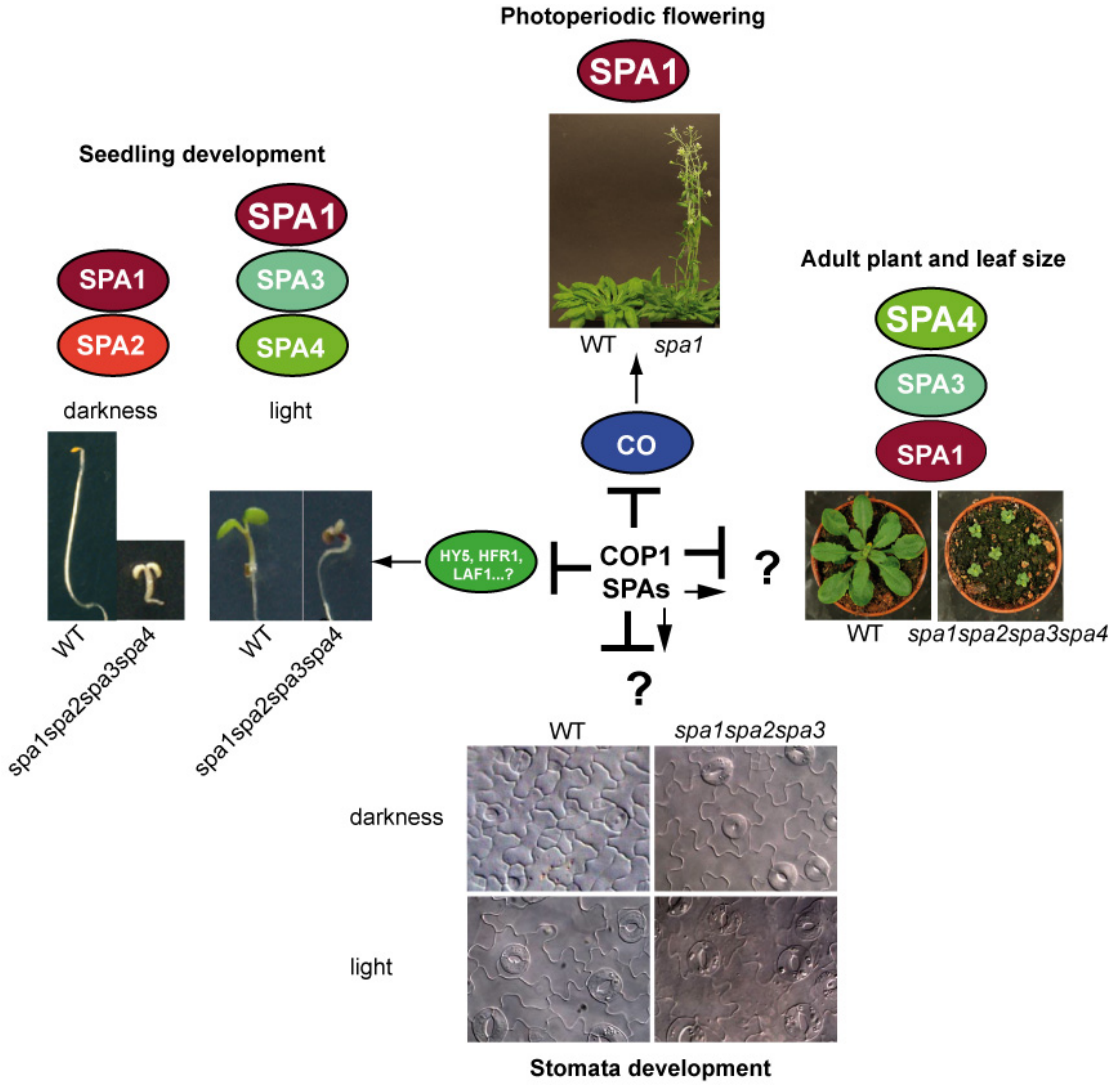

Figure 1.4: Contribution of SPA proteins to *Arabidopsis* plant development. Shown are the developmental processes in which SPA proteins have been characterized. Also given are the transcription factors known to be regulated by COP1 and the SPA proteins. SPA1 plays a major role in seedling development in darkness and light as well as in the regulation of flowering time. It is also involved in the determination of plant size. SPA2 only plays a role in seedling development in darkness. SPA3 regulates seedling development as well as adult plant and leaf size. SPA4 has its major role in adult plants but also contributes to seedling development in light. SPAs are involved in stomata development in darkness (Stomata pictures: Kang et al., 2009).

I.3 COP1 as part of protein complexes

The COP1 protein is part of higher molecular weight complexes (Saijo et al., 2003). COP1 is able to interact with the RING-finger domain of the ubiquitin-activating E2 variant COP10, another protein from the COP/DET/FUS group that is mediating the repression of photomorphogenesis in darkness (Suzuki et al., 2002). COP10 associates with DEETIOLATED 1 (DET1) and UV-DAMAGED DNA_BINDING PROTEIN 1 (DDB1), thereby assembling a small protein complex called CDD complex (Yanagawa et al., 2004). Some proteins from the COP/DET/FUS group were also found to interact with another multi-subunit complex, the COP9 signalosome CSN (von Arnim, 2003). CDD and CSN are involved in the proteasomal degradation of photomorphogenesis-promoting factors (Serino and Deng, 2003; Yanagawa et al., 2004; Yi and Deng, 2005). Further, CSN seems to be essential for the activity of E3-ubiquitin ligases of the SKIP/CULLIN/F-BOX (SCF)- type and is interacting with the proteasome (Kwok et al., 1999; Serino und Deng, 2003; Peng et al., 2003). Interestingly, in darkness COP1 is depleted in the nucleus in *csn* mutants (compared to wild type) suggesting that the CSN plays an important role in COP1 nuclear import and/or retention in the dark (Chamovitz et al., 1996; von Arnim et al., 1997). The CDD complex is able to associate with COP1 and CSN *in vivo*, indicating that all these factors may act together in ubiquitin-proteasome-mediated degradation of photomorphogenesis-promoting factors (Yanagawa et al., 2004).

CULLIN 4 (CUL4), a distinct member of the cullin protein family, binds to the RING-BOX 1 (RBX1)-protein as well as DDB1 to form the core of a CUL4-based E3-ubiquitin ligase (Groisman et al., 2003; Wertz et al., 2004; Chen et al., 2006). Mutants of *CUL4* have been shown to have an early flowering phenotype in short days and to enhance the photomorphogenic phenotype of a *cop1* mutation in darkness, suggesting the involvement of CUL4 in these processes (Chen et al., 2010). Furthermore, COP1 and the SPA proteins were shown to associate with CUL4 based E3-ubiquitin ligases by binding to the DDB1 protein (Chen et al., 2010). COP10 and DET1, the other two members of the CDD complex, can also interact with CUL4-DDB1 but seem to be not included in the complex when COP1 and the SPA proteins

are present. Therefore, DDB1 seems to be the adaptor protein that recruits so called DDB1–CUL4-associated WD40 domain proteins (DCAFs), like the SPA proteins, as substrate recognition receptors and modulates the specificity of the CUL4-based E3-ubiquitin ligase (Chen et al., 2010). The activity of DDB1-CUL4 complexes is regulated via the CSN, which rubylates and derubylates CUL4. Thus, rubylation seems to activate the DDB1-CUL4 complex (Chen et al., 2006).

I.4 Regulation of anthocyanin biosynthesis in *Arabidopsis thaliana*

Anthocyanins are purple natural pigments found in many plant species. They belong to secondary plant metabolites known as flavonoids, which play important roles in many plant functions. The major function of anthocyanin is to provide color to flowers and fruits, which can help to attract pollinating aminals and animals that will help to disperse seeds (Gould et al., 2009). Anthocyanins are also involved in processes such as protection of the photosynthetic apparatus, herbivory and free radical scavenging (Holton and Cornish, 1995; Gould, 2004; Koes et al., 2005; Tanaka et al., 2008). Over 6000 different flavonoids have been reported (Harborne and Williams, 2000) and subdivided into different classes that include flavonols, flavones, flavanols and anthocyanins, according to the oxidation level of the C-Ring (Figure 1.5 A). Additionally, stereochemistry, position, nature and combination of substitutions (hydroxyl, methyl, galloyl, glycosyl), degree of polymerization and linkages between the basic units allow for the multitude of these compounds in plants (Figure 1.5 A). The accumulation of anthocyanin in plants is stimulated by light and various environmental stress factors like UV-B light, nutrient depletion and low temperature (Winkel-Shirley, 2001; Ulm et al., 2004; Brown et al., 2005; Lillo et al., 2008; Olsen et al., 2009).

Biosynthesis of anthocyanins is mediated by multiple enzymes in a pathway that derives from the amino acid phenylalanine and is referred to as the anthocyanin branch of the phenylpropanoid pathway (Holton and Cornish, 1995; Winkel-Shirley, 2001; Koes et al., 2005). The genes encoding for the

enzymes of the biosynthesis pathway are subdivided into two groups designated as “early“ and “late“ genes (Pelletier et al., 1997; Dubos et al., 2008; Gonzalez et al., 2008; Figure 1.5 B). In *Arabidopsis*, analysis of the *transparent testa* (*tt*) mutants uncovered many enzymes that are involved in anthocyanin biosynthesis (Lepiniec et al., 2006; Figure 1.5 B). In other plant species presence, substrate recognition and number of homologues for each anthocyanin biosynthetic enzyme vary. Therefore, the division of the “early“ and “late“ genes varies too (Shi et al., 2010; Figure 1.5 B).

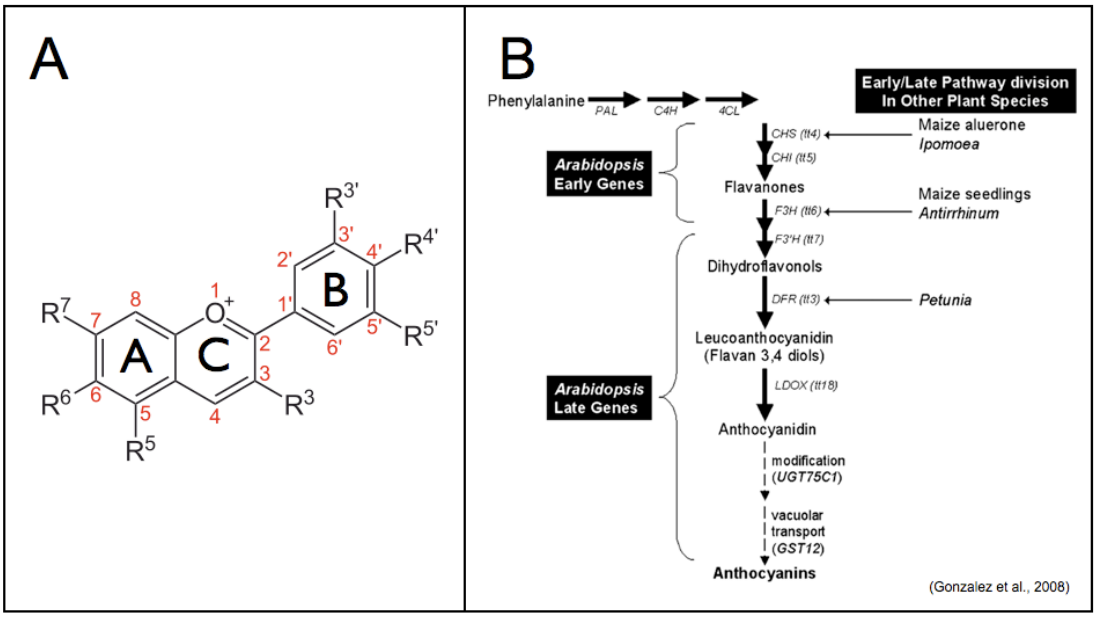

Figure 1.5: Structure and biosynthesis of anthocyanins in plants. (A) The core of anthocyanin is a structure of three aromatic rings, the A-, B- and C-Ring. Anthocyanins can be substituted with hydroxyl-, methyl-, galloyl-, glycosyl- groups at the positions R, indicating a number of various combinations possible. (B) Branch of the phenylpropanoid pathway yielding anthocyanin biosynthesis in plants (Gonzalez et al., 2008). The pathway is subdivided in „early“ and „late“ genes. Bisosynthethic enzymes are *PHENYLALANINE AMMONIA-LYASE* (*PAL*), *CINNAMATE 4-HYDROXYLASE* (*C4H), 4-COUMAROYL-CoA-LIGASE* (*4CL*), *CHALCONE SYNTHASE* (*CHS*), *CHALCONE ISOMERASE* (*CHI*), *FLAVANOLE 3-HYDROXYLYASE* (*F3H*), *FLAVONOID 3’-HYDROXYLYASE* (*F3’H*), *DIHYDROFLAVONOL REDUCTASE* (*DFR*), *LEUCOANTHOCYANIDIN SYNTHASE* (*LDOX*) *UDP FLAVONOID GLUCOSYL TRANSFERASE* (*UGT*) and *GLUTATHIONE S-TRANSFERASE LIKE 12* (*GST12*). The name of the mutants is shown in brackets. The horizontal arrows indicate the first structural gene that is regulated in other plant species.

In *Arabidopsis* and other plant species, many transcription factors including members of the MYB, bHLH and WD40-repeat protein families were found to regulate anthocyanin biosynthesis (Nesi et al., 2000; Zhang et al., 2003; Koes et al., 2005; Stracke et al., 2007; Dubos et al., 2008; Gonzalez et

al., 2008; Matsui et al., 2008; Rowan et al., 2009), e.g. the WD-repeat protein TRANSPARENT TESTA GLABRA 1 (TTG1) and the bHLH proteins TRANSPARENT TESTA 8 (TT8), ENHANCER OF GLABRA 3 (EGL3) and GLABRA 3 (GL3). Additionally, the Myb transcription factors PRODUCTION OF ANTHOCYANIN PIGMENT1 (PAP1, also called MYB75) and PAP2 (also called MYB90), MYB113 and MYB114 and TRANSPARENT TESTA 2 (TT2) have been shown to be involved in the regulation in *Arabidopsis* (Zhang et al., 2003; Broun, 2005; Cominelli et al., 2008; Gonzalez et al., 2008).

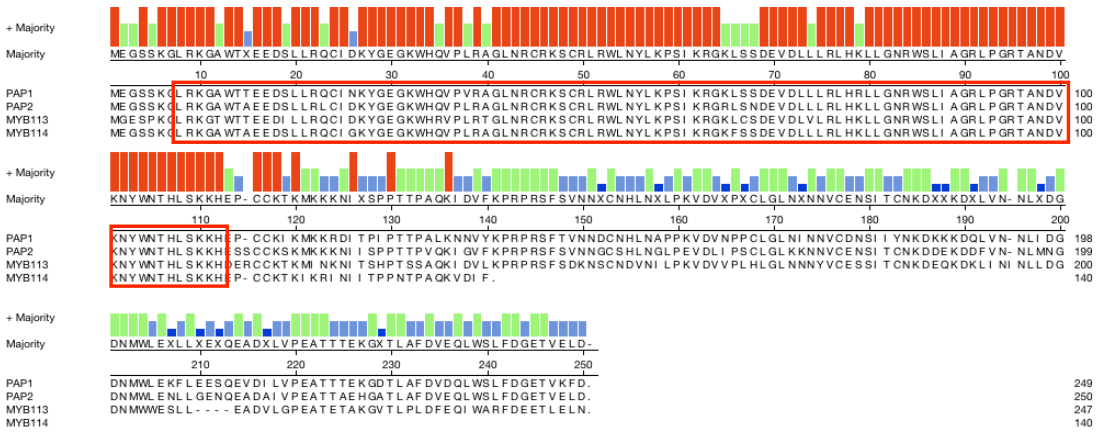

Figure 1.6: Amino acid alignment of the R2R3 MYB domain of the PAP1, PAP2, MYB113 and MYB114 transcription factors. The R2R3-MYB domain is boxed in red. Identical amino acids are indicated by the colored bars. Red bars indicate four, green bars three and blue bars two matches. The majority of amino acids is also given.

PAP1, PAP2, MYB113 and MYB114 carry a DNA binding motif that consists out of two imperfect repeats named R2 and R3, which designates them as R2R3-MYB transcription factors (Ogata et al., 1994; Figure 1.6). The R2R3-MYB domain contains a consensus motif that has been reported to be plant specific (Braun and Grotewold, 1999; Kranz et al., 2000). PAP1, PAP2, MYB113 and MYB114 are very similar to each other regarding amino acid sequences, indicating high redundancy in their mode of action (Figure 1.6). For instance, PAP1 and PAP2 share 85% identical amino acids with each other. *RNAi* lines targeting the mRNA of all four genes exhibited down-regulation of anthocyanin biosynthesis genes, highlighting the major impact of those proteins on anthocyanin biosynthesis (Gonzalez et al., 2008). The MYB transcription factor PAP1 was found by activation tagging screen experiments in *Arabidopsis* (Weigel et al., 2000). Nearby insertion of four enhancer

elements from the *35S CaMV* (Cauliflower Mosaic Virus) promoter to the *PAP1* gene triggered its expression resulting in purple pigmentation of nearly all vegetative organs, what indicated an upregulation of the phenylpropanoid biosynthesis pathway in the activation tagged plants referred to as *production of anthocyanin pigment 1-Dominant* (*pap1-D*; Borevitz et al., 2000). This phenotype was also observed in other transgenic lines overexpressing both PAP proteins (Borevitz et al., 2000; Teng et al., 2005) or their homologues MYB113 and MYB114, respectively (Gonzalez et al., 2008). Whether these four members perform their function in concert with each other or in an independent manner is an interesting question that remains so far unanswered.

Ectopic overexpression of *PAP1* in *Arabidopsis* results in upregulation of genes across the entire flavonoid biosynthetic pathway, including “early“ and “late“ genes of the anthocyanin biosynthetic branch. This implies a broad function of PAP1 in these metabolic processes (Borevitz et al., 2000; Tohge et al., 2005b; Bhargava et al., 2010). Also, this results in a lost of proanthocyanins and a gain of anthocyanins in the seed coat. Proanthocyanins accumulate predominatly in the seed coat and embryo (Tohge et al., 2005a). Overexpression of the *Arabidopsis PAP1* gene in tobacco and tomato caused similar effects of anthoyanin overaccumulation, indicating the conservation of PAP1 function in other plants (Borevitz et al., 2000; Xie et al., 2006; Zuluaga et al., 2008). However, genetic analysis from Gonzalez and co-workers (2008) revealed that the function of PAP1, PAP2, MYB113 and MYB114 is dependent on the presence of GL3 or TT8, EGL3 and TTG1 and that these factors together induce specifically the “late“ anthocyanin biosynthetic genes. Consistent with this, the expression of *MYB113* and *MYB114* in *egl gl3* double mutant background causes reduced anthocyanin levels compared to *egl gl3* mutants. In addition, *pap1-D ttg1* mutants fail to accumulate anthocyanin, showing the dependence of PAP1 function on TTG1 (Borevitz et al., 2000). Further studies revealed that TTG1 strengthens TT2 - TT8 interactions in yeast and thus might stabilize bHLH-MYB complexes (Baudry et al., 2004). Thus, a protein complex including WD-repeat, bHLH and MYB factors is likely to act in the regulation of anthocyanin biosynthesis genes. The hypothesis of complex formation is also supported by

the fact that EGL3 is able to interact with PAP1, PAP2, MYB113 and MYB114 in yeast (Zimmermann et al., 2004a). Also, TTG1 is able to interact with GL3 and EGL3 in yeast (Payne et al., 2000). Nevertheless a direct interaction between the PAP proteins, MYB113, MYB114 and TTG1 has never been shown.

The amount of different bHLH and MYB factors that is most likely involved in the regulation of anthocyanin biosynthesis, points to a complex network of transcription factors with highly redundant functions (Shi et al., 2010). This is for example supported by the fact that overexpression of GL3 and EGL3 in a *tt8* mutant background (*tt8* mutants fail to accumulate anthocyanin) led to either partial or complete restoration of a wild-type seedling phenotype (Zhang et al., 2003).

Transcript levels of *PAP1, PAP2, EGL3* and *GL3* as well as *TT8* are strongly regulated by light. They accumulate in dark-adapted adult plants upon exposure to white, blue, UV-A, UV-B and red light. In contrast, the expression of *TTG1* is unaltered under all light conditions (Cominelli et al., 2008). Since in darkness transcript levels of *PAP1, PAP2, EGL3* and *GL3* in seedlings are very low and overexpressors of *PAP1* and *PAP2* fail to accumulate anthocyanin, it was postulated that anthocyanin biosynthesis can only occur in the light, when all factors are present (Cominelli et al., 2008).

Besides anthocyanin biosynthesis, WD/bHLH/MYB containing complexes are also involved in proanthocyanin synthesis, mucilage synthesis, root hair patterning and trichome initiation (Figure 1.7). In this context, many bHLH and MYB transcription factors have been identified that mediate those responses and are interacting with each other (Broun et al., 2005; Figure 1.7). The WD-repeat protein TTG1 participates in all these responses providing a scaffold to facilitate the interactions between MYB and bHLH proteins. However, there is also cross-reaction of factors. CAPRICE (CPC), a single-repeat R3 MYB transcription factor known to play a role in developmental processes such as root hair differentiation and trichome-initiation was shown to be a negative regulator of anthocyanin biosynthesis by competing with PAP1 and PAP2 for the binding of bHLH factors (Zhu et al., 2009).

Taken together, it seems to be clear that the control of transcription factors over secondary metabolism in plants occurs within complex regulatory

networks, which integrate metabolism and development. The exact mode of action of TTG1 and its orhologues on the DNA remains so far unclear.

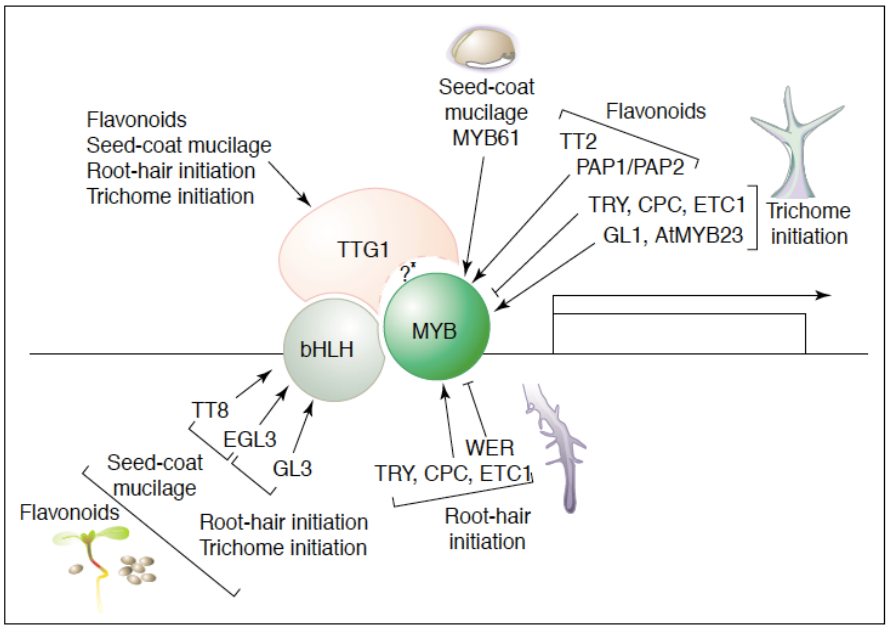

Figure 1.7: The composition and function of WD / bHLH / MYB containing complexes throughout *Arabidopsis* plant development (Broun et al., 2005). Shown are the transcription factors and the regulatory outcome. The questionmark between MYB and TTG1 indicates that only interaction between TTG1 and TT2 has been demonstrated.

I.6 Light-mediated regulation of anthocyanin biosynthesis

For light-mediated regulation of anthocyanin biosynthesis detailed information has been provided on the light regulation of *CHALCONE SYNTHASE* (*CHS)* expression. Light induction of *CHS* expression as an "early" expressed gene (Figure 1.5 B) is very complex and involves UV-B-, UV-A-, cryptochrome- and phytochrome signaling (Jenkins, 1997). phys were shown to induce *CHS* in young *Arabidopsis* seedlings (Kaiser et al., 1995), whereas the induction of *CHS* in leaf tissue of later stages is mediated by the phytochrome, cryptochrome and UV-B phototransduction pathways together (Fuglevand et al., 1996; Wade et al., 2001). Analysis of the *CHS* gene from parsley revealed a light-responsive unit carrying a G-Box and MYB recognition element supporting the notion that *CHS* is regulated by bHLH, bZIP and MYB transcription factors (Schulze-Lefert et al., 1989; Feldbrügge et al., 1994; 1997). Nearly all promoters of anthocyanin biosynthetic genes, like

CHS, *CHI*, *F3H*, *F3'H*, *DFR* and *LDOX* contain such elements (Shin et al., 2007).

In 2010, Zhang and co-workers showed that low temperature-induced anthocyanin accumulation is influenced by HY5 and HYH. Recently, chromatin immunoprecipitation (ChIP) analysis revealed more than 3000 *in vivo* HY5 targets in the *Arabidopsis* genome. The class of HY5-binding targets was enriched for light-responsive genes, indicating that HY5 is a major regulator in light responsiveness besides other developmental processes (Lee et al., 2007). HY5 was also found to bind promoters of "early" and "late" genes of anthocyanin biosynthesis, such as *CHS* and *DFR,* underlining the integration of photomorphogenic and metabolic responses (Ang et al., 1998; Chattopadhyay et al., 1998; Holm et al., 2002; Lee et al., 2007; Shin et al., 2007; Zhang et al., 2010). In addition, PIF3, another factor in phytochrome signaling that is known to promote anthocyanin biosynthesis (Kim et al., 2003), was found to act in a HY5-dependent manner. Both proteins are able to bind to various promoters of anthocyanin biosynthetic genes (Shin et al., 2007). HY5 is also necessary but not sufficient for the induction of *LIGHT-REGULATED ZINC FINGER PROTEIN 1 (LZF1)* expression. LZF1 is a C2C2-CO B-box transcription factor that promotes *PAP1* expression and therefore leads to accumulation of anthocyanin (Chang et al., 2008).

Previous studies revealed higher accumulation of anthocyanin in *cop1-* and *spa-* mutants compared to wild type (Deng et al., 1991; Baumgardt et al., 2002; Laubinger et al., 2004). As described above, HY5 is a target of COP1 dependent ubiquitination in photomorphogenic responses (Osterlund et al., 2000a). In agreement, HY5 protein levels were show to be stabilized in both *cop1-* and *spa-* mutants (Saijo et al., 2003; Yang et al., 2006; Favory et al., 2009; Nixdorf et al., 2010).

Since an E3-ubiquitin ligase (UPL3 / KAKTUS) is known to target the transcription factor GL3 in the context of branching and endoreplication in *Arabidopsis* trichomes (Downes et al., 2003; El Refy et al., 2003), one could assume that COP1 acts equivalently in anthocyanin biosynthesis by targeting bHLH, Myb and bZIP factors from WD/bHLH/MYB complexes. Interestingly, the PAP1 and PAP2 protein were found to interact with COP1 and SPA proteins in a recent Yeast Two-Hybrid- screen using a transcription factor-

library (Falke, 2008; L.Kokkelink, G. Fiene and U. Hoecker, unpublished). However, little is known about the regulation of anthocyanin biosynthesis via E3-ubiquitin ligases so far.

I.7 Aims of this PhD thesis

(i) **Analysis of SPA protein contribution to COP1 containing complexes by testing SPA -SPA dimeric interactions**: The four SPA proteins carry out distinct but also overlapping functions throughout plant development. Since they were found to act in concert with the E3-ubiquitin ligase COP1 and to physically interact with COP1, I studied in a first project whether SPA proteins can also interact with each other *in vitro* and *in planta*, indicating the existence of larger COP1/SPA containing complexes.

(ii) **Generation of COP1, SPA1 and SPA2 antibodies:** In order to detect endogenous COP1, SPA1 and SPA2 proteins, I started generating polyclonal antibodies employing recombinant protein from *E.coli* or artificially designed peptides. Using SPA1 and SPA2 antibodies, I tested how COP1/SPA1 and COP1/SPA2 complex assembly is regulated in light versus darkness.

(iii) **The PAP1 and the PAP2 proteins are potential targets for COP1/SPA complexes:** Ubiquitination of downstream targets via COP1/SPA complexes seems to be a major way of regulating protein levels at multiple stages in plant development. PAP1 and PAP2 proteins are transcription factors, which were found to be involved in the regulation of anthocyanin biosynthesis. In addition, they interact with COP1 and SPA proteins in yeast, which designates them to be potential COP1/SPA complex targets. Since it is known that *PAP1* and *PAP2* expression is regulated by light, I studied the influence of light on PAP1 and PAP2 protein levels by using overexpressing *Arabidopsis* plants. Further, I studied the effect of COP1 function on anthocyanin biosynthesis by analyzing crosses of *cop1-4* mutant with *PAPRNAi* mutant and *PAP* overexpressing plants by determination of anthocyanin contents and protein levels. In parallel, antibodies against PAP1 were generated in order to study the endogenous PAP1 protein levels.

II. Results

II.1 Analysis of SPA-SPA protein interactions

All SPA proteins share a high similarity with each other in regard of the amino acid sequence, which is also the case for the arrangement of the protein domains (Laubinger and Hoecker 2003; Laubinger et al., 2004). Previous studies showed that *COP1* and *SPA* genetically interact in the repression of photomorphogenesis and all SPA proteins can associate with the COP1 protein (Hoecker and Quail, 2001; Laubinger and Hoecker; 2003; Laubinger et al., 2004; Lin and Wang, 2007). In addition, SPA1 was found to modulate COP1 E3-ubiquitin ligase activity *in vitro* (Saijo et al., 2003; Seo et al., 2003), indicating that COP1 works in concert with the SPA proteins in the repression of photomorphogenesis. COP1 is also part of different higher molecular weight complexes (Yanagawa et al., 2004; Chen et al., 2010).

Since the contribution of SPA proteins to the architecture of COP1 complexes is not clear, it was interesting to test whether SPA proteins can also interact with each other in homo- and heterodimers, indicating the existence of larger protein complexes including multiple SPA proteins and COP1. Two configurations of COP1/SPA complexes would be possible: A large supercomplex involving all SPAs and COP1 or smaller complexes with a set of certain SPA proteins and the COP1 protein. Since many proteins of other known protein complexes were found to interact with COP1 or SPA proteins, a participation of these factors in a protein complex is also possible. The composition of such COP1/SPA complexes may explain the distinct but also overlapping functions of SPA proteins throughout plant development.

II.1.1 SPA proteins interact with each other *in vitro*

In order to test whether the four SPA proteins can interact with each other, pairwise *in vitro* CoIP studies were performed. Recombinant [^{35}S]-radioactively labeled SPA and GAD-SPA fusion proteins (SPA proteins fused to GAL4-activation domain) were produced in a cell free transcription and translation system. Using specific antibodies against the GAD domain, bait

proteins were precipitated and the amount of bound SPA prey protein was analyzed.

In the experiment, all SPA proteins were able to associate with each other in every combination tested (Figure 2.1 A). The interactions between GAD-SPA1 and SPA1, GAD-SPA1 and SPA2, GAD-SPA2 and SPA1 and GAD-SPA2 and SPA2 appeared to be the strongest with 1 % to nearly 2 % of precipitated prey protein. Further, the homodimer of SPA3 showed also a strong interaction. In contrast, all negative controls with GAD exhibited almost no binding to the prey proteins (Figure 2.1 A, B).

II.1.2 The N-terminus of SPA1 mediates SPA1 self-association and SPA1-SPA2 interaction

As described above, all SPA proteins could associate with each other. Also, previous studies revealed that the coiled-coil domain of SPA1 mediates the interaction with the COP1 protein (Hoecker and Quail, 2001; Yang et al., 2005a), whereas the WD40-repeat domain is involved in binding substrates like HY5 and HFR1 (Hoecker et al. 1999; Saijo et al., 2003; Yang and Wang, 2006). In this regard, deletion derivates of SPA1 were tested in pairwise *in vitro* binding assay together with non-labeled GAD-SPA1 and GAD-SPA2 full-length bait proteins to determine the part of the SPA proteins that is mediating the interactions within the SPAs. Since only weak interactions between SPA1 and SPA3 as well as SPA4 could be observed in the previous experiments (Figure 2.1), interactions of GAD-SPA3 and GAD-SPA4 with deletion derivates of SPA1 were not tested. For the deletion derivates SPA1-NT696, which lacks the C-terminal WD40-repeat domain, SPA1-NT545, which lacks the WD40-repeat and coiled-coil domain, and SPA1-CC, which encodes only for the coiled-coil domain of SPA1 were employed, respectively (Hoecker and Quail, 2001; Figure 2.2 A). As Figures 2.2 B and C show, the SPA1-NT696 protein was able to bind to SPA1 and SPA2 protein as efficiently as the full-length SPA1 protein, whereas deletion of the coiled-coil domain strongly reduced, but did not abolish the interaction. The coiled-coil domain itself also mediated weak interactions. Hence, the N-terminus of SPA1 including the

coiled-coil motif is mediating the interaction of SPA1 with SPA2 and full-length SPA1.

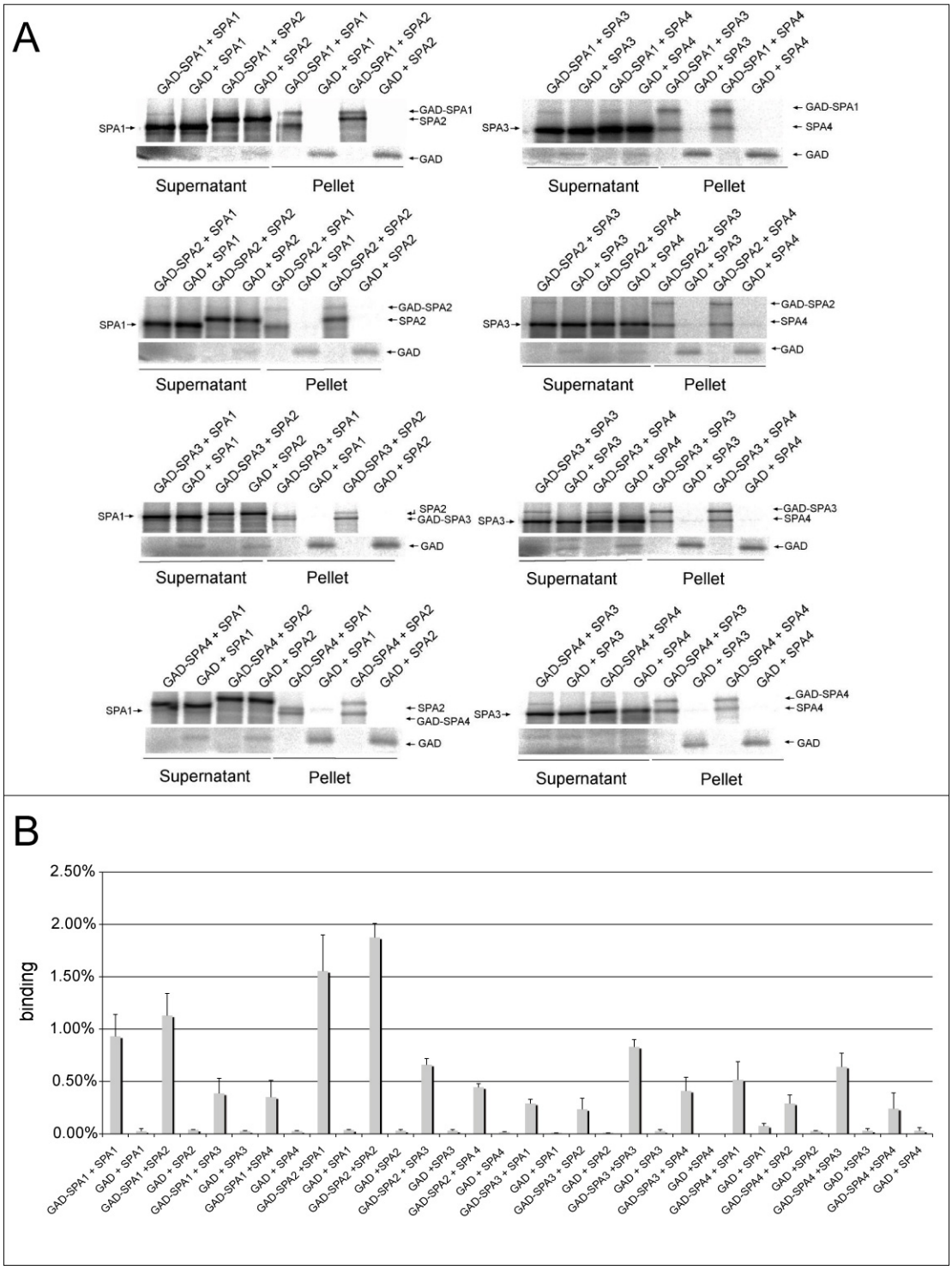

Figure 2.1: All SPA proteins interact with each other *in vitro*. (A) Recombinant [^{35}S]-labeled SPA proteins as preys were incubated with partially [^{35}S]-labeled GAD-SPA baits and precipitated with GAD specific antibodies. 2.5% of the supernatant fraction and 33% of the pellet fraction were analyzed on 7.5% and 10% SDS-PAGE gels. The protein was visualized using a phosphoimager. (B) Quantification of two independent CoIP experiments. The error bar shows the standard error of the mean.

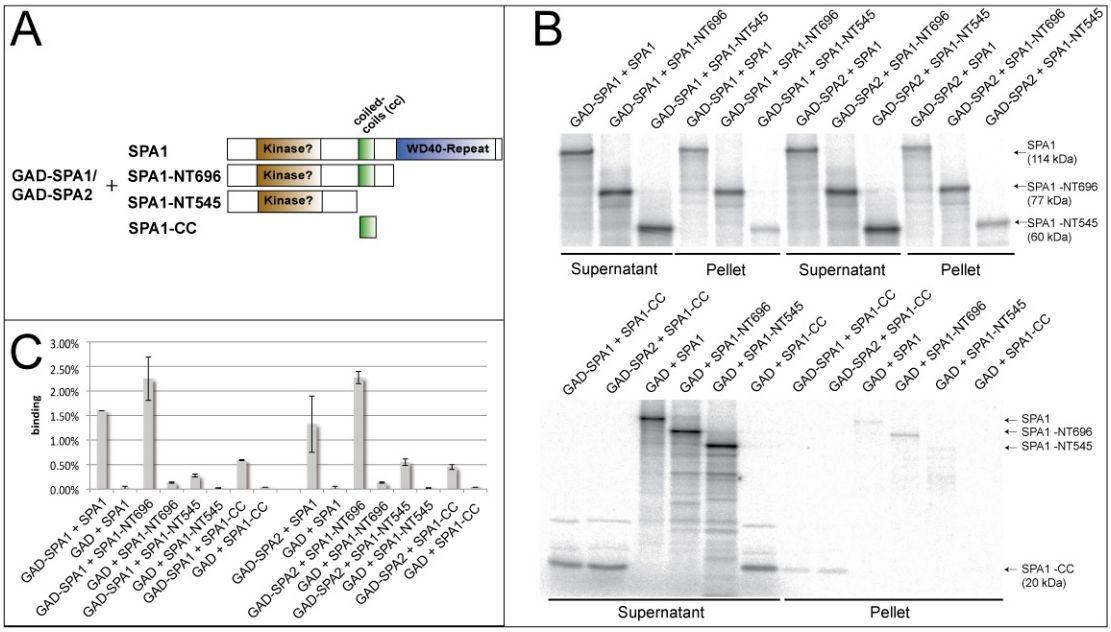

Figure 2.2: The N-terminus of SPA1 is important for SPA-SPA interaction. (A) Schematic overview of the tested constructs. (B) Results from *in vitro* CoIP using recombinantly produced deletion derivates of [^{35}S]-labeled SPA1 protein. Non-labeled GAD-SPA1 and GAD-SPA2 were employed as bait proteins. 2.5% of the supernatant fraction and 33% of the pellet fraction were analyzed on 7.5% and 10% SDS-PAGE gels. (C) Quantification of two independent CoIP experiments. The error bar shows the standard error of the mean.

II.1.3 SPA proteins interact *in planta*

In order to verify the results for full-length SPA interactions obtained from *in vitro* CoIP, *in planta* Bimolecular Fluorescence Complementation (BiFC)-analysis was performed. Therefore, the YFP N-terminal fragment (YN) and the YFP C-terminal fragment (YC) fused to SPA1 and/or SPA4 were coexpressed from the 35S promoter of Cauliflower mosaic virus (*35S CaMV*) in onion (*Allium cepa*) epidermal cells. CFP-talin was co-bombarded to monitor transfected cells. YN and YC fusions of the nuclear protein CPRF1 co-transfected with respective SPA1 or SPA4 fusions served as negative controls. For SPA2 and SPA3 no reliable results could be obtained using the BiFC assay, as they exhibited weak YFP signals upon co-transfaction with CPRF1.

A strong YFP signal was detected for SPA1 self-interaction exclusively in the nucleus of the cell, whereas no signal was detectable for the negative controls with CPRF1 (Figure 2.3). SPA1 was also able to interact with the SPA4 protein, although the signal was much weaker than in case of SPA1

self-interaction, and occurred in the cytoplasm as well as the nucleus of the cell when SPA4 was fused to YN. SPA4 fusions with YC co-transfected with YN-SPA1 did not exhibit a stronger YFP-signal in the cytoplasm of the cell in all repetitions of the experiment, indicating differences due to the direction of the tagging. SPA4 was also able to interact with itself and again the YFP signal was detectable in the nucleus, but also in the cytoplasm. Nevertheless, the signal in the nucleus was much weaker than in case of SPA1-SPA4 interaction. The fact that SPA4-SPA4 interaction signals also occurred in the cytoplasm of the cells is most likely due to the lack of an NLS sequence in SPA4. Since the YFP signals of SPA4-SPA4 interactions are also detectable in the nucleus, it could be that a portion of SPA4-SPA4 is targeted to the nucleus by other factors. However, why then SPA1, which carries NLSs, is able to interact with SPA4 in the cytoplasm remains unclear and could be only explained by impaired nuclear transport or an artifact due to strong overexpression. CPRF1 together with SPA4 showed a significantly weaker YFP signal compared to the SPA interactions in all cases. CPRF1 protein also associated with itself as described by Stolpe et al., 2005 (Figure 2.3).

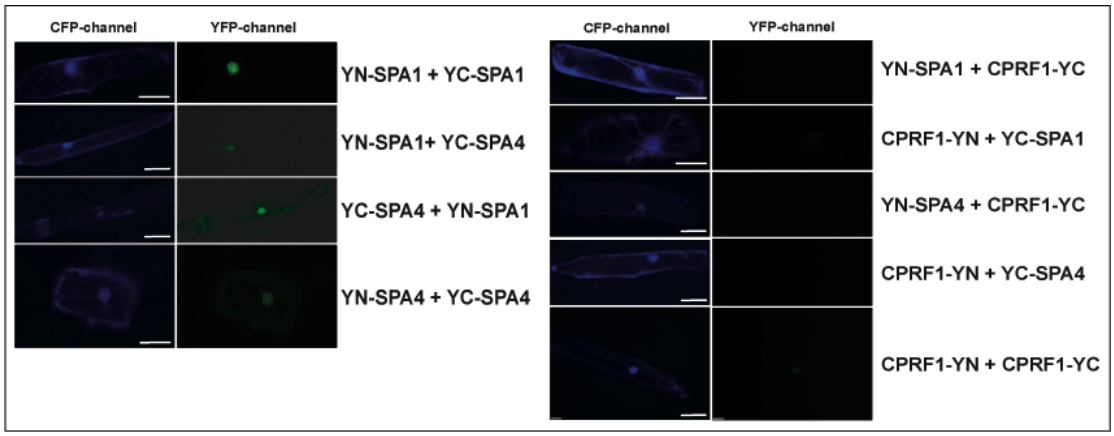

Figure 2.3: SPA1 and SPA4 interact with each other and with themselves using Bimolecular Fluorescence Complementation (BiFC). YN-SPA1, YN-SPA4, YC-SPA1 and YC-SPA4 were transiently expressed in onion (*Allium cepa*) epidermal cells and visualized using fluorescence microscopy (YFP-channel). The YN and YC fusions of the nuclear protein CPRF1 were used as negative controls. The homodimerization of CPRF1 served as positive control. CFP-talin displayed successful transformation (CFP-channel). Bar =100 µm.

II.1.4 SPA proteins co-localize in nuclear speckles

Besides BiFC analysis of SPA-SPA interactions, co-localization studies were performed by co-expressing CFP- and YFP- fusions of SPA proteins in transiently transfected *Arabidopsis* leaf epidermal cells. All constructs were expressed from the *35S CaMV* promoter. As controls the full-length CFP and YFP proteins were co-transfected, respectively.

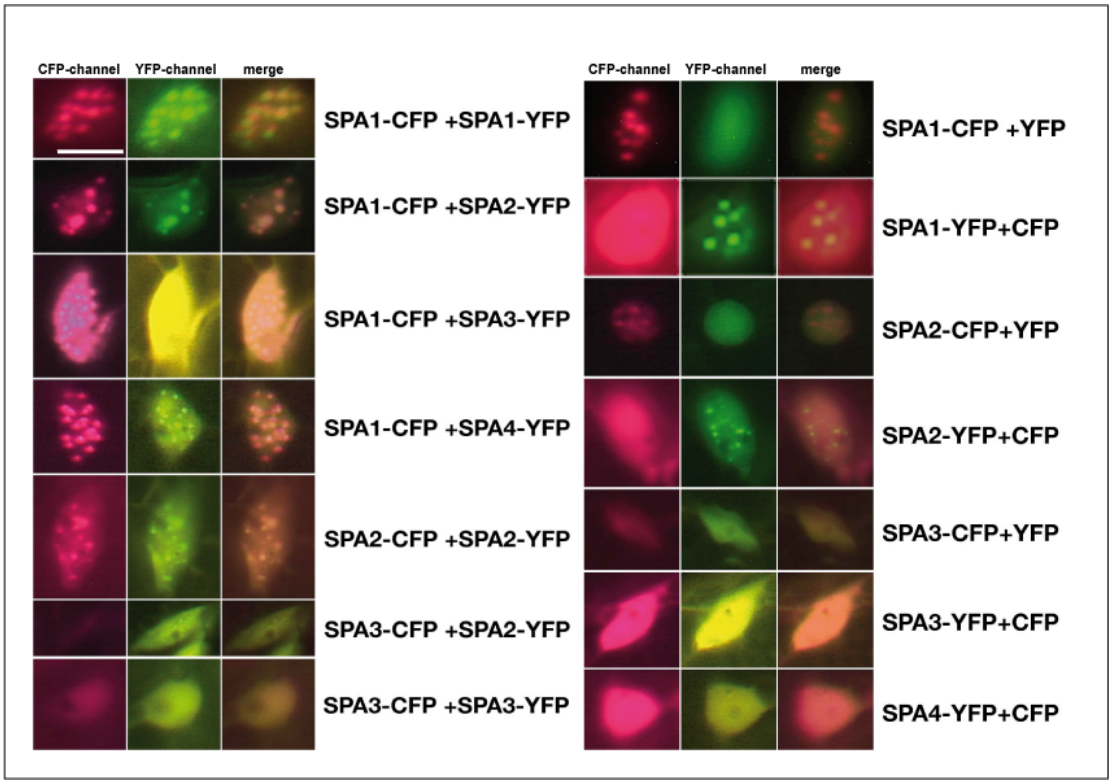

Figure 2.4: SPA proteins co-localize in nuclear speckles. Shown are nuclei from four-day-old white-light-grown *Arabidopsis* leaf epidermal cells. CFP and YFP fusions of SPA proteins were transiently coexpressed and visualized using fluorescence microscopy. Only cases in which cotransfection was successful are shown. CFP and YFP full-length proteins served as negative controls. The magnification is the same in all images. Bar= 10 µm.

CFP-SPA1 co-localized in nuclear speckles with YFP-SPA1, YFP-SPA2 and YFP-SPA4. Interestingly, YFP-SPA4 only accumulated in nuclear speckles when SPA1 was present, indicating that SPA1 can recruit SPA4 into nuclear speckles. CFP-SPA2 co-localized with YFP-SPA2, supporting the notion that SPA2 can interact with itself in the nucleus. In case of the SPA3 fusions no speckles were detected in any case (Figure 2.4).

Taken together, all SPA proteins were able to interact with each other *in vitro*, supporting the notion of homo- and heterodimeric complexes with the

COP1 protein. At least in the case of SPA1, the N-terminus including the coiled-coil domain, mediates the interaction with the SPAs. Interactions of the SPA1-SPA1 homodimer, SPA1-SPA4 heterodimer, and the SPA4-SPA4 homodimer could be confirmed *in planta*. SPA1 and SPA2 as well as SPA2 and SPA2 co-localize in nuclear speckles in *Arabidopsis* leaf epidermal cells. SPA4, which lacks any known NLS sequence, seems to be recruited to nuclear speckles by the SPA1 protein.

II.2 Production of COP1-, SPA1- and SPA2- antibodies

In order to detect endogenous COP1, SPA1 and SPA2 proteins *in vivo,* polyclonal antibodies were generated using either truncated recombinant protein from *E.coli* or artificially designed peptides, in case of SPA2. After purification and processing (in case of COP1) of the recombinant proteins, the samples were sent for immunization.

II.2.1 Production of anti-COP1 antibodies

II.2.1.1 Purification and processing of COP1-915 protein

The first 915 bp of *COP1* cDNA were cloned for expression of a truncated recombinant COP1 protein (COP1-915) in *E.coli* as described under IV.4.12.1. The COP1-915 protein was tagged with a Thioredoxin- (Trx), 6x Histidine- (His_6) and Streptavidin- (S) tag at the N-terminus as well as an additional 6x Histidine- (His_6) tag at the C-terminus (Figure 2.5 A; predicted size of the recombinant protein 57 kDa). As Figure 2.5 B shows, COP1-915 protein was expressed (about 55 kDa) and could be purified via His_6-tag from 500 ml *E.coli* culture, although most of the protein was not bound to the Ni-NTA resin (see flow through). Elution step number 2 in buffer E showed the greatest amount of eluted protein and was therefore used for the following steps. Even though the COP1-915 protein migrated in two bands in the SDS-PAGE, this was of no importance for further analysis and protein production. In order to send the protein for immunization, the multi tagged COP1-915

protein needed to be processed with enterokinase protease to cleave off the tags at the N-terminus. A test digest with 50 µg of dialyzed COP1-915 protein from elution 2 buffer E and 4 µl enterokinase (0.3 µg/µl) digested for one, three, six or 24 hours was performed to determine the size and amount of processed COP1-915 protein (Figure 2.5 C). After 24 hours the digest showed the highest amount of processed protein (about 40 kDa, asterisk, Figure 2.5 C), although about ten-fold of protein was lost during this procedure (data not shown). In addition, the cleaved off tag was visible in the SDS-PAGE (diamond, Figure 2.5 C).

To confirm the processed protein, which still carried a His_6-tag at the C-terminus, an immunoblot using His_6- specific antibodies was performed. The asterisk in Figure 2.5 C marks the processed COP1-915 protein, which is not present in the dialyzed lysate from protein purification used as a control. Processed COP1-915 protein from 500 ml *E.coli* preparative culture was cut out from a preparative gel and sent for immunization as described under IV.4.12.5.

II.2.1.2 Detection of native COP1 protein

For immunization of the processed COP1-915 protein six rabbit preimmune sera obtained from Agrisera AB (Sweden) were screened for unspecific signals at the predicted size of the native *Arabidopsis* COP1 protein (76 kDa). Therefore, Col-0 wild-type protein extracts from white-light-grown seedlings were analyzed with the preimmune sera in immunoblot analysis (data not shown). The rabbits Melker and Niger displayed almost no unspecific signal at the predicted size of endogenous *Arabidopsis* COP1 protein and were selected for immunization. The secondary anti-rabbit antibody also showed no unspecific signals (Figure 2.6 A). After nine months of immunization the rabbits were taken to final bleed. Analysis of the serum from Niger exhibited a specific signal in Col-0 wild-type extracts at the size of COP1 protein that was not present in protein extracts from *cop1-4* mutants (arrow, Figure 2.6 B; *cop1-4* mutants are EMS mutants, Supplemental figure

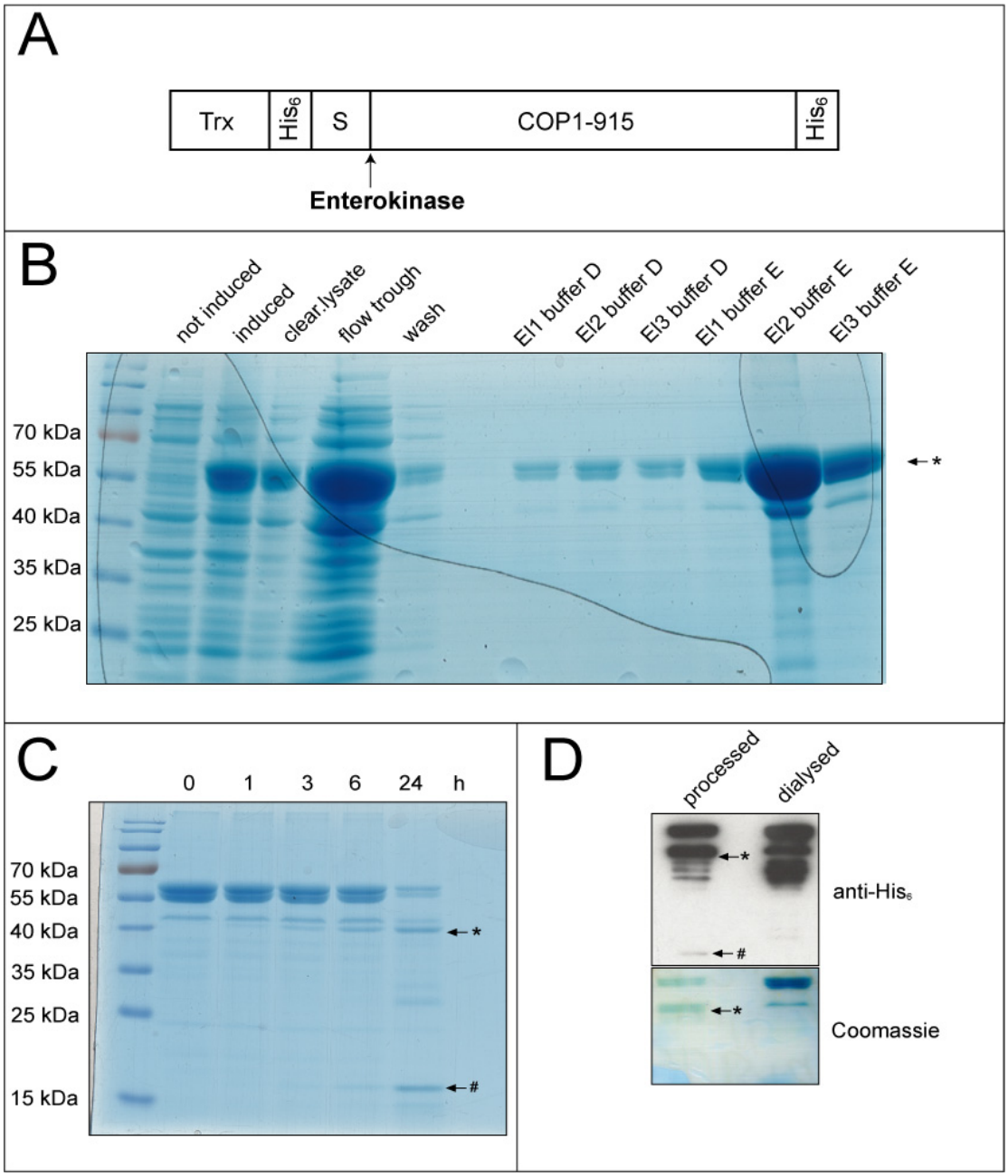

Figure 2.5: Purification of COP1-915 recombinant protein. (A) Thioredoxin- (Trx), 6x Histidine (His_6)-, Streptavidin (S)- tagged COP1-915 protein used for protein purification. (B) Protein purification using Ni-NTA agarose resin from 500 ml *E.coli* culture. 40% of not induced, 20% of induced samples, 100% of the cleared lysate sample, 0.9% of the flow through sample, 0.5% of the pooled wash sample and 7.2% of all elutions were resolved on a 10% SDS-PAGE gel. The gel was stained with Coomassie Brilliant Blue. The asterisk marks the COP1-915 protein. (C) Test digest with enterokinase protease. 50 µg of fusion protein was incubated with 4 µl (0.3 µg/µl) enterokinase for one, three, six or 24 hours. 2.1% of the digested samples each were analyzed on a 12.5% SDS-PAGE gel. The gel was stained with Coomassie Brilliant Blue. The asterisk marks the processed COP1-915 protein. The diamond marks the cleaved off tags. (D) Immunoblot analysis of processed COP1-915 protein. 2 µg of processed and 10 µg of dialysed protein were loaded on a 10% SDS-PAGE gel. The asterisk marks the processed COP1-915 protein. The diamond shows the cleaved off tags. Coomassie staining of the PVDF membrane served as a control.

5.1). In contrast, the serum from Melker showed an unspecific signal in *cop1-4* protein extracts.

Since the immunoblot with the obtained sera featured a lot of unspecific signals, the anti-COP1 antibodies from Melker- and Niger- sera were purified with COP1-915 recombinant protein on PVDF membrane as described under IV.4.12.6. The first elution of the purified serum of Melker displayed a strong reduction of unspecific signal background (Figure 2.6 C). A signal at the size of COP1 was detectable in Col-0 wild-type protein extracts and missing in the protein extracts from *cop1-4* mutant plants (arrow, Figure 2.6 C). Two unspecific signals above and directly under the specific signals that were present in the first elution were no longer detectable in the second elution. The purified antibodies from Niger serum also showed a strong reduction of unspecific signal background. A band occurred at the predicted size of native COP1 protein. No differences between the two elutions of the purified antibodies were detected (Figure 2.6 C).

Purified sera from both rabbits exhibited a specific signal for the truncated COP1-4 protein at the size of about 35 kDa (asterisk, Figure 2.6 C), which is in agreement with Mc Nellis et al. (1994). The second elution of purified antibodies from Melker serum was also tested with a second *cop1* mutant allele, *cop1-6*. No signal at the size of native COP1 was detected in protein extracts from *cop1-6* mutants (arrow, Figure 2.6 D). However, this is contradictory to Mc Nellis et al. (1994), since they stated that COP1 protein of wild-type size and abundance accumulates in *cop1-6* mutants. The *cop1-6* mutation changes the splicing junction “AG” at the 3’ end of intron 4 to “GG” and leads to three principal cryptically spliced mRNA transcripts (Transcripts 1-3) and a transcript with an unspliced intron (Transcript 4). Transcript 2 produces a protein with five novel amino acids inserted in frame between Glu-301 and Phe-302 of the wild-type protein and is hypothesized to be the accumulating protein reported by Mc Nellis et al. (1994) (Supplemental figure 5.1).

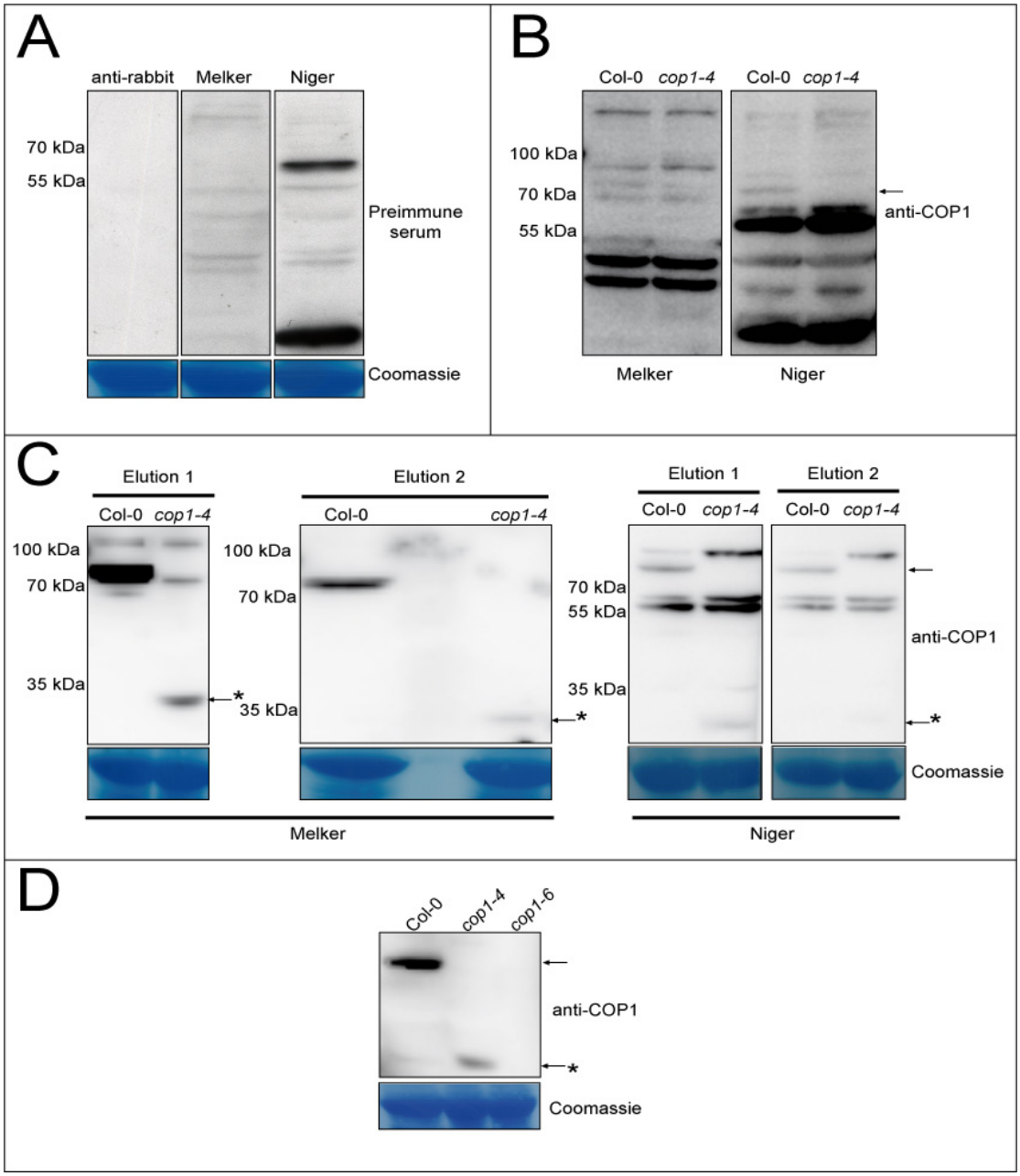

Figure 2.6: Detection of native COP1 protein in *Arabidopsis* plant cell extracts. (A, B) Preimmune sera test and immunoblot analysis of the immunized sera (B) from the rabbits Melker and Niger. 30 µg of total protein from 4 day-old white-light-grown Col-0 and *cop1-4* seedlings were analyzed by immunoblot analysis following SDS-PAGE. Preimmune sera and immunized sera were diluted 1:1000 in 1x TBS containing 3% non-fat-dried milk powder. Coomassie staining of the PVDF membrane served as loading control. (C) Purification of COP1 antibodies using PVDF membrane. 30 µg of total protein from white-light-grown Col-0 and *cop1-4* seedlings were analyzed by immunoblot following SDS-PAGE. The antibody elutions were diluted 1:500 in 1x TBS containing 3% non-fat-dried milk powder. Coomassie staining of the PVDF membrane served as loading control. (D) Detection of native COP1 protein with purified antibodies (second elution) from the serum of Melker including the *cop1-6* mutant. 30 µg of total protein from white-light-grown Col-0, *cop1-4 and cop1-6* seedlings were separated by SDS-PAGE and analyzed by immunoblot analysis. The antibody elution was diluted 1:300 in 1x TBS containing 3% non-fat-dried milk powder. Coomassie staining of the PVDF membrane served as loading control.

II.2.2 Production of anti-SPA1 antibodies

II.2.2.1 Purification of SPA1 recombinant protein

The first 570 bp of the *SPA1* cDNA were cloned for expression of a recombinant truncated version of the SPA1 protein (SPA1-570) as described under IV.4.12.1. The protein was tagged with a 6x His- (His_6) tag in the N-terminus (predicted size of the recombinant protein 27 kDa). As Figure 2.7 A shows, the protein could be expressed (asterisk, about 30 kDa) in 50 ml *E.coli* culture, although the amount of protein was very low. Several modifications in the expression system (variation of induction period and temperature) were performed to increase the amount of recombinant protein without any success (data not shown). Nevertheless, SPA1-570 protein could be enriched from 500 ml of *E.coli* culture by purification using Ni-NTA agarose resin (asterisk, Figure 2.7 B). The greatest amount of protein could be obtained from elution 2 in buffer E, which was then used for purification of the protein from large preparative cultures.

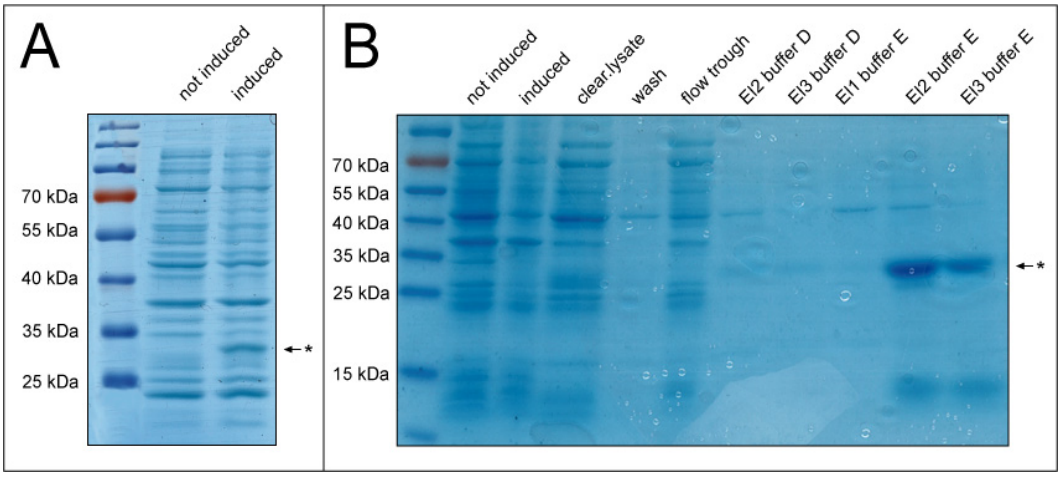

Figure 2.7: Expression and purification of His_6-tagged SPA1-570 recombinant protein. (A) Expression of SPA1-570 protein. 40% of induced and 20% of not induced samples were separated on a 10%SDS-PAGE gel. The gel was stained with Coomassie Brilliant Blue. The asterisk marks the SPA1-570 protein. (B) Purification of SPA1-570 protein using Ni-NTA resin. 40% of induced and 20% of not induced samples, 100% of the cleared lysate sample, 0.9% of the flow through sample, 0.5% of the pooled wash sample and 7.2% of all the elutions were resolved by a 12.5% SDS-PAGE gel. The gel was stained with Coomassie Brilliant Blue. The asterisk marks the SPA1-570 protein.

II.2.2.1 Detection of native SPA1 protein in *Arabidopsis* plant extracts

24 preimmune sera obtained from Agrisera AB (Sweden) were screened for unspecific signals. The rabbits Tracy and Velmer showed low unspecific signal at the predicted size of native SPA1 protein (115 kDa). The secondary anti-rabbit antibody alone also displayed no specific signal (Figure 2.8 A). After seven month of immunization with SPA1-570 recombinant protein, sera from the final-bleed of Tracy and Velmer were tested on Col-0 wild type, *spa1-3* mutant, *spa1-7* mutant and *SPA1::SPA1-HA* plant cell extracts. *spa1-3* is an EMS mutant in RLD background, whereas *spa1-7* is a T-DNA insertion mutant in Col-0 background (see Supplemental figure 5.1). *SPA1::SPA1-HA* seedlings express SPA1 protein C-terminally fused to an HA tag under the control of its own promoter in *spa1-3* mutant background (Fittinghoff et al., 2006).

No signal was visible at the size of native SPA1 protein using the sera from the final bleed. In contrast, the background of unspecific signals was increased compared to before immunization (Figure 2.8 B). Since no signal could be detected, the antibodies from both rabbits were purified using the His_6-tagged SPA1-570 as an antigen and PVDF membranes. As Figure 2.8 C shows, the purified antibodies in elutions one and two from the serum of Tracy exhibited no signal for native SPA1. Elution number one from Velmer, however, showed a specific signal at about 130 kDa (asterisk), that was lacking in the mutant and increased in *SPA1:SPA1-HA* plant extracts. In agreement with Zhu et al. (2008), the signal occurred as a double band and is designated to be native SPA1. Using the second elution only the signal from *SPA1:SPA1-HA* plant extracts was detectable, indicating that SPA1 antibodies were eluted mainly in the first elution. Since *spa1-3* mutant and *SPA1:SPA1-HA* plants are in the RLD background, an immunoblot using the first elution of purified antibodies from Velmer serum with RLD wild-type plant protein extracts was performed. The immunoblot showed also a specific signal for native SPA1 in RLD wild-type plants. Again, no signal was detected in *spa1-3* and *spa1-7* protein extracts (Figure 2.8 D).

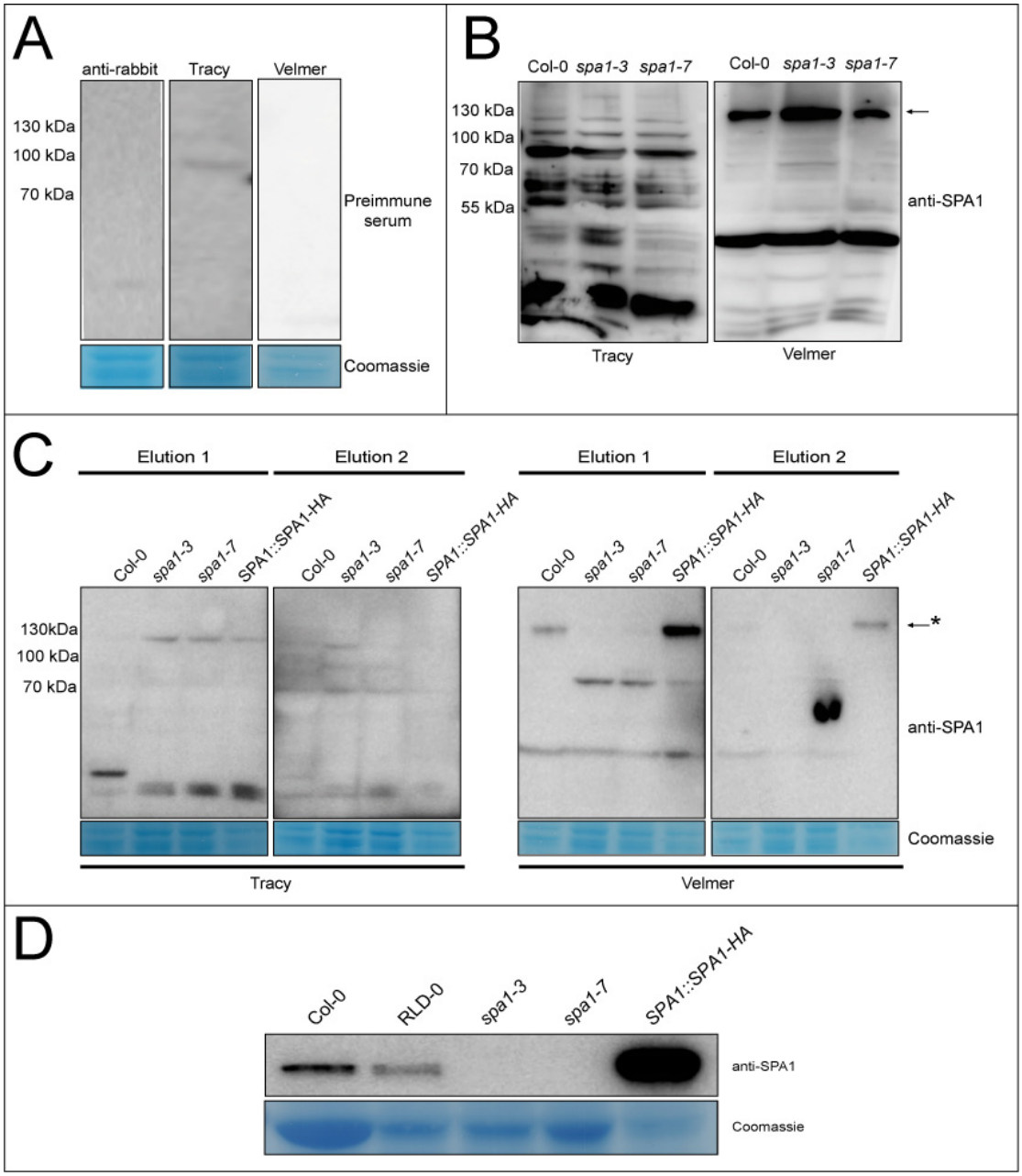

Figure 2.8: Detection of native SPA1 protein. (A,B) Test of preimmune sera and sera after immunization from the rabbits Tracy and Velmer. 30 µg total protein of Col-0 wild-type, *spa1-3* and *spa1-7* mutants seedlings grown on 1x MS plates for 4 days in darkness transferred for two hours to 30 µmol m^{-2} s^{-1} red light were analyzed by immunoblot followed by SDS-PAGE. The sera each were diluted 1:1000 in A and 1:500 in B in 1x TBS containing 3% non-fat-dried milk powder. The secondary anti-rabbit antibody was diluted as described under 2.10. Coomassie staining served as loading control. (C) Purification of anti-SPA1 antibodies. 30 µg total protein of Col-0, *spa1-3*, *spa1-7* and *SPA1::SPA1-HA* seedlings grown as described in A were separated by SDS-PAGE and analyzed using immunoblot. The elutions were diluted 1:300 in 1x TBS containing 3% non-fat-dried milk powder**.** Coomassie staining served as loading control. (D) Immunoblot including protein extracts from RLD wild type. 30 µg of total protein were analyzed by SDS-PAGE and subsequent immunoblotting. Col-0 wild-type plants and *spa1-7* mutant were grown for 4 days on 1x MS plates in white light, whereas RLD, *spa1-3* and *SPA1::SPA1-HA* plants were grown as described in A. The first elution of Velmer was diluted 1:300 in 1x TBS containing 3% non-fat-dried milk powder. Coomassie staining of the PVDF membrane served as loading control.

II.2.3 Production of anti-SPA2 antibodies

For production of anti-SPA2 antibodies two synthetic peptide sequences (amino acid 22-35 and 349-359) that are unique for SPA2 among the SPA protein family were designed (performed by Agrisera AB, Sweden). Peptide sequences were confirmed to be unique using the BLAST algorithm (data not

MMDEGSVGDVSRIDEADVAHLQFKNSEQSFKPENIEVREVKEVQVQREAGSPDCSYGVIADFLDGKNGGDH
VELIGNEPCSSRQNTNDEGDVVEELTVKTCEGSSMAIVGRPSSRARLEMNRSQFLHRFPLDGDLPGSSSMSK
KVIDRGTVSILRNAGKMSLPETSNGQLAIIAVNGEANEHLTNVERNPVPVEALSHEGIKTKMLSQSGFSQFFVR
KTLKGKGVTFRGPPNNRSKARNMDQQTVASSGSALVIANTSAKISSSIPLAAYDDTHRGCGGEGLSLREWLK
SERQEVNKAECMYIFRQIVDHVDCSHSQGVVLCDLRPSSFKIFKENAVKYVVSGSQRESFDSNMNKETLSQL
ENPLVRRRLGDTSSLSIPAKKQKSSGPSSRQWPMFQRAGGVNIQTENNDGAIQEFHFRSSQPHCSTVACPFT
SVSEQLEEKWYASPEELRGDMRSASSNIYSLGILLYELLSQFQCERAREAAMSDIRHRILPPKFLSENPKEAGF
CLWLLHPESSCRPSTRDILQSEVVNGIPDLYAEGLSLSIEQEDTESELLQHFLFLSQEKRQKHAGNLMEEIASV
EADIEEIVKRRCAIGPPSLEEASSSSPASSVPEMRLIRNINQLESAYFAARIDAHLPEARYRLRPDRDLLRNSDN
TVAEVENSETWSSDDRVGAFFDGLCKYARYSKFETRGVLRTSELNNTSNVICSLGFDRDEDYFATAGVSKKIKI
YEFNSLFNESVDIHYPAIEMPNRSKLSGVCWNNYIRNYLASSDYDGIVKLWDVTTGQAISHFIEHEKRAWSVDF
SEACPTKLASGSDDCSVKLWNINERNCLGTIRNIANVCCVQFSPQSSHLLAFGSSDFRTYCYDLRNLRTPWCI
LSGHNKAVSYAKFLDNETLVTASTDNTLKLWDLKKTTHGGLSTNACSLTFGGHTNEKNFVGLSTSDGYIACGS
ETNEVYAYHRSLPMPITSYKFGSIDPISGKEIEEDNNLFVSSVCWRKRSNMVVSASSNGSIKVLQLV*

Figure 2.9: Amino acid sequence of SPA2 protein. Highlighted in red are the two peptides used for immunization (QFKNSEQSFKPENI) 22-35 and (SFDSNMNKETL) 348-358. The kinase-like domain of SPA2 is underlined. The coil-coil domain is highlighted in yellow. The WD40-repeat domain in the C-terminus is highlighted in green.

shown). Preimmune sera from twelve rabbits were screened for unspecific signals at the predicted size of native *Arabidopsis* SPA2 protein (115 kDa). Since all rabbits tested displayed unspecific signals at this size, sera from the rabbits Rex and Ogert were selected, that exhibited the weakest unspecific signals at the size of interest. No signal was detected using the secondary anti-rabbit antibody (Figure 2.10 A). After six months of immunization of each rabbit with both peptides no specific signal of SPA2 could be detected in immunoblot analysis using protein extracts from Col-0 wild type and *spa2-2* mutant seedlings (Figure 2.10 B; *spa2-2* carries a T-DNA insertion 1331 bp downstream from the initial ATG of the *SPA2* gene; Supplemental figure 5.1). In order to reduce the strong background that may hide a specific SPA2 signal, the antibodies were purified. Sera from both rabbits were mixed and purified using each peptide separately (performed at Agrisera AB, Sweden). After purification immunoblot analysis was performed. In this regard, protein extracts from Col-0 wild type, *spa2-1* mutant (T-DNA insertion mutant;

Supplemental figure 5.1), *spa2-2* mutant and *35S::GUS-SPA2* transgenic plants (N-terminal GUS fusion of SPA2 protein driven by *35S CaMV* promoter in *spa1spa2* double mutant background) were analyzed. In case of detection with the 22-35 peptide, a signal at 130 kDa could be detected in Col-0 wild-type protein extracts. However, this signal and/or a weak background signal of the same size were also observed in protein extracts from *spa2-1*, *spa2-2* and *35::GUS-SPA2* plants. The GUS-SPA2 fusion protein was also detected, migrating much slower than endogenous SPA2 as it is expected to have a size of approximately 170 kDa. In the case of the 348-358 peptide, signals at the predicted size of SPA2 protein could be also detected, but they were also present in the protein extracts from the mutants. The GUS-SPA2 fusion protein was not detected (Figure 2.10 C)

Since repetition and modification of the experiments did not provide a reliable result using anti-SPA2 antibodies, nuclei were isolated to enrich samples for SPA2 protein and to reduce the background caused by the cross-reaction with cytosolic proteins. As the asterisk in Figure 2.10 D shows, native SPA2 could be detected in protein extracts of Col-0 and *35S::GUS-SPA2* plants from nuclei-enriched fractions at a size of about 130 kDa. Since GUS-SPA2 as a fusion protein is supposed to have a higher molecular size, the signal at size of native SPA2 in *35S::GUS-SPA2* protein extracts must be a truncated version of SPA2 maybe lacking the GUS protein. Since *35S::GUS-SPA2* fusions are in *spa1spa2* mutant background and SPA3 and SPA4 are of smaller size the detected signal was not likely due to cross-reaction. Even the truncated, faster migrating SPA2-1 protein resulting from the *spa2-1* mutation as described by Zhu et al. (2008) was detectable (diamond, Figure 2.10 D). The *spa2-2* mutant did not exhibit a signal for native SPA2 protein.

Taken together it was possible to generate antibodies against endogenous COP1, SPA1 and SPA2 proteins from *Arabidopsis*. The designation of the sera and purified antibody solutions as well as antigens, dilutions and protein isolation methods used for the detection of the proteins are given in Table 2.1. Since all antibodies were generated in rabbit, the secondary antibody is goat-anti-rabbit (IV.1.10).

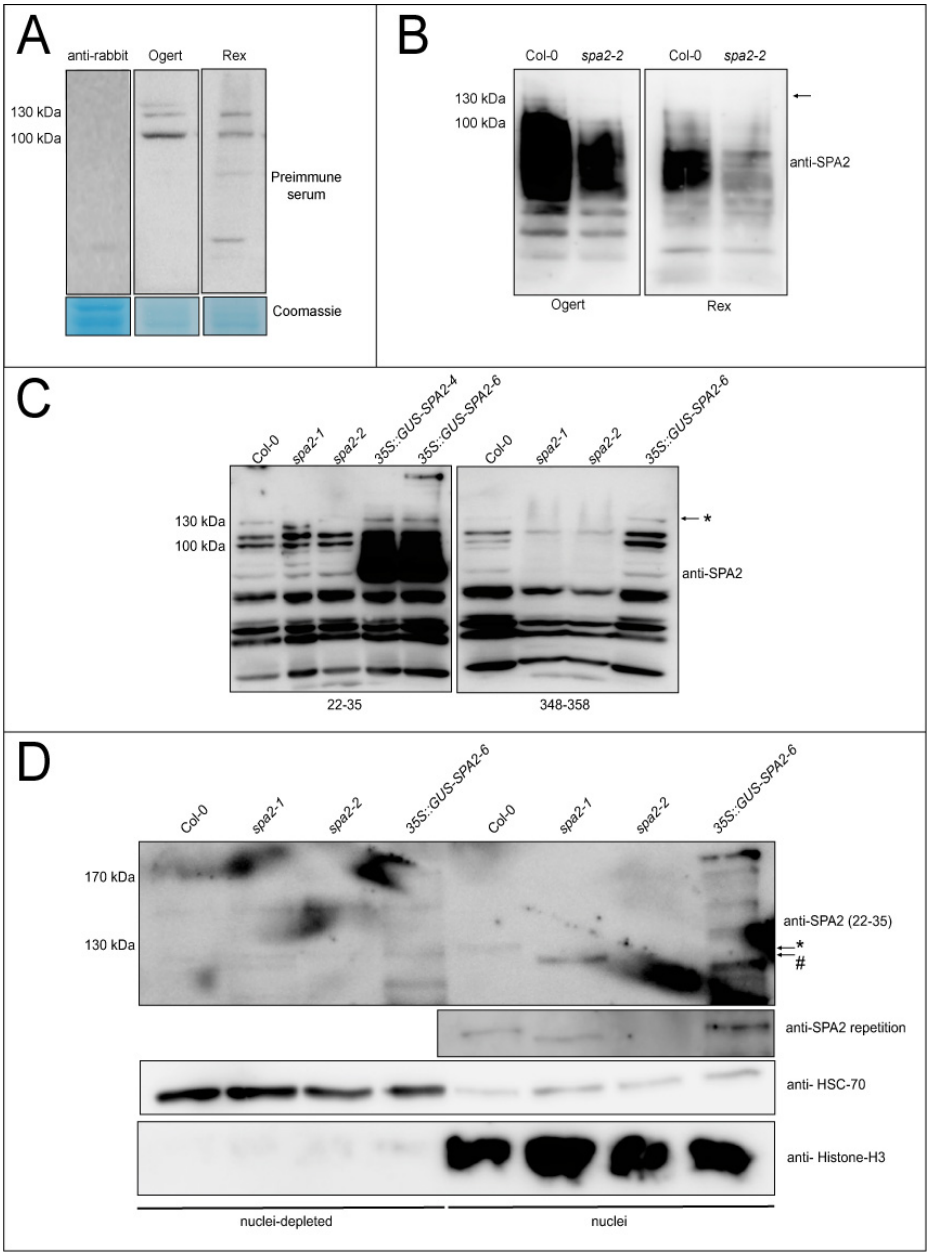

Figure 2.10: Production of anti-SPA2 antibodies. (A,B) Test of preimmune sera and sera after final bleed from the rabbits Rex and Ogert. 30 µg of total protein from Col-0 wild type and *spa2-2* mutant plants grown for 4 days in darkness were analyzed by immunoblot following SDS-PAGE. The sera were diluted 1:1000 in 1x TBS containing 3% non-fat-dried milk powder. Coomassie staining served as loading control. Arrow indicates predicted size of SPA2 (C) Analysis of anti-SPA2 antibodies from the purification with peptide 22-35 and peptide 348-358. 30 µg of total protein from Col-0 wild-type, *spa2-1*, *spa2-2* mutant and *35S::GUS-SPA2* plants (line 4 and 6) grown for 4 days in darkness were analyzed by Immunoblot following SDS-PAGE. Asterisk marks predicted size of native SPA2 protein. Purified antibodies from the sera were diluted 1:300 in 1x TBS containing 3% non-fat-dried milk powder (D) Nuclei preparations using the purified anti-SPA2 antibodies from peptide 22-35. Col-0 wild-type, *spa2-1* mutant, *spa2-2* mutant and *35S::GUS-SPA2* transgenic seedlings were grown as described under Figure A. 16% of nuclei depleted and 25% of nuclei-enriched samples were analyzed by immunoblot subsequent to SDS-PAGE. Asterisk marks the predicted size of native SPA2 protein. The diamond marks the faster migrating SPA2-1 protein. The blot was technically repeated once (anti-SPA2 repetition). Purified antibodies from the sera were diluted 1:300 in 1x TBS containing 3% non-fat-dried milk powder. Anti-HSC-70 served as cytosolic- and anti-Histone-H3 as nuclear- marker.

Table 2.1: Antibodies generated against native COP1, SPA1 and SPA2

Antibody	Antigen	Description	Dilution	Method
anti-COP1 Niger	COP1-915	Serum from Niger	1:1000 in 1x TBS containing 3% non-fat-dried milk powder	Total protein extraction (IV.4.1)
anti-COP1 2EL Melker	COP1-915	Purified: second elution /serum of Melker	1:300 in 1x TBS containing 3% non-fat-dried milk powder	Total protein extraction (IV.4.1)
anti-SPA1 1EL Velmer	SPA1-570	Purified: first elution / serum of Velmer	1:300 in 1x TBS containing 3% non-fat-dried milk powder	Total protein extraction (IV.4.1)
anti-SPA2 (22-35)	QFKNSEQSFKPENI peptide	Sera purified with 22-35 peptide	1:300 in 1x TBS containing 3% non-fat-dried milk powder	Nuclear protein extraction (IV.4.3)

II.2.4 *in vivo* CoIP of SPA1-HA and native COP1 protein using COP1-specific antibodies

SPA1 is known to interact with the E3-ubiquitin ligase COP1 *in vitro* and *in vivo* (Hoecker and Quail, 2001; Saijo et al., 2003; Seo et al., 2003; Saijo et al., 2008). CoIP studies from *Arabidopsis* seedling extracts with HA-tagged SPA1 protein from *SPA1::SPA1-HA* plants as a bait were performed (see IV.4.8) and bound endogenous COP1 protein was detected using anti-COP1 antibodies that were generated in this study. In order to increase the amount of SPA1-HA protein, which is under the control of its native promoter, the plants were grown for four days in darkness and then transferred to red light as described by Fittinghoff et al. (2006). As the comparison between input and supernatant fraction in Figure 2.11 shows, SPA1-HA protein could be precipitated efficiently from plant cell extracts using an anti-HA Affinity Matrix, although the amount of SPA1-HA in the pellet was very low. Nevertheless, native COP1 protein could be detected in the input, supernatant and pellet samples, whereas the samples from *cop1-4* mutants did not exhibit any specific COP1 signal.

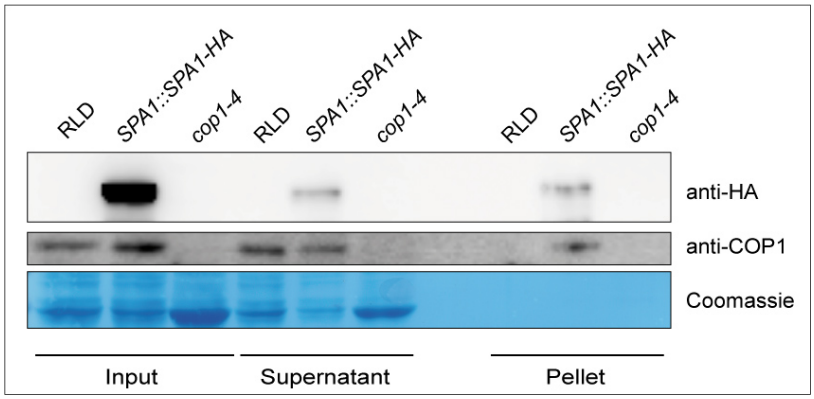

Figure 2.11: *In vivo* CoIP using HA-tagged SPA1 protein and anti-COP1 antibodies. 30 µg of total protein of input and the same volume of supernatant samples from RLD, *SPA1::SPA1-HA* and *cop1-4* protein extracts from 4 day-old seedlings were analyzed by Immunoblot following SDS-PAGE. 50% of the pellet samples were analyzed. The Immunoblot was incubated with HA- and COP1- specific antibodies. Coomassie staining served as loading control.

II.2.5 Endogenous SPA1 and SPA2 protein levels are reduced under far-red light

COP1 and SPA proteins were found to repress photomorphogenesis in dark- and light-grown seedlings together. Genetic analysis revealed that the four members of the *SPA* gene family have overlapping but also distinct functions throughout development. Thus, the *SPA1* and *SPA2* genes differ in their function in light-grown seedlings and adult plants but not in dark grown seedlings. While both genes can cause full suppression of photomorphogenesis in dark-grown seedlings, only SPA1 is inhibiting light signaling also in light-grown seedlings. SPA2 loses its function when seedlings grown in darkness are exposed to even very low fluences of light. (Laubinger et al., 2004). It seems to be unlikely that the different expression of *SPA* mRNAs is the only reason for distinct function of SPA1 and SPA2 (Fittinghoff et al., 2006). Alternative hypotheses are differences in SPA1 and SPA2 protein levels or varying activities of COP1/SPA1 and COP1/SPA2 complexes. Post-translational regulation, interactions with the photoreceptors and/or exclusion of COP1 from the nucleus upon light exposure are possible mechanisms, which could explain inhibition of COP1/SPA function. However, an exclusion of COP1 from the nucleus requires at least 24 h of light exposure and is therefore only a long-term response (von Arnim and Deng, 1994),

further supporting the existence of faster mechanisms regulating COP1/SPA function. Due to the fact that the difference of *SPA1* and *SPA2* function is only uncovered in light, it is likely that their function varies especially in the light-induced inactivation of COP1/SPA complexes.

In order to analyze potential differences in SPA1 and SPA2 protein abundance, four-day-old seedlings grown in darkness or continuous far-red light were analyzed by immunoblot using SPA1- and SPA2-specific antibodies. As Figures 2.12 A and D show, SPA1 protein levels from wild-type seedlings were slightly reduced when grown in continuous far-red light compared to darkness, although the transcript levels of *SPA1* were far-red-light-induced (Figure 2.12 C). In contrast, SPA2 protein levels were strongly reduced in far-red-light-grown wild type compared to dark-grown seedlings, whereas the transcript levels were not affected (Figure 2.12 D, E and F). This points to a post-translational regulation of SPA1 and SPA2 protein by light. Since SPA proteins are stabilized in *cop1* mutants (Zhu et al., 2008) and SPA1 and SPA2 can be stabilized by the application of the proteasome inhibitor MG132 (Balcerowicz et al., 2011), I tested whether there are differences in the stabilization of SPA1 and SPA2 protein in darkness and continuous far-red light in *cop1-4* mutants compared to wild type. A stronger stabilization in *cop1-4* mutants would imply that COP1/SPA complexes promote autoubiquitination of SPA1 and SPA2 protein, and would therefore point to a COP1-dependent regulation of SPA protein abundance. As Figure 2.12 shows, the amount of SPA1 and SPA2 protein was elevated in dark- and far-red-light-grown *cop1-4* mutants in comparison to wild type grown under same conditions, which is in agreement with Zhu et al. (2008). Nevertheless, the difference in protein levels observed between darkness and far-red light showed the same fold change of SPA1 protein levels like in wild type, indicating no influence of COP1 on far-red-light-dependent protein stabilization of SPA1 under the conditions tested. However, the standard error was very high in two experiments and this needs to be verified in additional experiments. For SPA2 a slighter reduction could be observed in in *cop1-4* mutants compared to wild type (2 fold in *cop1-4* mutants compared to 4 fold in wild type). The transcript levels of *SPA1* and *SPA2* in *cop1-4* mutants displayed no differences in darkness compared to far-red light (slight increase

for *SPA2* transcript levels). Interestingly, the far-red-light-dependent induction of *SPA1* transcript was not detected in *cop1-4* mutants.

Taken together, my results point to a post-translational effect of light on SPA1 and SPA2 protein abundance. However, a COP1 regulatory effect on SPA1 and SPA2 protein levels in light regulation needs to be verified.

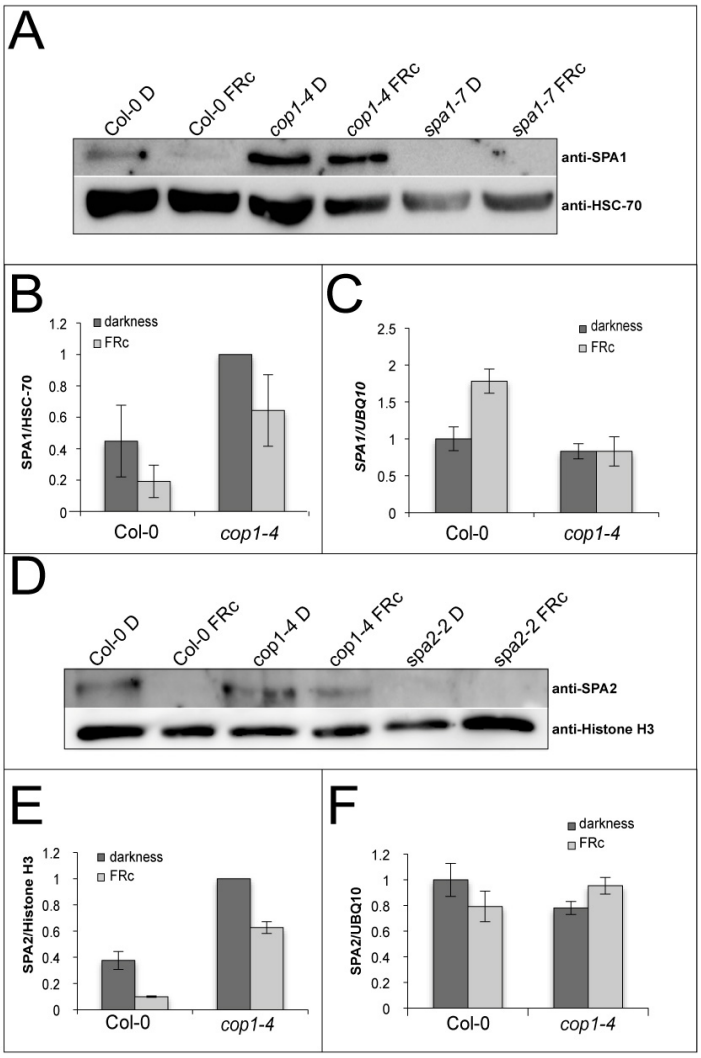

Figure 2.12: Endogenous SPA1 and SPA2 protein levels in dark- and light-grown seedlings. (A, D) Immunoblot analysis of endogenous SPA1 and SPA2 protein levels in Col-0 wild type and *cop1-4* mutant plants using anti-SPA1 and anti-SPA2 antibodies. 30 µg of total protein for immunodetection of SPA1 and 25% of nuclei samples from nuclei-enriched fractions for SPA2 immunoblot were analyzed. Seedlings were grown for 4 days in darkness (D) and 0.35 µmol m^{-2} s^{-1} far red light (FRc), respectively. HSC-70 protein levels in case of SPA1 and Histone-H3 protein levels in case of SPA2 served as loading controls. (B, E) Quantification of SPA1 and SPA2 protein levels relative to HSC-70 or Histone-H3 levels, respectively. Two biological replicates were analyzed. SPA1/HSC-70 and SPA2/Histone-H3 levels from *cop1-4* mutants grown in darkness were set to 1. Error bars indicate the standard error of the mean. (C, F) Transcript levels of *SPA1* and *SPA2* relative to *UBQ10* in RNA extracts from Col wild-type and *cop1-4* mutant seedlings used in (A) and (D). Error bars indicate the standard error of the mean.

II.3 New targets proteins for the COP1/SPA complex involved in anthocyanin biosynthesis

SPA proteins can build complexes with the COP1 protein that cause degradation of downstream targets. This seems to be a major way of integrating signals in *Arabidopsis* light signaling. I analyzed two new potential targets of COP1/SPA complexes, PAP1 and PAP2, which are involved in anthocyanin biosynthesis. Since COP1/SPA complexes repress photomorphogenesis-promoting factors in darkness by targeting them for degradation, they might act in a similar way on PAP1 and PAP2, providing an additional mechanism for the rapid regulation of these factors.

II.3.1 *cop1-* and *spa-* mutants exhibit increased amounts of anthocyanin in darkness and white light

At the seedling stage *cop1* and *spa* mutants accumulate higher levels of anthocyanin in darkness and light in comparison to wild type. The anthocyanin contents of *spa* triple and quadruple mutants are pointing to a redundant effect. Enhanced anthocyanin accumulation in a single *spa* mutant is not detectable, but it can be observed in double and triple mutants (Deng et al., 1991; Baumgardt et al., 2002; Laubinger et al., 2004; Figure 2.13 A). The transcription factor HY5, which is necessary for a broad spectrum of light responses is also known to promote anthocyanin biosynthesis in light. Mutants of HY5 exhibit aberrant light-mediated phenotypes, including increased hypocotyl elongation, reduced chlorophyll accumulation and reduced anthocyanin accumulation (Holm et al., 2002; Oyama et al., 1997; Figure 2.13 B). As described before, HY5 is known to be a substrate for the COP1/SPA complex. To test whether high anthocyanin accumulation in *cop1* mutants is exclusively due to hyperaccumulation of HY5 protein, a *cop1-4 hy5-215* double mutant was examined for anthocyanin content. Since the anthocyanin levels in *cop1-4 hy5-215* double mutants in light and darkness are similar to wild type, whereas the *hy-5-215* single mutant exhibits nearly no anthocyanin, other factors influenced by COP1-activity in addition to HY5

must be involved in the COP1-dependent regulation of anthocyanin biosynthesis at the seedling stage (Figure 2.13 B). COP1 as an E3-ubiquitin ligase could thereby take direct influence on the post-translational level or indirect influence on the transcriptional level of those factors.

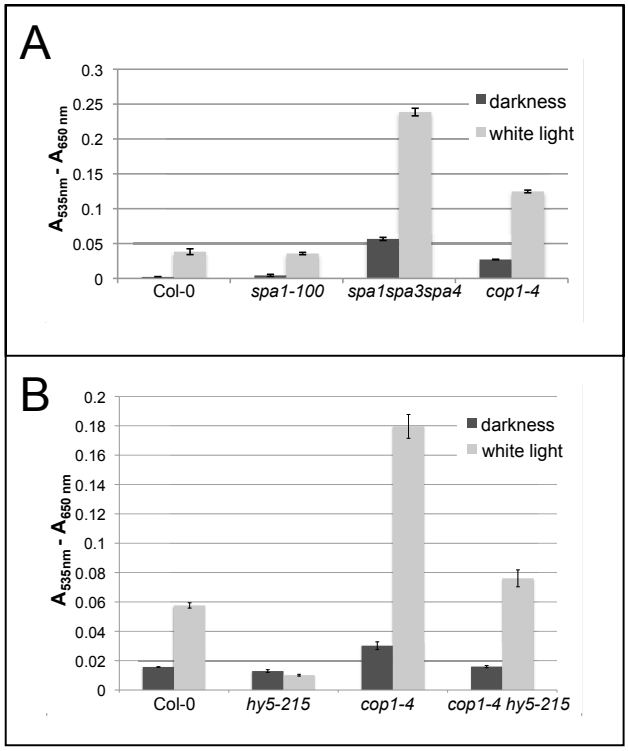

Figure 2.13: Anthocyanin content in dark- and light- grown mutants defective in photomorphogenesis. (A, B) Three times 40 seeds of *spa1-100*, *spa1spa3spa4, hy5-215, cop1-4 hy5-215* and *cop1-4* mutants were grown for 4 days in darkness or 40 µmol m^{-2} s^{-1} white light on 1x MS plates containing 1% sucrose. Error bars indicate the standard error of the mean.

II.3.2 *PAP* proteins interact with COP1 and SPA proteins in Yeast Two-Hybrid analysis

A Yeast Two-Hybrid screen with a transcription factor library obtained from Franziska Turcks laboratory (MPIZ, Cologne, Germany) using SPA1, SPA4 and COP1 as bait proteins revealed PAP1 and PAP2 as new potential interactors of COP1/SPA complexes (Falke, 2008; L. Kokkelink, G. Fiene and U. Hoecker, unpublished). As Figure 2.14 shows, the interactions could be verified by direct Yeast Two-Hybrid analysis using the *HIS3* reporter gene. PAP1 was found to interact with SPA1, SPA3 and SPA4 on selective media,

whereas PAP2 was found to interact with SPA1, SPA4 and COP1. SPA2 showed autoactivation in the negative control. On selective media containing 5 mM 3-AT the interaction of SPA1 with PAP1 was suppressed indicating PAP1-association with SPA3 and SPA4 to be stronger. The interaction of SPA1 and PAP2 showed also a reduction. On plates containing 10 mM and

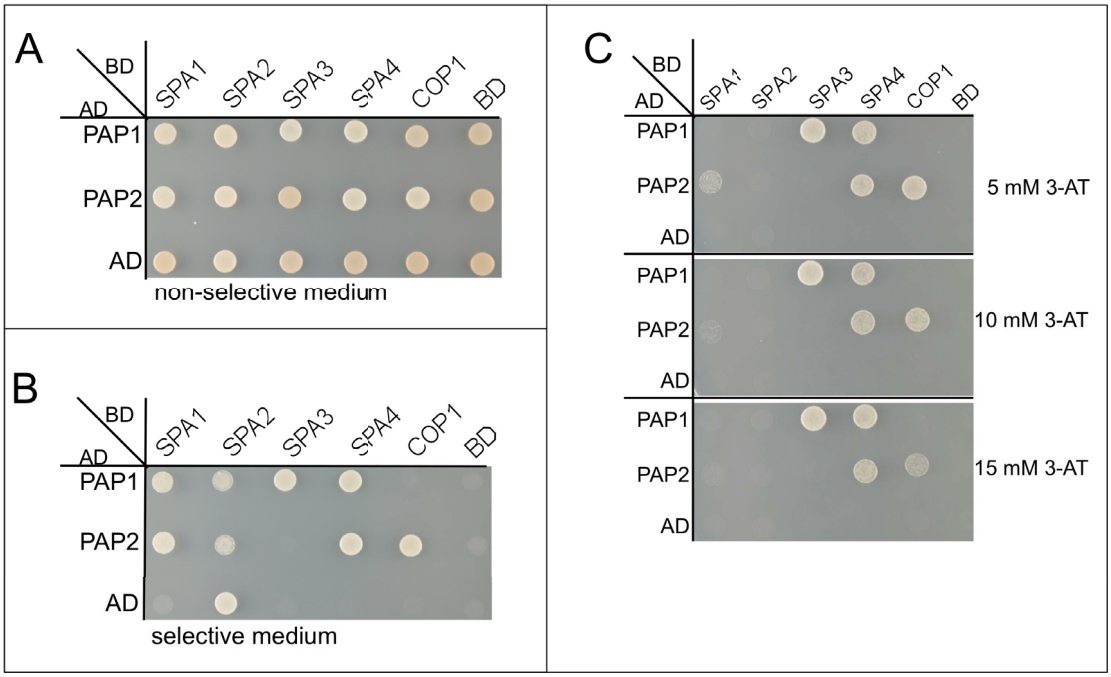

Figure 2.14: PAP1 and PAP2 interact with members of COP1/SPA complexes in Yeast Two-Hybrid analysis. (A) Transformation control of tested COP1- and SPA- interactions with PAP1 and PAP2 on non-selective media (-Leu –Trp). SPA proteins and the COP1 protein are expressed fused to GAL4-binding domain (BD). PAP1 and PAP2 were expressed fused to GAL4-activation domain (AD). Empty vectors expressing BD and AD served as controls. (B) Interactions of COP1 and SPA proteins with PAP1 and PAP2 on selective media lacking Histidine (-Leu –Trp –His). (C) Interaction of COP1- and SPA- proteins with PAP1 and PAP2 on selective media using 3-AT as an inhibitor of autoactivation.

15 mM 3-AT, the interactions of SPA3, SPA4 with PAP1 and SPA4 with COP1 were still visible, whereas the interaction of PAP2 with SPA1 was not detectable any longer. SPA3 and SPA4 together with PAP1 and SPA4 and COP1 together with PAP2 showed therefore the strongest affinity to each other in yeast. Since SPA2 autoactivation and interactions were not detectable on plates containing 5 mM 3-AT compared to the selective media plates, potential interactions with the SPA2 protein could not be determined.

II.3.3 Overexpression of *PAP1* and *PAP2* results in increased anthocyanin contents in darkness and white light

Since it is known that *PAP1* and *PAP2* transcript abundance is regulated by light in seedlings and adult plants (Schmid et al., 2005; Cominelli et al., 2008) and PAP proteins interact with the members of COP1/SPA complexes, I investigated the general effect of light on PAP1 and PAP2 protein levels. In this regard, I created transgenic *Arabidopsis* plants that overexpress *PAP1* and *PAP2* cDNA, respectively. Activation-tagged *pap1-D* plants, which are expressing the endogenous *PAP1* under the control of four enhancer elements from *CaMV 35S* promoter, were also employed for these experiments (Borevitz et al., 2000).

For the generation of overexpressing plants, N-terminal HA-tagged fusions of PAP1 and PAP2 were expressed from a single *CaMV 35S* promoter in Col-0 wild-type plants. Additionally, PAP1 was expressed from the *CaMV 35S* promoter fused to an N-terminal *AcV5*-tag in Col-0 background, and from the *CaMV 35S* promoter without a tag in Col-0 background. Seeds from these overexpressing plants exhibited a strong accumulation of anthocyanin in light as previously reported (Borevitz et al., 2000; Thoge et al., 2005; Figure 2.15 A). For strongly expressing plants like *35S::HA-PAP1* L8/3, the anthocyanin was visible at the margin of cotyledons and underneath the shoot meristem one day after germination (arrows, Figure 2.15 A). After four days cotyledons exhibited a dark green color and the accumulation of anthocyanin underneath the shoot meristem was still visible (arrow, Figure 2.15 A). In agreement with Gonzalez et al. (2008), anthocyanin was not observed in the mucilage or testa. Seedlings grown in darkness for four days displayed a strong accumulation of anthocyanin in the cotyledons, indicating that *PAP1* overexpression was able to promote flavonoid biosynthesis in darkness (Figure 2.15 B).

Quantitative analysis of four-day-old seedlings confirmed the observation of the qualitative analysis. As Figure 2.16 A shows most of the plants overexpressing either HA-PAP1 or HA-PAP2 fusion proteins displayed more anthocyanin compared to wild type when grown in light. The *cop1-4* mutant, the *spa* triple mutant and *pap1-D* plants showed the strongest accu-

mulation of anthocyanin. In darkness, plants overexpressing either PAP1 or PAP2 also showed a higher amount of anthocyanin when compared to wild

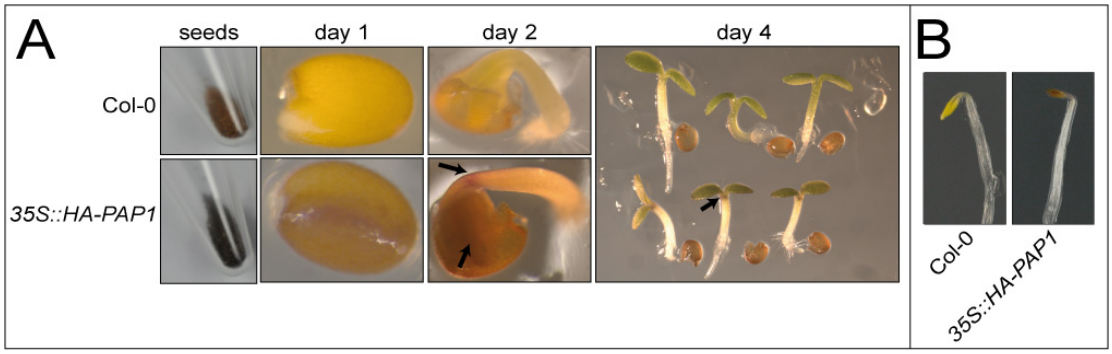

Figure 2.15: Overexpression of HA-PAP1 leads to strong accumulation of anthocyanin in seedlings grown in light and darkness. (A) Seeds and seedlings from Col-0 wild type and *35S::HA-PAP1* L8/3 overexpressing plants. Seedlings were grown for 1, 2 or 4 days on 1x MS plates containing 1% sucrose. (B) Seedlings from Col-0 and *35S::HA-PAP1* L8/3 plants were grown for 4 days in darkness on 1x MS plates containing 1% sucrose.

type. Among the plants expressing *AcV5*-tagged PAP1 one line displayed an even higher accumulation of anthocyanin than *pap1-D* plants in light and darkness (Figure 2.16 B). In order to exclude the possibility that overexpression phenotypes result from a stabilized protein due to tagging of the proteins, PAP1 was also expressed without a tag from *CaMV 35S* promoter as shown in Figure 2.16 C. Two of the three corresponding overexpressing plants exhibited a slightly stronger accumulation of anthocyanin in white-light-grown seedlings compared to wild type. In dark-grown seedlings all of the lines displayed a stronger anthocyanin content compared to wild type. These results indicate that overexpression of tagged and non-tagged PAP fusion proteins results in an increase in anthocyanin content for all generated overexpression lines in darkness and light.

II.3.4 PAP1 and PAP2 proteins accumulate in white-light-grown seedlings

As shown under II.3.3, transgenic lines expressing HA-tagged PAP1 and PAP2 protein accumulate higher amounts of anthocyanin in comparison to Col-0 wild type in light and darkness (Figure 2.16 A). In order to test, whether this high anthocyanin content is due to stabilized PAP proteins,

immunoblot studies were performed using protein extracts from dark- and white light grown transgenic seedlings. Such a stabilizing effect could be

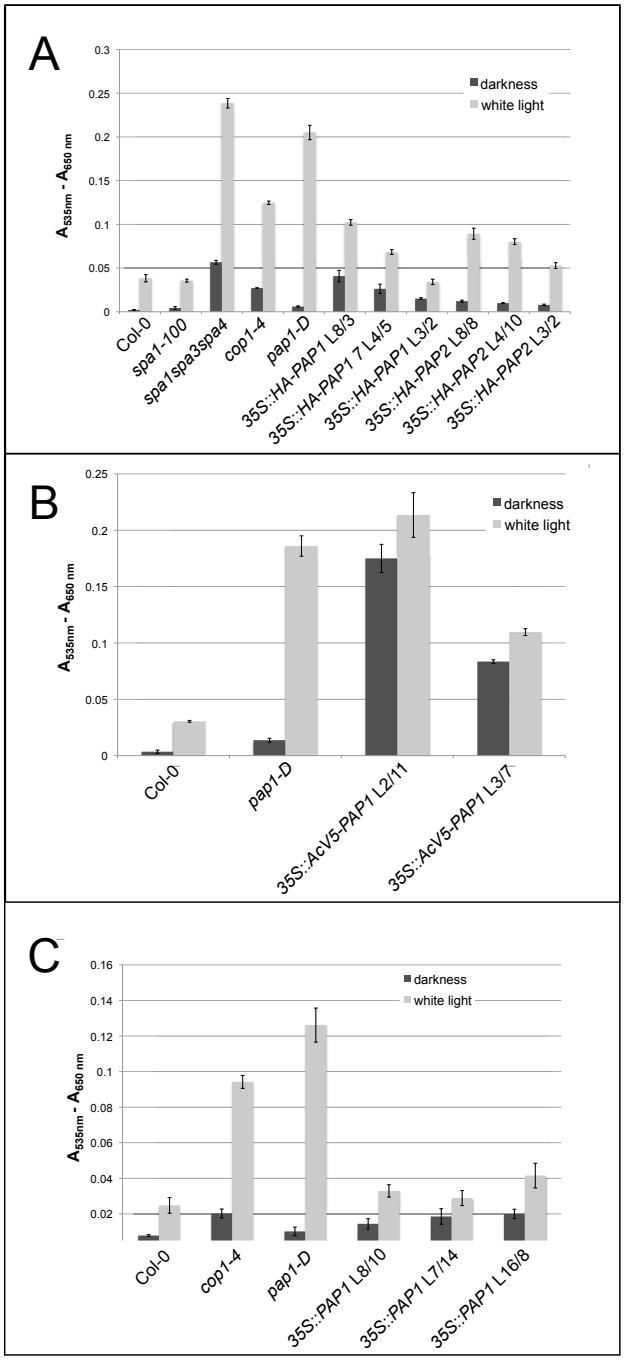

Figure 2.16: Overexpression of PAP1 and PAP2 results in increased anthocyanin accumulation in dark- and light-grown seedlings. (A, B) Measurement of anthocyanin content in ectopic-expressing *HA*-tagged PAP1 and PAP2 or AcV5-tagged PAP1 lines in Col-0 wild-type background. Three times 40 seeds were grown for 4 days on 1x MS plates containing 1% sucrose. The error bar indicates the standard error of the mean. (C) Measurement of anthocyanin content in wild-type plants constitutively expressing non-tagged PAP1 protein. Three times 20 seeds were grown for 4 days in 1x MS plates containing 1% sucrose. The error bar indicates the standard error of the mean.

therefore due to transcriptional and/or post-translational regulation of the PAP proteins by light. Figure 2.17 shows two independent experiments of the respective immunoblot analysis. Since *35S::HA-PAP* transgenic lines showed in all cases strong silencing effects in the T_4 -generation and different batches of seeds were used for analysis, it was difficult to directly compare different experiments with each other.

As Figures 2.17 A and D show, the HA-tagged PAP1 and PAP2 proteins could be detected specifically and the signal was not present in Col-0 wild-type protein extracts. HA-PAP2 ran as a slower migrating band compared to HA-PAP1 protein what was unexpected, since both proteins are predicted to be of same size (28 kDa). This could be due to post-translational modifications or different charges of the proteins. Both immunoblots showed an enrichment of PAP proteins in light compared to darkness (Figure 2.17 B, E). For some lines the repetition of the experiment showed minor differences due to experimental variation. To verify that light indeed affects the PAPs on the protein level transcript levels of the *35S::HA-PAP1* and *35S::HA-PAP2* lines were analyzed (Figure 2.17 C, F). Only small differences between dark- and light-grown seedlings were observed supporting the hypothesis that HA-PAP proteins are regulated post-translationally. Differences in the mRNA levels between individual lines and experiments were most likely due to silencing effects. Although the transcript data showed nearly no differences between darkness and light, hardly any correlation between mRNA and protein levels was detected.

II.3.5 PAP1 and PAP2 proteins are regulated over time

Since HA-PAP protein levels are regulated by light, I tested whether the accumulation of these proteins is changed over time. Therefore, HA-PAP1 and HA-PAP2 lines were grown for four days in darkness and then transferred to continuous white light for additional four days. As a control four-day-old plants were kept in darkness for four more days. As Figures 2.18 A, B, C and D show, HA-PAP1 and HA-PAP2 proteins accumulated six hours after transition to white light. After one day the protein levels decreased and in-

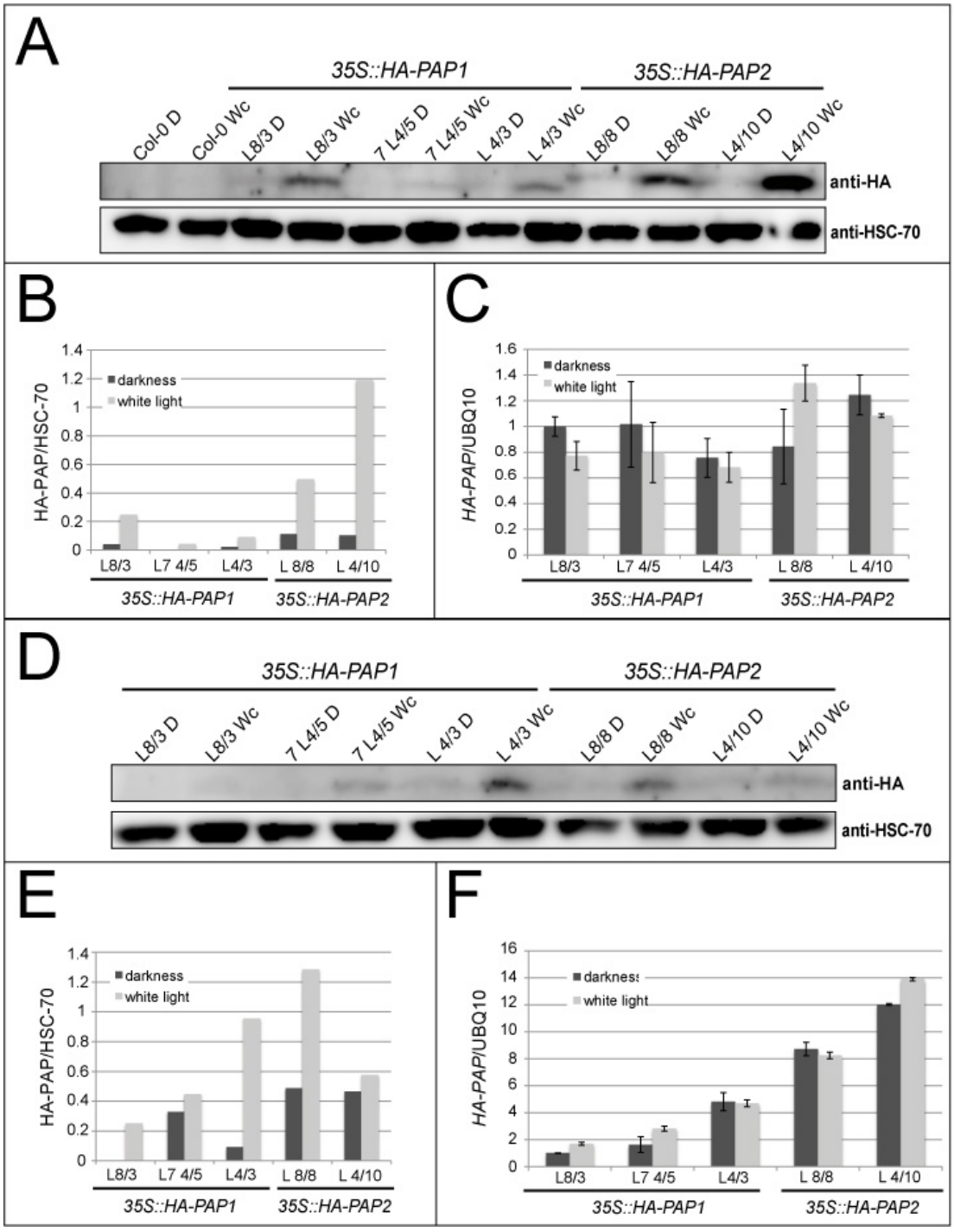

Figure 2.17: PAP1 and PAP2 accumulate in white-light-grown seedlings. (A, D) Protein analysis of transgenic *35S::HA-PAP1* and *35S::HA-PAP2* lines. 90 µg of total protein from 4 day-old dark- (D) and white light- (Wc) grown seedlings were analyzed using immunoblot subsequently to SDS-PAGE. Col-0 served as negative control. HSC-70 protein served as loading control. Shown are two independent experiments (B, E). Quantification of HA-PAP protein levels relative to HSC-70 protein levels of the blots shown in Figures A and D. (C, F) Transcript levels of *HA-PAP1* and *HA-PAP2* relative to *UBQ10* in RNA extracts from *35S::HA-PAP1* and *35S:: HA-PAP2* seedlings used in A and D. Error bars indicate the standard error of the mean.

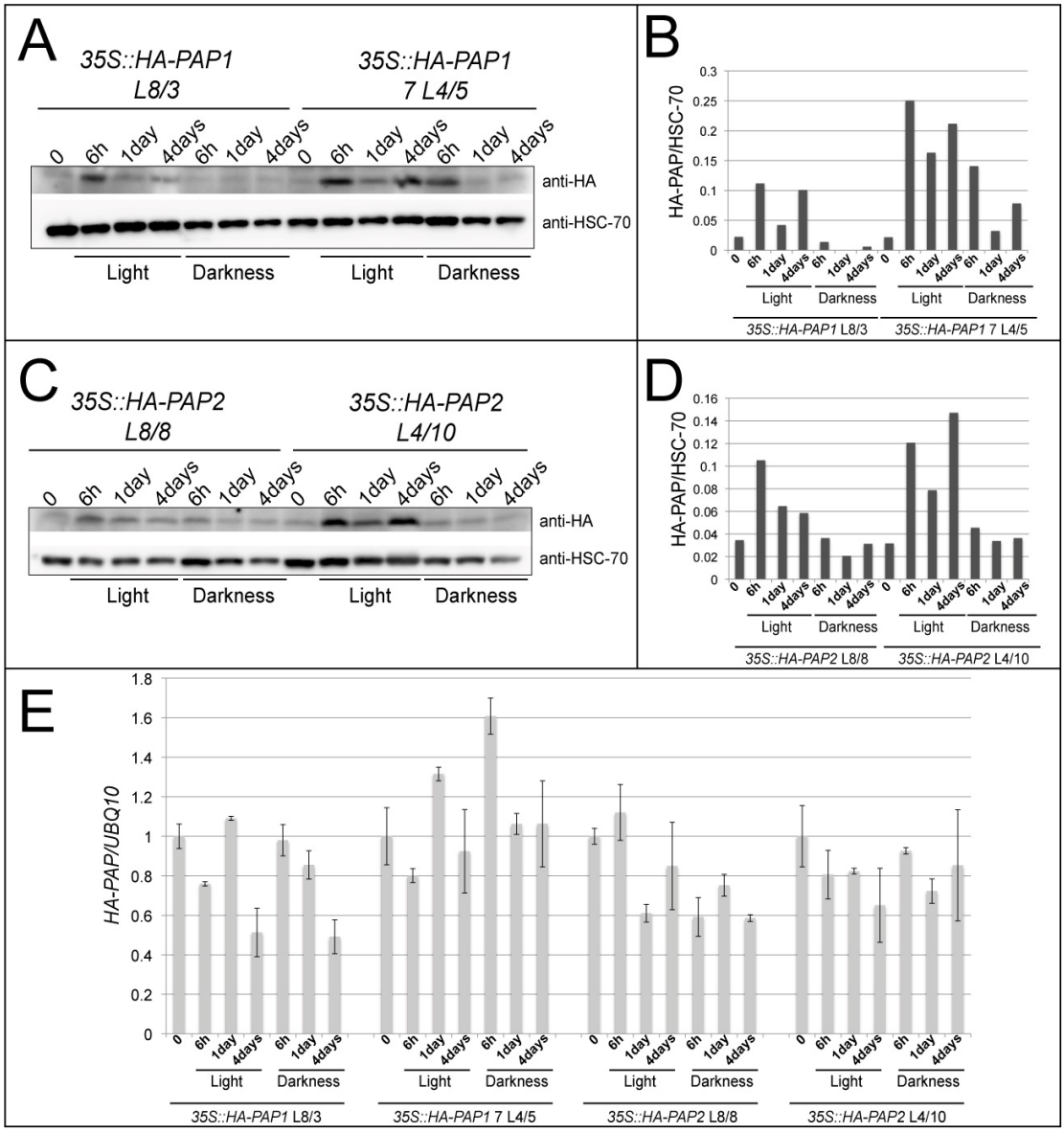

Figure 2.18: HA-PAP protein levels over time. (A, C) Transfer experiment using *35::HA-PAP* transgenic lines grown for 4 days in darkness (0) and then transferred for additional 6 hours, 1 day and 4 days to continuous white light. As a control seedlings were kept in darkness for additional 6 hours, 1 day and 4 days. 90 µg of total protein were analyzed by immunoblot using HA-specific antibodies. HSC-70 protein levels served as loading control (B, D) Quantification of HA-PAP protein levels relative to HSC-70 protein levels from the immunoblots in Figures A and C. Transcript levels of *HA-PAP1* and *HA-PAP2* relative to *UBQ10* in RNA extracts from *35S::HA-PAP1* and *35S:: HA-PAP2* seedlings used in A and C. Error bars indicate the standard error of the mean.

creased again after four days. This is the case for all lines tested, however *35S::HA.PAP2* L8/8 shows no increase of protein levels after four days. The amount of protein of the samples kept in darkness did not increase that strong. Nevertheless, the decrease after one day in dark-kept samples indicated a light-independent effect, although the protein levels were very low. The amount of protein was therefore only increased in transferred samples.

The transcript levels of all samples remained more or less the same, although there were slight up- and down-regulations (Figure 2.18 E). Again the level of expression correlated only partially with the amount of protein observed.

II.3.6 Anthocyanin levels in *cop1-4* mutants are dependent on PAP function

Gonzalez et al. (2008) generated *PAP1*RNAi mutants that harbor a construct targeting *PAP1* mRNA and *Myb*RNAi mutant plants carrying a construct targeting all four *MYB* mRNAs (*PAP1, PAP2, MYB113* and *MYB114*). They showed that the anthocyanin content is reduced in all RNAi mutants. Since *PAP2*RNAi mutants did not exhibit reduced amounts of anthocyanin, Gonzalez et al. (2008) concluded PAP1 to be the major player in anthocyanin biosynthesis in light. Thus, I included only *PAP1*RNAi and *Myb*RNAi mutants in my analysis. In order to understand the contribution of *PAP1* to increased anthocyanin levels known from *cop1-4* mutants, I crossed *PAP1*RNAi and *Myb*RNAi lines into *cop1-4* mutants and analyzed the anthocyanin content in four-day-old seedlings. As Figure 2.19 shows, the anthocyanin amount of *cop1-4* seedlings was strongly increased in light- and dark- grown seedlings when compared to wild type as described previously. Furthermore, in agreement with Gonzalez et al. (2008), *PAP1*RNAi plants exhibited slightly reduced anthocyanin content compared to wild type in light, whereas the decrease was stronger in *Myb*RNAi plants. *PAP1*RNAi *cop1-4* double mutants displayed reduced levels of anthocyanin in light, whereas MybRNAi *cop1-4* mutants showed almost no anthocyanin accumulation compared to *cop1-4* mutants. This clearly indicated strong contribution of PAP1, PAP2, Myb113 and Myb114 to COP1-dependent anthocyanin biosynthesis in light. It was hard to determine an effect in dark-grown seedlings because of only minor differences between the lines (*PAP1*RNAi and MybRNAi plants showed an increase of anthocyanin compared to wild type in darkness). Nevertheless, the anthocyanin amount in the crosses was slightly decreased in comparison to *cop1-4* mutants indicating a regulatory

effect of COP1 in darkness. However, to verify the effect in darkness more properly, the experiments need to be repeated with more seeds.

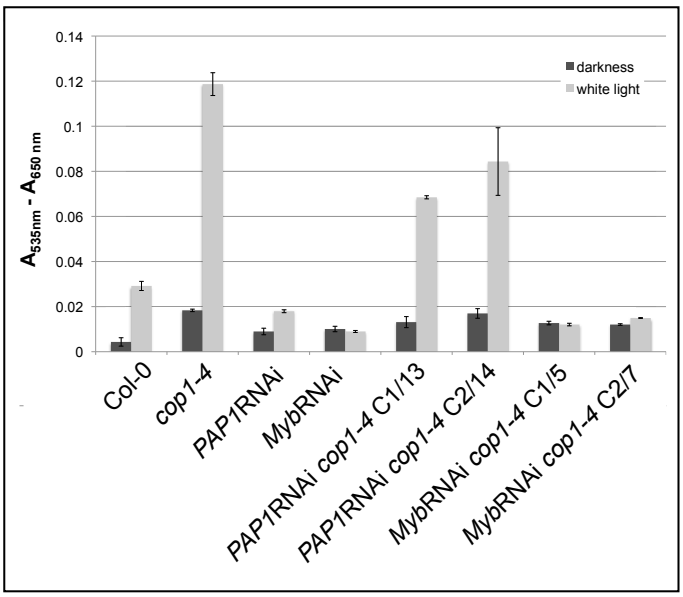

Figure 2.19: Contribution of PAP proteins to COP1-dependent anthocyanin biosynthesis. Measurement of anthocyanin content in Col-0, *cop1-4*, *PAP1*RNAi, *Myb*RNAi and *PAP1*RNAi *cop1-4* as well as *Myb*RNAi *cop1-4* seedlings. Three times 25 seedlings were grown for 4 days on 1x MS containing 1% sucrose in darkness and white light. Two independent crosses (C1 and C2) each were analyzed. The error bar indicates the standard error of the mean.

II.3.7 Overexpression of PAP1 and PAP2 in *cop1-4* mutant background results in increased anthocyanin content in darkness and light

In order to study the effect of COP1 on PAP1 and PAP2 protein and anthocyanin levels, I crossed *35S::HA-PAP1* and *35S::HA-PAP2* overexpressing plants into *cop1-4* mutant plants. In addition, *pap1-D* plants were crossed into *cop1-4* mutant plants to verify the effect of the *cop1-4* mutation on anthocyanin levels. As Figure 2.20 shows, the anthocyanin contents of *pap1-D cop1-4* (A) as well as *35S::HA-PAP2 cop1-4* seedlings (B) were strongly increased in darkness and light compared to wild type, *pap1-D*, *cop1-4* and the overexpressor *35S::HA-PAP2* L8/8. Interestingly, the effect in darkness seemed to be more than additive when compared to the overexpressors in Col-0 background and the *cop1-4* mutant. However, *35S::HA-PAP1 cop1-4* crosses did not exhibit an increase in anthocyanin

levels compared to *35S::HA-PAP1* lines and *cop1-4* mutants, which might be due to silencing of the *35S::HA-PAP1* transgene.

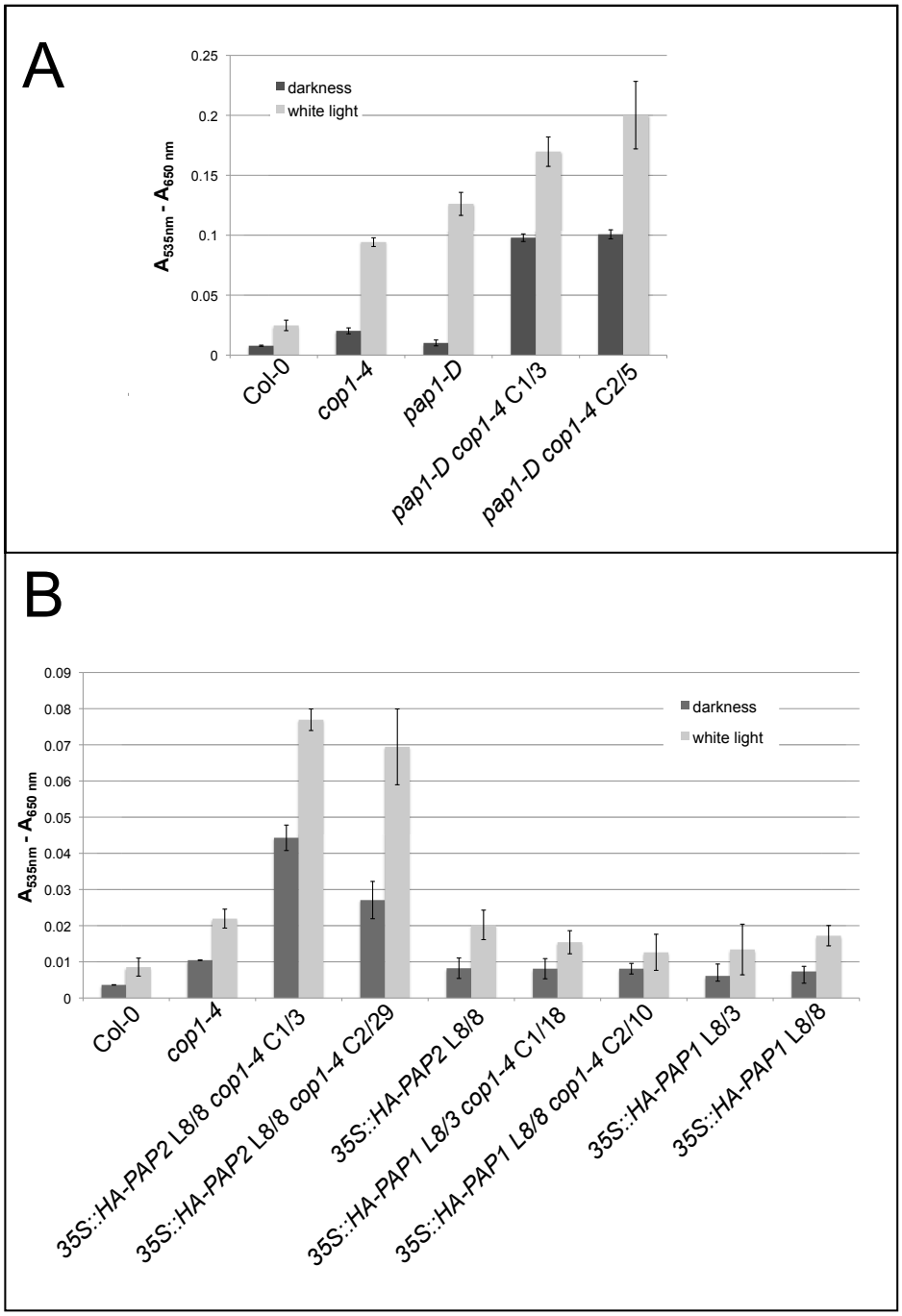

Figure 2.20: Overexpression of PAP1 and HA-PAP2 in the *cop1-4* mutant background results in strong accumulation of anthocyanin in darkness and white light. (A, B) Measurement of anthocyanin content in *PAP1* and *PAP2* overexpressing plants in the *cop1-4* mutant background. Three times 15 seedlings were grown for 4 days on 1x MS containing 1% sucrose. Two independent crosses (C1 and C2) each were analyzed. The error bar indicates the standard error of the mean.

The overaccumulation of anthocyanin in PAP overexpressing plants crossed to *cop1-4* mutant indicates a strong contribution of COP1 to PAP-dependent regulation of anthocyanin biosynthesis in light and darkness. Since the effect of the *cop1-4* mutation in darkness is that strong, a regulation of PAP function via COP1 predominantly in darkness is most likely.

II.3.8 HA-PAP2 protein accumulates in the *cop1-4* mutant background

Since crosses of *35S::HA-PAP* lines with the *cop1-4* mutant showed high accumulation of anthocyanin in darkness and light, pointing to a COP1-regulatory effect, I started analyzing the protein levels in these crossings in darkness versus light. An initial experiment using the HA-PAP overexpressing lines in wild-type background showed that HA-PAP1 and HA-PAP2 protein can be stabilized by the application of MG132 (Figure 2.21 A), which implies regulation by protasomal degradation. This could be caused by the activity of COP1 protein. Indeed, in a first experiment *35S::HA-PAP2 cop1-4* plants displayed an enrichment of the protein in darkness and white light compared to *35S::HA-PAP2* plants in wild-type background (Figures 2.21 A, B). Thus, the crossings exhibited three times more protein in darkness compared to the *35S::HA-PAP2* L8/8 line grown in darkness indicating an effect of COP1 on HA-PAP2 steady-state levels. Nevertheless, this preliminary result needs to be verified in further western blots with different lines to be sure that this is an effect due to the lack of COP1 protein rather than an artifact of the experiment.

II.3.9 Production of anti-PAP1 antibodies

For detection of endogenous PAP1 in *Arabidopsis* and to further verify the effect of COP1/SPA on endogenous PAP1 protein levels, antibodies were raised against a truncated His_6-tagged recombinant protein from *E.coli* consisting of the last 132 amino acids of the PAP1 protein (PAP1-396). PAP proteins share a high identity to each other especially in the N-terminus of the proteins, where the DNA binding domains are located. Thus, the C-terminal

part of PAP1 protein was chosen for expression and immunization. As the asterisk in Figure 2.22 A shows, the PAP1-396 protein (17 kDa) could be expressed and purified from 500 ml *E.coli* culture using Ni-NTA resin. For unknown reason, the PAP1-396 protein was found to migrate slower in the

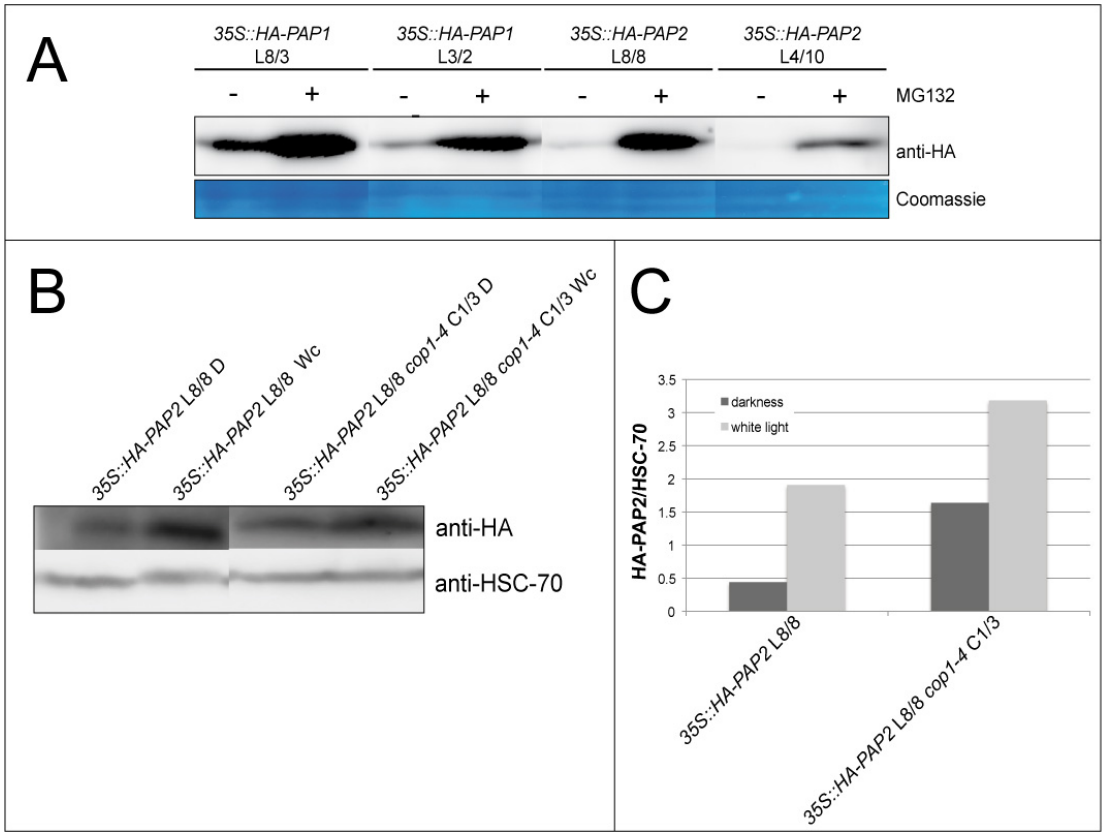

Figure 2.21: HA-PAP proteins are post-translationally regulated. HA-PAP2 protein is stabilized in the *cop1-4* mutant. (A) HA-PAP proteins accumulate after application of MG132. 90µg of total protein from 4-day-old *35S::PAP1* and *35S::PAP2* expressing seedlings in wild-type background were analyzed by immunoblot using HA-specific antibodies. Coomassie staining served as loading control. (B) Immunoblot analysis of HA-PAP2 protein levels from *35S::HA-PAP2 cop1-4* C1/3 seedlings. Seedlings were grown for 4 days in darkness (D) or continuous white light (Wc) on 1x MS plates containing 1% sucrose. 90 µg of total protein were loaded. For comparison protein extracts from *35S::HA-PAP2* seedlings were loaded. HSC-70 protein levels served as loading control. (B) Quantification of HA-PAP2 protein levels relative to HSC-70.

SDS-PAGE (about 25 kDa) than its predicted size would suggest. The greatest amount of protein was again obtained from elution 2 in Buffer E. The protein from this elution was used for immunization of two rabbits.

Screening six rabbit preimmune sera revealed the sera of the rabbits Hawai and Pusta to have the weakest background at the predicted size of native PAP1 protein (about 33 kDa), which were then chosen for immunization (Figure 2.22 B). After nine months of immunization no specific

signal for endogenous PAP1 could be detected in Col-0 wild type, *pap1-D* or *35S::AcV5-PAP1* overexpressing plants using the sera from Hawai and Pusta. *PAP1*RNAi and *Myb*RNAi plants were employed as negative controls. Extracts from those seedlings showed an unspecific band at the expected size of PAP1 protein (arrow, Figure 2.22 C). Since the unspecific background from the sera was very strong, the antibodies were purified using PAP1-393 protein as the antigen blotted on PVDF membranes. Since *PAP1* mRNA expression is induced by the application of sucrose (Solfanelli et al., 2006), all experiments were also carried out on MS plates containing 1% and 3% sucrose in order to increase PAP1 amounts. Using purified antibodies from Hawai, protein extracts from seedlings grown in white light on plates containing 3% sucrose directly isolated in 2x Laemmli buffer displayed a specific signal for endogenous PAP1 running slightly higher as expected at about 35 kDa (arrow, Figure 2.22 D) at least in case of *pap1-D*. This signal was also present in protein extracts from Col-0 wild type. Since *PAP1*RNAi, *Myb*RNAi and *myb75 Ds* (T-DNA insertion mutant, Supplemental figure 5.1) mutant plants also showed an unspecific band at the same size, it is hard to conclude whether the signal from *pap1-D* seedling extracts is specific for endogenous PAP1 protein. Since the *myb75 Ds* mutation is in No-0 wild-type background, protein extracts from No-0 seedlings were also included to the analysis. However, the signal observed in *PAP1*RNAi and *Myb*RNAi mutants could be due to incomplete silencing of the *PAP* transcripts (*Myb*RNAi mutants still exhibit low amounts of *PAP1* transcript according to Gonzalez et al. (2008)). Further, the signal in *myb75 Ds* mutants could result from the insertion of the T-DNA at the very end of *PAP1* coding sequence (Supplemental figure 5.1). The purified antibodies from Pusta did not display any specific signal in the same experiments (data not shown). In addition, nuclei-enriched fractions from plants grown on plates with sucrose did not provide reliable results (data not shown), raising the possibility that the PAP1 protein is degraded during the nuclei enrichment procedure.

Taken together, I was able to show that PAP1 and PAP2 proteins were able to interact with members of COP1/SPA complexes in yeast. The overexpression of HA-PAP1, HA-PAP2, AcV5- and non-tagged versions of the proteins showed an increase in anthocyanin content in light and darkness.

Ectopically expressed HA-PAP1 and HA-PAP2 proteins were regulated by light since both proteins accumulated strongly in light, but were reduced in darkness. In addition, HA-PAP1 and HA-PAP2 protein levels were regulated

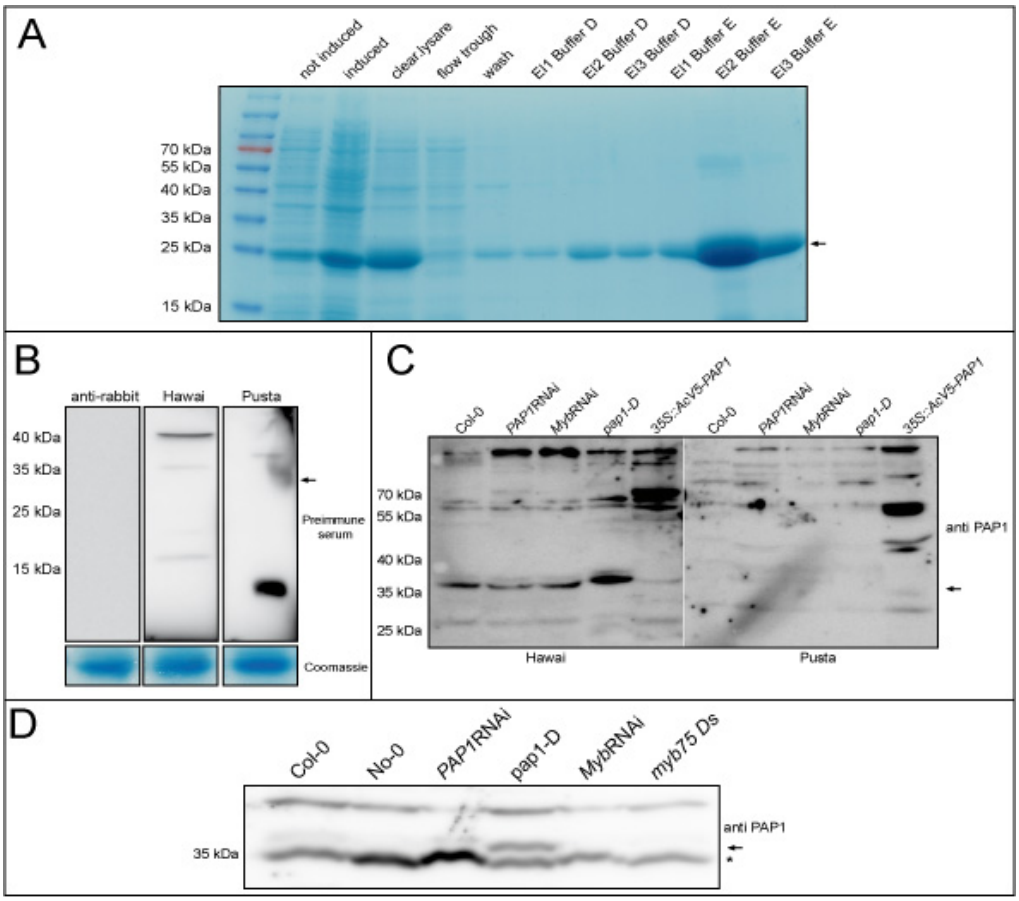

Figure 2.22: Production of anti-PAP1 antibodies. (A) Expression and purification of His_6-tagged PAP1-396 recombinant protein from *E.coli*. 40% of induced and 20% of not induced samples, 100% of the cleared lysate sample, 0.9% of the flow through sample, 0.5% of the pooled wash sample and 7.2% of all the elutions were resolved by a 12.5% SDS-PAGE gel. The gel was stained with Coomassie Brilliant Blue. The arrow marks the PAP1-396 protein. (B) Test of the sera from the rabbits Hawai and Pusta prior to immunization. 30 µg of total protein from four-day-old seedlings grown in white light on 1 xMS containing 1% sucrose were analyzed by Immunoblot following SDS-PAGE. Coomassie staining of the membrane served as loading control. The sera were diluted 1:1000 in 1xTBS containing 3% non-fat-dried milkpowder. The arrow marks the predicted size of *Arabidopsis* PAP1 protein. (C) Analysis of the sera from Hawai and Pusta after immunization. 30 µg of total protein from Col-0, *pap1-D* and *35S::AcV5-PAP1* four-day-old seedlings as positive control, as well as 30 µg of total protein from *PAP1*RNAi and *Myb*RNAi seedlings as negative control were analyzed by immunoblot subsequently to SDS-PAGE. All seedlings were grown in white light. The sera were diluted 1:1000 in 1xTBS containing 3% non-fat-dried milkpowder. The asterisk marks the predicted size of endogenous PAP1 protein. (D) Immunoblot analysis of the purified serum from Hawai. 50 µg of total protein from white-light-grown Col-0 wild type, No-0 wild type and *pap1-D* seedlings served as positive control. 50 µg of *PAP1*RNAi and *Myb*RNAi as well as *myb75 Ds* protein extracts from seedlings served as negative control. All seedlings were grown on 1x MS containing 3% sucrose. The purified antibodies from Hawai were diluted 1:300 in 1xTBS containing 3% non-fat-dried milkpowder. The arrow marks the predicted size of endogenous PAP1 protein. The asterisk labels an unspecific band used as loading control.

over time. Pointing to a dependence of PAP protein function on COP1, I observed a decrease of anthocyanin in RNAi *cop1-4* double mutants in light as well as an increase of the anthocyanin amounts in PAP1 overexpressing lines crossed in *cop1-4* mutants in light and darkness. Further, HA-PAP1 and HA-PAP2 proteins were enriched by the application of MG132. Supporting the notion that COP1 post-translationally regulates PAP proteins, I observed that HA-PAP2 protein levels were increased in a *cop1-4* mutant background in an initial experiment. However, generation of an anti-PAP1 antibody to detect the endogenous PAP1 protein in plant cells extracts remained so far unsuccessful since the specific signal could not be verified.

III. Discussion

III.1 SPA proteins interact with each other *in vitro* and *in planta*

Since SPA proteins regulate photomophogenesis in concert with the E3-ubiquitin ligase COP1, which also includes physical interaction with COP1, I tested *in vitro* and *in planta* whether SPA proteins can interact with each other, implying the existence of a larger protein complex including several SPA proteins and the COP1 protein. COP1/SPA complex composition could represent one reason for the distinct but also overlapping functions of SPA proteins during *Arabidopsis* plant development. In this regard, different COP1/SPA complexes would carry out distinct biochemical activities to various targets under different conditions. The absence of a single SPA protein in the complex at the stage where it is normally needed may lead to a reduction or defect of the E3-ubiquitin ligase activity of COP1.

Indeed, I could show that SPA proteins are able to interact pairwise with each other *in vitro* and *in planta*. Therefore, it is most likely that SPA proteins can also be part of larger COP1-containing protein complexes. The N-terminus including the coiled-coil domain was important at least for the interactions of SPA1 with itself and with SPA2, and therefore may also be required for the interactions between the other SPAs. Even though the coiled-coil domain alone was not able to restore interaction completely, this domain seems to be very important for SPA-SPA interaction, like it was shown for COP1-SPA1 interaction (Hoecker and Quail, 2001).

By co-localization experiments I showed that SPA1 is able to recruit SPA4 to nuclear speckles in *Arabidopsis* leaf epidermal cells. Therefore, it could be that SPA1 recruits SPA4 to protein complexes. This could be further studied for instance by investigating SPA4 function in *spa1* mutant backgrounds. Recently, *SPA4* overexpressing plants in a *spa3spa4* double mutant background harboring an artificial *NLS* sequence showed overcomplementation in photomorphogenic responses compared to plants overexpressing of the wild type *SPA4* sequence (Fackendahl, unpublished). This supports the hypothesis that SPA4 has to be imported into the nucleus

for proper function. However, *spa* triple mutant plants only expressing functional *SPA4* showed only small differences in seedling and adult plant phenotype compared to wild type, indicating only a minor contribution of SPA4 nuclear import via SPA1 to SPA protein function (Laubinger et al., 2004).

In agreement with my results from pairwise interactions studies, Zhu et al. (2008) found that SPA proteins can build homo- and heterodimers *in vivo*, in which every combination of SPA proteins is possible (Figure 3.1 A). In addition, *in vivo* co-immunoprecipitation as well as gel filtration analysis suggests that SPA-SPA dimers form a complex with COP1 homodimers, building tetrameric complexes (Figure 3.1 B). These complexes have a variable composition of SPA dimers, whereas the COP1 homodimer is always included. The notion that multiple COP1/SPA complexes exist, rather than one supercomplex involving all SPAs and COP1, is supported by several other evidences: SPA protein levels were variable in *in vivo* immunoprecipitation experiments using anti-SPA antibodies, which indicates the presence of multiple protein complexes involving SPAs. In addition, the gel filtration pattern of SPA proteins and the COP1 protein under different light conditions was similar, and the COP1 pattern in such experiments was not altered in *spa* single and double mutants, what showed that these proteins can be members of similar protein complexes but COP1 complexes are not affected by the loss of SPA proteins (Zhu et al., 2008). The large number of possible complexes with COP1 may therefore explain differences in SPA function. This hypothesis is strengthened by the different light-regulated and tissue-specific expression patterns of SPA proteins (Zhu et al., 2008; Fittinghoff, 2008).

Chen et al. (2010) revealed that COP1/SPA tetrameric complexes also associate with CUL4-DDB1 proteins building a protein complex in the absence of the CDD complex. COP10 protein, previously described to interact with COP1 (Yanagawa et al., 2004), was therefore shown to associate with COP1 as monomer rather than as a part of the CDD complex. In addition, COP1 was shown not to interact with the DET1 protein. According to Chen et al. (2010) this determines COP1 to be part of CUL4-DDB1 complexes rather than interacting with the CDD complex. Since the DDB1 protein works as an adaptor protein that interacts with DCAF substrate recognition receptors,

which the SPA proteins are designated to be, the association of COP1/SPA complexes with CUL4-DDB1 most likely represents a way of modulating E3-ubiquitin ligase activity towards target proteins for the regulation of different developmental stages in plants. The CDD complex was also found to interact

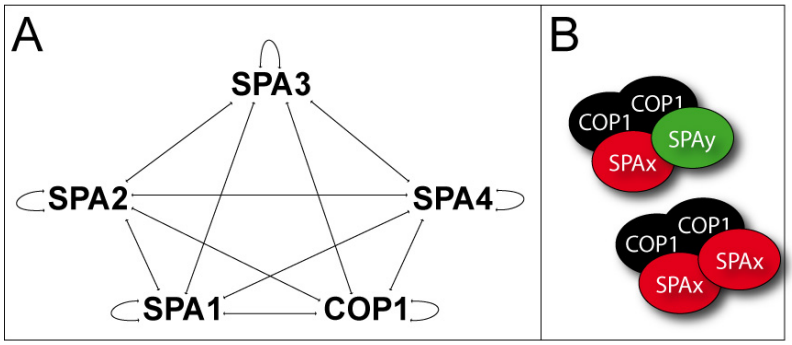

Figure 3.1: SPA proteins interact with each other and with the COP1 protein forming tetrameric protein complexes. (A) SPA proteins can interact pairwise with each other and the COP1 protein. (B) SPA proteins together with the COP1 protein form tetrameric complexes in which the SPAs form homo- and hetero-dimers, whereas a homodimer of COP1 is always included (Zhu et al., 2008).

with CUL4-DDB1 ligases. CDD may therefore have a regulatory relationship to CUL4-DDB1-COP1/SPA complexes, a relation that requires further study. This hypothesis is further supported by the fact that *DET1* and *SPA1* were found to act synergistically in the control of photomorphogenesis at the seedling stage and later developmental stages (Nixdorf et al., 2010; Chen et al., 2010). Since COP1 is part of other protein complexes, it could also be that light inactivates COP1's own ligase function by integrating it into other complexes. It is known from mammals that the factor c-Jun is ubiquitinated by a CUL4-based E3-ubiquitin ligase under participation of humanCOP1 (hCOP1), but although hCOP1 interacts with c-Jun, it does not function as c-Jun E3-ubiquitin ligase. hCOP1 recruits c-Jun to an E3 complex containing DET1, DDB1, cullin4A, and Roc (Wertz et al., 2004). COP1 in CUL4-DDB1-COP1/SPA complexes in plants may act in a similar way. This would imply that COP1 is able to carry out E3-ubiquitin ligase function on its own but can also work as an adaptor protein and may provide an additional mechanism in the regulation of its function as the inclusion into a complex could also change the target specificity in light-regulated ubiquitination. However, this needs to be further elucidated.

Nevertheless, the basic question remains, which kind of mechanism decides about COP1/SPA complex composition and/or activity. Since protein accumulation and mRNA expression do not correlate in all cases, there must be other mechanisms determining SPA function in COP1/SPA complexes. Therefore, promoters and/or protein sequences can regulate SPA function. SPA2 protein levels in seedlings for instance are reduced in light, even though the mRNA expression remains unaffected. In adult plants *SPA1* and *SPA4* were found to be expressed at a similar strength, but the genetic analysis of *SPA* function revealed that *SPA1* plays only a minor role at this developmental stage. Furthermore, *SPA1*, *SPA2* and *SPA4* promoters express very strongly in roots, whereas only the proteins of SPA2 and SPA4 are detectable in roots, indicating post-translational regulation of SPA1 (Zimmermann et al., 2004b; Fittinghoff, 2008; Zhu et al., 2008).

III.2 Inactivation of COP1/SPA complexes by light

Balcerowicz et al. (2011) showed that SPA2 expressed from the strong *SPA1* promoter lacks any repressor function in the light, whereas SPA1 expressed from the *SPA2* promoter retained repressor function under the same conditions. COP1/SPA2 complexes therefore seem to function in darkness equally to COP1/SPA1 complexes, whereas they become hyper-inactivated in the light. This reveals that the distinct functions of the SPAs are due to their protein sequence. Furthermore, SPA1 and SPA2 proteins could be enriched by the application of the proteasome inhibitor MG132, clearly indicating regulation via proteasomal degradation. In this regard, I analyzed SPA1 and SPA2 protein levels in far-red light- and dark-grown seedlings using anti-SPA1 and anti-SPA2 antibodies generated in this study. Indeed, in my experiments endogenous SPA1 and SPA2 protein levels were decreased in far-red light compared to darkness. SPA2 protein levels showed a stronger reduction by far-red light compared to darkness than those of SPA1 protein. This effect was due to the lower *SPA2* transcript abundance relative to *SPA1* as well as the lower stability of SPA2 protein when compared to SPA1 protein and indicates that light might regulate the respective protein levels through

proteasomal degradation. SPA1 protein abundance was only slightly reduced in light-grown seedlings compared to dark grown ones. The transcript of *SPA1* was slightly induced, an effect that indicates that light-induced degradation of SPA1 protein may be counteracted by light- induced expression of *SPA1*. The *SPA1* promoter is considered to be strongly induced by red and far-red light (Fittinghoff et al., 2006) and in addition Zhu et al. (2008) showed stronger accumulation of SPA1 protein in far-red light. In this regard, the reduction of SPA1 protein may be due to the fact that seedlings were grown in lower fluences of continuous far-red light and the strong light induction of *SPA1* expression may over-compensate the decrease in protein stability.

SPA1 and SPA2 protein levels were shown to be elevated in *cop1-4* mutants indicating that COP1 reduces SPA1 and SPA2 steady-state protein levels as described previously (Zhu et al., 2008). In order to investigate a regulatory effect of COP1 on SPA protein levels in light versus darkness, which would imply that COP1/SPA complexes promote light-dependent autoubiquitination of the SPAs, the SPA1 and SPA2 protein levels were analyzed in a *cop1-4* mutant background under the respective light conditions using the generated anti-SPA1 and anti-SPA2 antibodies. The fold change of light-dependent degradation of SPA1 remained in my experiments the same in *cop1-4* mutants compared to wild-type seedlings grown under the same conditions, which points to a COP1-independent effect on light-regulated SPA protein abundance. Since the differences between two experiments in case of SPA1 protein levels were very high, this needs to be repeated. However, in case of SPA2 protein levels in *cop1-4* mutants, the differences between light and darkness were weaker, implying a regulatory function of COP1 on SPA2 protein levels. On the other hand, this could also in part be due to the slight increase of *SPA2* transcript levels in the light. In order to determine the effect of the *cop1* mutation more properly, these experiments need to be verified and could be repeated using other *cop1* mutations like the *cop1-6* mutation.

Recently, it was shown that the deletion of the N-terminus of SPA1 results in a far-red-light-dependent increase of the deletion derivate protein levels (Fackendahl, unpublished). Hence, the N-terminal kinase-like domain of SPA proteins seems to be a good candidate to mediate the de-stabilization in response to light. In addition the deletion of the coiled coil domain, which is

essential for the interaction with COP1, also leads to a light-dependent increase of protein amounts (Fackendahl, unpublished). Since these domains have been shown to be essential for SPA-COP1 interaction, this could also be crucial for the regulation of SPA protein stability.

Taken together, the inactivation of COP1/SPA complexes and therefore regulation of COP1/SPA function is likely to be regulated by multiple mechanisms. My data together with those of Balcerowicz et al. (2011) indicate that inactivation is most likely mediated by an E3-ubiquitin ligase, which, at least in case of SPA2, might be COP1. As described previously, changes in the interactions with the photoreceptors are also a possible mechanism for regulating COP1/SPA complex activity. A third mechanism could be the change of post-translational modifications like phosphorylation, even though this still needs to be studied (Fittinghoff, 2008; Balcerowicz et al., 2011; Figure 3.2). An inactivation by nuclear exclusion of COP1 seems to be unlikely since

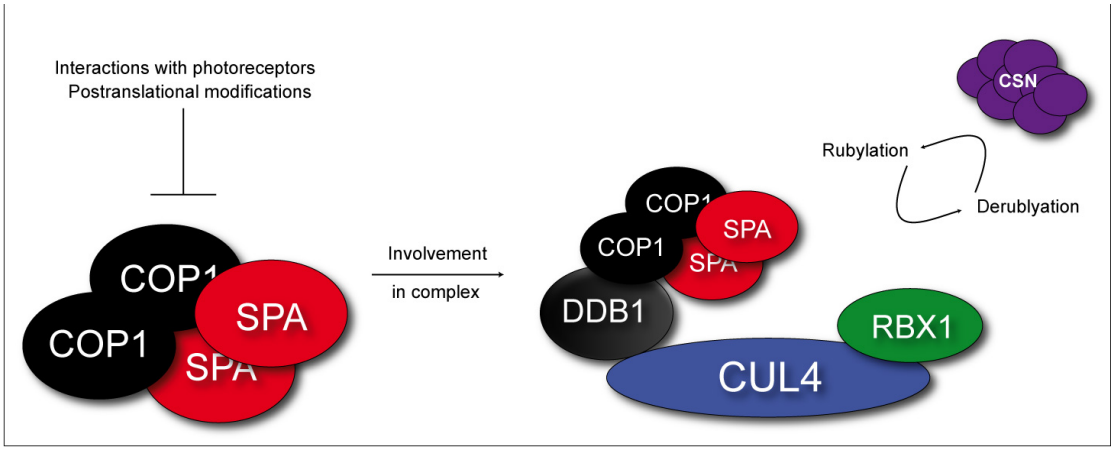

Figure 3.2: Regulation of COP1/SPA function. Complex composition can be affected by interactions with the photoreceptors and / or post-translational modifications like ubiquitination or phosphorylation. COP1/SPA complexes interact with CUL4-DDB1, providing an additional mode of action during Arabidopsis development. The CSN is known to regulate CUL4-DDB1 activity via rubylation and derubylation (Chen et al., 2010).

changes in the gene expression are detectable 2 h after light exposure (C.Falke and U.Hoecker, unpublished), whereas exclusion of COP1 protein from the nucleus takes up to 36 h (von Arnim und Deng, 1994). As described above, COP1/SPA complexes could also be regulated in their function by integration in CUL4-DDB1 protein complexes. However, whether COP1/SPA complexes are permanently associated with CUL4/DDB1 complexes *in planta*

or COP1/SPA carries out most functions on its own remains so far unclear and requires further study (Figure 3.2).

III.3 PAP proteins, potential targets of COP1/SPA complexes

Since COP1/SPA complexes act as repressors in multiple developmental processes in plants especially at early stages, I analyzed whether two new potential targets, the PAP1 and PAP2 protein, which are involved in anthocyanin biosynthesis at the seedling stage, can be also repressed in their function by COP1/SPA complexes in a light-dependent manner. Even though regulation via COP1/SPA complexes is designated to occur at the post-translational level, there could be also an indirect effect of COP1/SPA on *PAP1* and *PAP2* transcription. PAP1 and PAP2 were recently found to regulate TTG1-, GL3- and EGL3-dependent anthocyanin biosynthesis via “late” biosynthesis genes (Gonzalez et al., 2008). I could show in my experiments that COP1 and the SPA proteins were interacting with PAP1 and PAP2 in Yeast Two-Hybrid assays, providing some evidence for a COP1/SPA-dependent regulation of anthocyanin biosynthesis. PAP1 interacted with SPA1, SPA3 and SPA4, whereas PAP2 interacted with SPA1, SPA4 and COP1. The fact that PAP1 and PAP2 were not able to associate with all members of the SPA protein family or the COP1 protein could suggest that PAP proteins *in planta* could interact with different COP1/SPA complexes. Nevertheless, all interactions were only observed in yeast and need to be verified in other interaction assays. The fact that SPA2 was not able to interact either with PAP1 or PAP2 could be due to SPA2s function in darkness, whereas *PAP* expression is considered to be light dependent. However, COP1/SPA complexes could regulate PAP protein levels also in darkness, as it has been characterized for other transcription factors involved in photomorphogenic responses. The observed interactions of PAP1 with SPA3 and PAP1 and PAP2 with SPA4 might indicate an association during adult plant development, since SPA3 and SPA4 function preferentially during these stages (Laubinger et al., 2004). However, this needs to be verified in further interaction studies. In addition, it would be interesting to test which part

of the PAP1 and PAP2 protein mediates the interactions because PAP1 was exclusively interacting with SPA3 while only PAP2 was only found to interact with the COP1 protein. Analyzing the importance of the protein domains for substrate recognition in anthocyanin biosynthesis could also be interesting. In this regard, functional analysis of deletion derivates lacking the coiled-coil domain, the N-terminus or the WD40 domain of SPA proteins could at least give an idea about the mechanism of SPA-PAP association in light and darkness.

III.4 Regulation of PAP-dependent anthocyanin biosynthesis in light and darkness

The results from this study show that ectopic overexpression of PAP1 and PAP2 in a wild-type background resulted in enhanced anthocyanin amounts in light and darkness compared to wild-type seedlings grown under the same conditions. Such hyperactivation of the phenylpropanoid pathway in light is in agreement with previous studies, underlining the contribution of PAP1 and PAP2 to anthocyanin biosynthesis in light. Therefore, overexpression most likely results in an upregulation of the entire biosynthesis pathway including “early” and “late” genes (Borevitz et al., 2000; Gonzalez et al., 2008; Shi et al., 2010). However, overexpression of HA-PAP1 and HA-PAP2 as well as AcV5-tagged and non-tagged PAP1 proteins resulted in my experiments in a strong accumulation of anthocyanin in darkness as well. This is contradictory to previous results on first sight since Cominelli et al. (2008) showed in their experiments that anthocyanin biosynthesis occurs only in light because certain components of WD/bHLH/MYB complexes like GL3 and EGL3 are very low expressed in seedlings in darkness and need to be induced upon light exposure to gain function. Confirming their hypothesis, *pap1-D* seedlings failed to accumulate anthocyanin in darkness in their experiments. Nevertheless, my experiments showed accumulation of anthocyanin in darkness. Several scenarios could explain this. First, there are most likely differences between ectopic overexpression in my lines and *PAP1* expression in *pap1-D* plants. Hence, it could be that *PAP1* expression in

pap1-D seedlings is lowered or kept silent in darkness like it was shown for the wild-type *PAP1* gene (Cominelli et al., 2008). In this regard, Weigel et al. (2000) observed in their experiments that activation-tagged *FT* expression matches more or less the endogenous regulation of the genes rather than ectopic expression of the transgene via 35S promoter. In order to verify potential differences between expression via *35S CaMV* and enhanced expression of the endogenous gene via four 35S enhancer elements, *PAP1* transcript levels in *pap1-D* plants need to be analyzed in darkness.

Further, besides the possibility of so far mostly uncharacterized WD/bHLH/MYB complex-independent stimulation of anthocyanin biosynthesis via PAP proteins in the overexpressing lines, the observed accumulation of anthocyanin in darkness could be due to the fact that overexpression of PAP proteins stimulates transcription or stabilization of light induced factors that may also interact with the PAP proteins. In this regard, a microarray analysis from Tohge et al. (2005b) revealed that *TT8* transcript levels are increased in *35S::PAP1* and *pap1-D* plants. According to other studies, PAP1 is able to bind to the promoter of the *TT8* gene (Baudry et al., 2006). Since TT8 protein was also found to interact with PAP1, PAP2 and TTG1 (Zimmermann et al., 2004a) and *TTG1* expression is constitutive in light and darkness (Cominelli et al., 2008), it could be that WD/bHLH/Myb complexes in PAP overexpressing lines can also assemble in darkness to switch on anthocyanin biosynthesis. Furthermore, of course other bHLH factors could be stabilized in *35S::PAP* overexpressors and trigger anthocyanin biosynthesis. However, *GL3* and *EGL3* transcription levels were at least found to be unaffected in *35S::PAP1* adult plants (Tohge et al., 2005b; Rowan et al., 2009).

Due to the observed accumulation of anthocyanin in dry embryos of *35S::HA-PAP* seeds (Seeds from overexpressing constructs showed a strong blackening), another possibility for increased anthocyanin amounts in darkness could be that measured anthocyanin contents in darkness result from the amount already stored in the embryo from light-grown plants. In this regard, *de novo* synthesis needs to be analyzed in darkness by investigating for example biosynthetic gene expression of overexpressing lines. It is also possible to measure anthocyanin content in dark-grown seedlings over time,

even though an initial experiment failed due to high variation between the samples (data not shown).

III.5 COP1/SPA-dependent regulation of PAP1 and PAP2 function

This study revealed that PAP1 and PAP2 protein levels in 35S overexpressing plants are stabilized by light, indicating an additional post-translational mechanism involved in the regulation of PAP function besides the already characterized regulation via transcription (Cominelli et al., 2008). Since low amounts of HA-PAP proteins were still detectable also in darkness, the increased anthocyanin amounts in dark-grown *35S::HA-PAP* lines described under III.4, were due to constitutive synthesis of PAP proteins via the *35S CaMV* promoter. In this regard, PAP proteins are suggested to be repressed very strongly in darkness compared to light.

Together with the results of the Yeast Two-Hybrid analysis, COP1/SPA complexes could therefore be involved in the regulation of PAP protein levels in darkness and/or light. A few other evidences support the association of PAP with COP1/SPA complexes under both conditions: Anthocyanin accumulated very strongly in *spa* triple as well as *cop1-4* mutants in darkness and light. In addition, *cop1-4 hy5-215* double mutants accumulated anthocyanin levels that are similar to wild type under both conditions, indicating that HY5, a known target of COP1/SPA complexes, is not the only COP1/SPA target in the regulation of light-dependent anthocyanin biosynthesis. Furthermore, crosses of *PAP1*RNAi as well as *Myb*RNAi mutants with *cop1-4* mutants clearly indicate a strong contribution of PAP1, PAP2, MYB113 and MYB114 to increased anthocyanin levels in *cop1-4* mutants in the light (anthocyanin contents were reduced or nearly not detectable in *Myb*RNAi *cop1-4* double mutants). On the other hand, *PAP1*RNAi *cop1-4* as well as *Myb*RNAi *cop1-4* double mutants displayed only small reductions of anthocyanin levels in darkness compared to *cop1-4* mutants, what challenges the effect of COP1/SPA complexes on PAP function predominantly in darkness. Since the anthocyanin levels in darkness were

very low and the detection of differences was difficult, the experiments need to be repeated with more seed.

However, further supporting a repressive effect of COP1/SPA complexes on PAP-dependent regulation of anthocyanin biosynthesis *35S::HA-PAP2 cop1-4* crosses as well as crosses of *pap1-D* plants with the *cop1-4* mutant displayed dramatically increased anthocyanin levels in light and darkness compared to the *cop1-4* mutant under respective conditions. Since the increase of anthocyanin levels in darkness was stronger than in light, this suggests a regulatory effect of COP1 on PAP function like in other photmorphogenic responses predominantly in darkness.

Increased anthocyanin levels in *35S::HA-PAP2 cop1-4* and *pap1-D cop1-4* crosses compared to the *cop1-4* single mutant are at least in part due to a triggered biosynthesis by secondary promoting effects via other COP1-regulated targets. Accumulating HY5 protein, which is known to bind to promoters of the respective biosynthetic genes, is therefore considered to enhance anthocyanin biosynthesis observed in PAP overexpressing *cop1-4* mutant plants. Further, the fact that increased HY5 levels in *cop1-4* mutants in darkness also promote most likely the expression of the transcription factor LZF1 and thus the expression of the *PAP1* gene may represent an additional explanation for increased anthocyanin biosynthesis and the regulation of *PAP1* expression in *35S::HA-PAP cop1-4* plants and *pap1-D cop1-4* double mutants (Chang et al., 2008). In this regard, one could investigate how *LZF1* mRNA levels in *pap1-D cop1-4* crosses are regulated in darkness versus light. In order to test whether there is another COP1-dependent regulatory mechanism on *PAP1* transcription, *PAP1* expression could be also measured in *lzf1 cop1-4* double mutants. Further, PAP overexpression in already available *cop1-4 hy5-215* double mutant plants may help to study the HY5-independent regulation of PAP function via COP1/SPA complexes more detailed. How *PAP2* expression is affected in *cop1-4* mutants remains unknown and needs to be investigated in darkness versus light, too.

To verify cross-reactions of PAP proteins with other bHLH factors that could accumulate in *cop1-4* mutants and therefore COP1-dependent regulation of anthocyanin biosynthesis, the analysis of mutants for different bHLH proteins involved in anthocyanin biosynthesis, like GL3, EGL3 or TT8,

in a PAP overexpressor in *cop1* mutant background is necessary. Further, the analysis of *cop1-4* mutants crossed to *gl3*, *egl3*, *tt8* single-, double- and triple mutants may help to understand the contribution of bHLH factors involved in anthocyanin biosynthesis to light-dependent COP1 function in more detail. However, it is neither clear whether these proteins accumulate in *cop1-4* mutants nor if COP1 affects the transcription of these factors indirectly. In this regard, analysis of *GL3*, *EGL3* and *TT8* transcript levels in *cop1-4* mutants is highly necessary. In addition, there could be other PAP-independent regulations of anthocyanin biosynthesis by factors accumulating in *cop1-4* mutants besides bHLH factors and HY5.

In general, a complementation analysis of transgenic PAP proteins in *pap*-mutant background, as well as the analysis in *cop1-4* mutant background is required to elude native *PAP* expression and therefore further characterize PAP function in darkness versus light. Since a T-DNA knockout mutant of PAP1 is so far only available in No-0 background, whereas *cop1* mutants are only available in Col-0 background, and T-DNA knockouts, as well as EMS mutants for the other PAPs are difficult to generate because of high linkage of these genes (*MYB113*, *MYB114* and *PAP2* occur in a tandem on chromosome 1), this needs further attempt.

Since I was able to show that HA-tagged PAP proteins accumulate strongly when plants are treated with the proteasome inhibitor MG132, and HA-PAP as well as HA-PAP2 protein accumulates light-dependently in 35S overexpressing lines, while there are only minor changes at the transcript level in these transgenic seedlings in wild-type background, a post-translational mechanism regulating PAP protein levels is most likely. An initial experiment using *35S::HA-PAP2 cop1-4* seedlings showed indeed an increase in HA-PAP2 protein levels in light and darkness compared to wild-type plants expressing *35S::HA-PAP2*, indicating a regulatory function of COP1 on PAP2 protein steady-state levels. Since COP1/SPA complexes act mainly in darkness these results imply an additional function in light. Since there were only small effects observed on HA-PAP2 protein levels in *cop1-4* mutant background, whereas HA-PAP protein levels in wild-type background were decreased very strongly in darkness, additional post-translational mechanisms involved in the regulation of PAP protein levels in darkness are

most likely. However, in order to verify the differences of PAP2 proteins in *35S::HA-PAP2 cop1-4* in light and darkness more properly the experiments need to be repeated again. In addition, an analysis of transcript in light versus darkness is required to exclude an effect of COP1 on *35S::HA-PAP* transcript stability. In case of PAP1 an anti-PAP1 antibody may help to observe the endogenous PAP1 protein levels in *cop1-4* mutants since 35S::*HA-PAP1* overexpressing lines in the *cop1-4* background showed silencing. In addition, a transition experiment from light to darkness using the proteasomal blocker MG132 is necessary to further characterize the turnover of the proteins in light versus darkness.

Besides a direct regulation via COP1/SPA complexes, HA-PAP2 proteins in *cop1-4* mutant background could also be stabilized at least in part by interaction with other factors that accumulate due to the *cop1* mutation (bHLH and Myb factors can associate during many responses). To ensure that PAP proteins are direct targets of COP1/SPA complexes, an ubiquitination assay *in vitro* and/or *in planta* (Liu et al., 2010) needs to be performed.

To further study the contribution of SPA proteins to PAP-dependent anthocyanin biosynthesis, the PAP-overexpressing lines were crossed to *spa* triple mutants. However, the respective transgenic mutants were not available at the end of this study and still need to be analyzed. In addition to COP1/SPA complex regulation on its own, participation of the CUL4-DDB1 protein complex in the regulation of PAP function is also likely, since *cul4cs cop1-4* double mutants accumulate exceedingly strong anthocyanin amounts compared to *cop1-4* and *cul4cs* single mutants (Chen et al., 2010). This implies the involvement of CUL4 in light-dependent anthocyanin biosynthesis, probably as part of COP1/SPA and other protein complexes. It further emphasizes the importance of both proteins for anthocyanin biosynthesis.

Taken together, the analysis of *PAP*RNAi *cop1-4* and *Myb*RNAi *cop1-4* double mutants as well as PAP overexpressing lines crossed to *cop1-4* mutant background implies a strong regulation of PAP1 and PAP2 function via COP1 in anthocyanin biosynthesis in light and darkness at the seedling stage. To this end, anthocyanin biosynthesis was stimulated in PAP-overexpressing lines in wild-type background under respective conditions and even stronger

triggered in the PAP overexpressing lines in *cop1-4* mutant background. Other studies indicated that *PAP1* is regulated via COP1 function on the transcriptional level in darkness, whereas the impact of COP1/SPA complexes on *PAP2* expression is unknown. My experiments, using *35S::HA-PAP2* expression in a *cop1-4* mutant background, showed an additional effect of COP1 on the regulation of PAP protein levels. However, it is so far not clear whether PAP protein levels accumulate solely due to a direct effect of COP1 or, at least in part, due to stabilization via other factors (Figure 3.3). This needs to be verified.

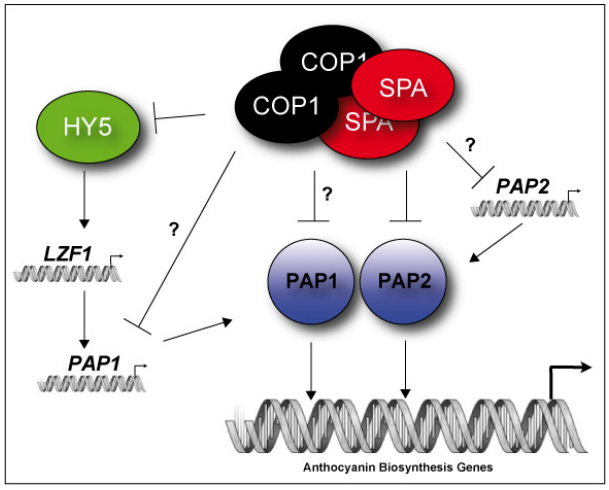

Figure 3.3: Possible regulatory mechanisms of PAP1 and PAP2 function via COP1/SPA complexes. HY5 was found to stimulate *PAP1* expression via the trans factor LZF1. Based on my results COP1/SPA complexes most likely regulate PAP2 protein levels post-translationally in light and darkness. The regulation of PAP1 protein remains so far unclear. In addition, other mechanisms could affect PAP transcript levels. How COP1/SPA complexes could inhibit *PAP1* and *PAP2* expression in addition to regulation via HY5 remains so far unclear.

III.6 PAP protein regulation during *Arabidopsis* plant development

Transfer experiments from darkness to white light using *35S::HA-PAP1* and *35S::HA-PAP2* overexpressing seedlings revealed that PAP protein levels are changed over time. They strongly accumulated six hours after light exposure, whereas protein levels in darkness remain more or less the same in comparison to the protein amounts before transition. In contrast, transcription seemed to be unaffected. This indicates a fast additional mechanism besides

the regulation of the transcript levels in controlling PAP protein levels in darkness and light. HA-PAP levels are decreased after one day in continuous white light and increase again after four days. This is also observed as a tendency in dark-grown seedlings. Thus, light seems to increase PAP protein levels overall, but does not have an effect on the decrease after one day. Therefore, the developmental stage of the seedlings seems to play a role in the regulation of PAP protein levels. It might be that PAP protein levels are only tolerated to a certain level at different developmental stages, and this level may also differ between light and darkness. However, it is difficult to postulate possible mechanisms explaining this turnover based on my experiments, although proteasomal degradation might represent the base for this regulation.

Anthocyanin accumulation is also part of stress responses; therefore a limitation of PAP protein levels appears to be reasonable to prevent the plant from overstimulation. The amounts of anthocyanin in crosses of *cop1-4* mutant plants with PAP-overexpressing plants are further underlining this, since the increase in the light was not that strong as in dark-grown seedlings. For future experiments it would be interesting to measure PAP protein and transcript levels at the early seedling stage during shorter time periods in order to get an idea about the rapid turnover of the PAPs and therefore fine tuning of anthocyanin biosynthesis in seedlings. It would also be interesting to test for tissue-specific regulation of PAP function since it was revealed that anthocyanin biosynthesis occurs in different cell types (Xie et al., 2006; Shi et al., 2010; this study). In this regard, correlating features of PAP function with those of COP1/SPA complex, which was found for some developmental processes to act in the phloem and mesophyll (Ranjan, 2010), might also be helpful. In order to analyze the involvement of SPA proteins in cell-specific anthocyanin biosynthesis, already existing lines expressing SPA1 under tissue-specific promoters could be analyzed. In general, differences regarding the tissue specificity of COP1/SPA regulation of the PAPs on the transcriptional and post-translational levels are possible.

IV Materials and Methods

IV.1 Materials

IV.1.1 Plant materials

Arabidopsis thaliana wild types, mutants, transgenic lines and crosses used and generated in this study are listed in tables 4.1, 4.2, 4.3 and 4.4, respectively.

Table 4.1 Wild-type *Arabidopsis* accessions used in this study

Accession	Abbreviation
Columbia	Col-0
Nossen	No-0
RLD	RLD

Table 4.2 Mutant lines used in this study

Mutant allele	Accession	Mutagen	Reference/Source
cop1-4	Col-0	EMS	Mc Nellis et al., 1994
cop1-6	Col-0	EMS	Mc Nellis et al., 1994
myb75 Ds	No-0	T-DNA	Teng et al., 2005
hy5-215	Col-0	EMS	Oyama et al., 1997
cop1-4 hy5-215	Col-0	EMS	Roman Ulm, University of Geneva (unpublished)
*PAP1*RNAi	Col-0	T-DNA RNAi	Gonzalez et al., 2008
*Myb*RNAi	Col-0	T-DNA RNAi	Gonzalez et al., 2008
spa1spa2spa3spa4	Col-0	EMS, T-DNA	Laubinger et al., 2004
spa1spa3spa4	Col-0	EMS, T-DNA	Laubinger et al., 2004
spa1-100	Col-0	T-DNA	Yang et al., 2005
spa2-1	Col-0	T-DNA	Laubinger et al., 2004

spa2-2	Col-0	T-DNA	Balcerowicz et al., 2011
spa1-3	RLD	EMS	Hoecker et al., 1998
spa1-7	Col-0	T-DNA	Fittinghoff et al., 2006

Table 4.3 Transgenic lines used in this study

Line	Accession	Reference/Source
SPA1::SPA1-HA (26)	RLD	Fittinghoff et al., 2006
35S::GUS-SPA2 (4/6)	Col-0	Laubinger et al., 2004
pap1-D	Col-0	Borevitz et al., 2000
35S::HA-PAP1	Col-0	Generated in this study
35S::PAP1	Col-0	Generated in this study
35S::AcV5-PAP1	Col-0	Generated in this study
35S::HA-PAP2	Col-0	Generated in this study

Table 4.4 crosses generated in this study

Cross	Accession	Reference/Source	Resistance
pap1-D cop1-4	Col-0	Generated in this study	BASTA^r
35S::HA-PAP1 cop1-4	Col-0	Generated in this study	BASTA^r
35S::HA-PAP2 cop1-4	Col-0	Generated in this study	BASTA^r
*PAP1*RNAi *cop1-4*	Col-0	Generated in this study	Kan^r
*Myb*RNAi *cop1-4*	Col-0	Generated in this study	Kan^r

BASTA^r: BASTA resistant; Kan^r: Kanamycin resistant

IV.1.2. Bacterial and Yeast Strains

IV.1.2.1 *Escherichia coli* (*E.coli*) strains

All *E. coli* strains were obtained from Invitrogen (Karlsruhe, Germany) and Stratagene (Santa Clara, USA).

DH5α

Genotype: F^- Φ80d*lac*ZΔM15 Δ(*lac*ZYA-*arg*F) U169 *deo*R *rec*A1 *end*A1 *hsd*R17(rk^-, mk^+) *pho*A *sup*E44 λ^- *thi*-1 *gyr*A96 *rel*A1

DB3.1

Genotype: F^- *gyrA462 end*A Δ(*sr*1-*rec*A) *mcr*B *mrr hsd*S20 (rB^-,-mB^-) *sup*E44 *ara*-14 *gal*K2 *lac*Y1 *pro*A2 *rps*L20 (SmR) *xyl*5 λ^- *leu mtl*1

BL21-CodonPlus (DE3)-RIL

Genotype: B F^- *ompT hsdS* (r_B^- m_B^-) dcm^+ Tet^r *gal* λ (DE3) *endA* Hte [*argU ileY leuW* Cam^r]

IV.1.2.2 *Agrobacterium tumefaciens* strains

DNA constructs for stable transformation of *Arabidopsis* plants were transformed in *Agrobacterium tumefaciens* strain GV3101 (pMK90RK) (Koncz et al., 1994).

IV.1.2.3 *Saccharomyces cerevisiae* strains

AH109

MATa, *trp1-901, leu2-3, 122, ura3-52, his3-200, gal4Δ, gal80Δ*,
LYS2::GAL1$_{UAS}$*-GAL1*$_{TATA}$*-HIS3,GAL2*$_{UAS}$*-GAL2*$_{TATA}$*-ADE2*,
URA3::MEL1$_{UAS}$*-MEL1*$_{TATA}$*-lacZ*
(James et al., 1996; A. Holtz unpublished)

IV.1.3 Vectors

The following vectors have been used or were generated in this study:

IV.1.3.1 Gateway™ Entry vectors

Vector	Description
pDONR 221	Gateway™ Entry vector. For cloning of PCR products using recombination (Invitrogen). Resistance in *E.coli:* Kanamycin (50 µg/ml).
SPA1-pENTR3c	Gateway™ Entry vector. Contains *SPA1* cDNA (Braun, 2005). Resistance in *E.coli:* Kanamycin (50 µg/ml).
SPA2-pENTR3c	Gateway™ Entry vector. Contains *SPA2* cDNA (Adrian, 2005). Resistance in *E.coli:* Kanamycin (50 µg/ml).
SPA3-pENTR2b	Gateway™ Entry vector. Contains *SPA3* cDNA (Adrian, 2005). Resistance in *E.coli:* Kanamycin (50 µg/ml).
SPA4-pENTR2b	Gateway™ Entry vector. Contains *SPA4* cDNA (Adrian, 2005). Resistance in *E.coli:* Kanamycin (50 µg/ml).
COP1-pDONR201	Gateway™ Entry vector. Contains *COP1* cDNA. (Braun, 2005). Resistance in *E.coli:* Kanamycin (50 µg/ml).
COP1-915-pDONR221	Gateway™ Entry vector. Contains first 915 bp of *COP1* cDNA. Resistance in *E.coli:* Kanamycin (50 µg/ml). (Created in this study)
SPA1-570-pDONR221	Gateway™ Entry vector. Contains first 570bp of *SPA1* cDNA. Resistance in *E.coli:* Kanamycin (50 µg/ml) (Created in this study)

PAP1-pENTR	Gateway™ Entry vector. Contains *PAP1* cDNA with stopcodon. (Kindly provided by Andrea Schrader, Huelskamp laboratory)
PAP1-396-pDONR221	Gateway™ Entry vector. Contains last 396 bp of *PAP1* cDNA. Resistance in *E.coli:* Kanamycin (50 µg/ml) (Created in this study)

IV.1.3.2 Vectors used in *in vitro* CoIP studies

Vector	Description
GAD-pET15b	Conventional cloning vector used for *in vitro* protein synthesis of GAL4 activation domain fused proteins driven by a T7 promoter. (Hoecker and Quail, 2001) Resistance in *E.coli:* Ampicillin (100 µg/ml).
GAD-SPA1-pET15b	*In vitro* protein synthesis of SPA1 protein fused N-terminally with GAL4 activation domain. (Hoecker and Quail, 2001)
SPA1-pET15b	*In vitro* protein synthesis of non-tagged SPA1 protein. (Obtained from U. Hoecker, unpublished)
GAD-SPA2-pET15b	*In vitro* protein synthesis of SPA2 protein fused N-terminally with GAL4 activation domain. (Laubinger et al., 2004)
SPA2-pET15b	*In vitro* protein synthesis of non-tagged SPA2 protein. (Obtained from U. Hoecker, unpublished).
GAD-SPA3-pET15b	*In vitro* protein synthesis of SPA3 protein fused N-terminally with GAL4 activation domain (Laubinger and Hoecker, 2003).
SPA3-pET15b	*In vitro* protein synthesis of non-tagged SPA3 protein (Obtained from U. Hoecker, unpublished).

GAD-SPA4-pET15b	*In vitro* protein synthesis of SPA4 protein fused N-terminally with GAL4 activation domain. (Laubinger and Hoecker, 2003)
SPA4-pET15b	*In vitro* protein synthesis of non-tagged SPA4 protein (Obtained from U. Hoecker, unpublished).
SPA1-NT696 -pET15b	Used for *in vitro* protein synthesis of the first 696 amino acids of SPA1 protein. Lacking WD40 repeat domain (Hoecker and Quail, 2001).
SPA1-NT545-pET15b	Used for *in vitro* protein synthesis of the first 545 amino acids of SPA1 protein. Lacking coiled coil and WD40 repeat domain (Hoecker and Quail, 2001).
SPA1-CC-pET15b	Used for *in vitro* protein synthesis. Contains the coiled-coil domain of SPA1 protein (Hoecker and Quail, 2001).

IV.1.3.3 Vectors used for Bimolecular Fluorescence Complementation assay studies

Vector	**Description**
pCL112	*CaMV 35S* promoter containing binary Gateway™ vector which carries the N-terminal part of YFP (YN) protein in front of the Gateway™ site. Christian Lauterbach (Scottish Crop Research Institute, Invergowrie, Dundee) Resistance in *E.coli:* Spectinomycin (100µg/ml). Resistance in plants*:* BASTA (10 µg/ml)
pCL113	*CaMV 35S* promoter containing binary Gateway™ vector which carries the C-terminal part of YFP (YC) protein in front of the Gateway™ site Christian Lauterbach (Scottish Crop Research Institute, Invergowrie, Dundee).

	Resistance in *E.coli:* Spectinomycin (100 µg/ml)
	Resistance in plants*:* BASTA (10 µg/ml)
SPA1-pCL112	N-terminal part of YFP fused to SPA1 protein (Created in this study).
SPA1-pCL113	C-terminal part of YFP fused to SPA1 protein (Created in this study).
SPA4-pCL112	N-terminal part of YFP fused to SPA4 protein (Created in this study).
SPA4-pCL113	C-terminal part of YFP fused to SPA4 protein (Created in this study).
CPRF1-YN	N-terminal part of YFP fused to CPRF1 protein (Stolpe et al., 2005).
	Resistance in *E.coli:* Ampicillin (100 µg/ml)
CPRF1-YC	C-terminal part of YFP fused to CPRF1 protein (Stolpe et al., 2005).
	Resistance in *E.coli:* Ampicillin (100 µg/ml)
CFP-m-Talin	CFP-talin constitutively expressed by *CaMV 35S* promoter (Saedler et al., 2004).
	Resistance in *E.coli:* Ampicillin (100 µg/ml)

IV.1.3.4 Vectors employed in Co-localization experiments (Created by Braun, 2005)

Vector	**Description**
pENSG-CFP	*CaMV 35S* promoter containing binary Gateway™ vector for N-terminal CFP fusions.
	Resistance in *E.coli:* Ampicillin (100 µg/ml)
	Resistance in plants*:* BASTA (10 µg/ml)
pENSG-YFP	*CaMV* 35S promoter containing binary Gateway™ vector for N-terminal YFP fusions.
	Resistance in *E.coli:* Ampicillin (100 µg/ml)
	Resistance in plants*:* BASTA (10 µg/ml)

CFP-SPA1	Full length CFP fused to SPA1 protein.
YFP-SPA1	Full length YFP fused to SPA1 protein.
CFP-SPA2	Full length CFP fused to SPA2 protein.
YFP-SPA2	Full length YFP fused to SPA2 protein.
CFP-SPA3	Full length CFP fused to SPA3 protein.
YFP-SPA3	Full length YFP fused to SPA3 protein.
CFP-SPA4	Full length CFP fused to SPA3 protein.
YFP-SPA4	Full length YFP fused to SPA3 protein.

IV.1.3.5 Vectors used for antibody production

Vector	**Description**
pDEST17	Gateway™ Destination vector for expression of His_6 -tagged recombinant protein in *E.coli* (Invitrogen). Resistance in *E.coli:* Ampicillin (100 µg/ml)
pet32b(+)-attR	Gateway™ Destination vector for expression of recombinant protein in *E.coli* (Backbone Merck™, modified Huelskamp laboratory, unpublished). Contains a Thioredoxin-, 2x His_6- and S-tag. Resistance in *E.coli:* Ampicillin (100 µg/ml)
COP1-915-pet32b(+)	Gateway™ Expression vector for expression of recombinant COP1-NT protein in *E.coli.* First 915 bp of *COP1* cDNA. Thioredoxin-, His_6- and S-tag (Created in this study).
SPA1-570-pDEST17	Gateway™ Expression vector for expression of His_6 tagged recombinant SPA1 protein in *E.coli.* The first 570 bp of *SPA1* cDNA were expressed (Created in this study).

PAP1-396-pDEST17	Gateway™ Expression vector for expression of His_6 tagged recombinant PAP1 protein in *E.coli.* The last 396 bp of *PAP1* cDNA were expressed (Created in this study).

IV.1.3.6 Vectors used for Yeast Two-Hybrid analysis

Vector	Description
pGADT7	Vector for conventional cloning, used for Yeast Two-Hybrid analysis. Contains GAL4-activation domain (Clontech™). Resistance in *E.coli:* Ampicillin (100 µg/ml). Resistance in *S.cerevisiae:* Leucin
pGBKT7	Vector for conventional cloning, used for Yeast Two-Hybrid analysis. Contains GAL4-binding domain (Clontech™). Resistance in *E.coli:* Kanamycin (50 µg/ml) Resistance in *S.cerevisiae:* Tryptophane
pAS2-attR	Gateway™ Destination vector for Yeast Two-Hybrid analysis. Contains GAL4 binding domain (Clontech™, modified by Huelskamp laboratory, unpublished). Resistance in *E.coli:* Ampicillin (100 µg/ml) Resistance in *S.cerevisiae:* Tryptophan
SPA1-GBKT7	Yeast Two-Hybrid vector. GAL4-binding domain fused to SPA1 (Obtained from U. Hoecker).
SPA2-GBKT7	Yeast Two-Hybrid vector GAL4-binding domain fused to SPA2. (Obtained from U. Hoecker).
SPA3-pAS2-attR	Yeast Two-Hybrid vector. GAL4-binding domain fused to SPA3 (Created in this study).
SPA4-GBKT7	Yeast Two-Hybrid vector. GAL4-binding domain fused to SPA4 (Obtained from U. Hoecker).

COP1-GBKT7	Yeast Two-Hybrid vector. GAL4-binding domain fused to COP1 (Obtained from U. Hoecker).
PAP1-pAct-attR	Yeast Two-Hybrid vector. GAL4-activation domain fused to PAP1 (Kindly provided by Andrea Schrader, Huelskamp laboratory).
PAP2-pAct-attR	Yeast Two-Hybrid vector. GAL4-activation domain fused to PAP2 (Kindly provided by Andrea Schrader, Huelskamp laboratory).

IV.1.3.7 Vectors used for generation of transgenic *Arabidopsis* plants

Vector	Description
pEGATE 100	*CaMV 35S* promoter containing binary Gateway™ vector (Early et al., 2006). Resistance in *E.coli:* Kanamycin (50µg/ml) Resistance in plants BASTA (10 µg/ml)
pEGATE 204	*CaMV 35S* promoter containing binary Gateway™ vector. Contains an *AcV5*-tag in front of the Gateway site (Early et al., 2006). Resistance in *E.coli:* Kanamycin (50 µg/ml) Resistance in plants BASTA (10 µg/ml)
PAP1-pEGATE100	*CaMV 35S* promoter containing binary Gateway™ vector. Constitutively expresses *PAP1* cDNA without a tag (Created in this study).
PAP1-pEGATE201	*CaMV 35S* promoter containing binary Gateway™ vector. Constitutively expresses *PAP1* cDNA fused to *HA*- tag (Kindly provided by Andrea Schrader, Huelskamp laboratory).
PAP1-pEGATE204	*CaMV 35S* promoter containing binary Gateway™ vector. Constitutively expresses *PAP1* cDNA fused to *AcV5*- tag (Created in this study).

PAP2-pEGATE201 — *CaMV 35S* promoter containing binary Gateway™ vector. Constitutively expresses *PAP2* cDNA fused to *HA*- tag (Kindly provided by Andrea Schrader, Huelskamp laboratory).

IV.1.4 Oligonucleotides

Primers used in this study are listed in Table 4.5. Oligonucleotides were purchased from Invitrogen (Karlsruhe, Germany) or Metabion (Martinsried, Germany). Start- and stop-codons are highlighted in red. Lyophilized primers were resuspended in ddH_2O to a final concentration of 100 pmol/µl (=100µM). Working solutions were diluted to 10 pmol/µl (=10 µM).

Table 4.5 Oligonucleotides used in this study

Primer	Sequence (5'>3')	Characteristics	Purpose
COP1-attB1	GGGGACAAGTTTGTACAAAAAAGCAGGC TGCATGGAAGAGATTTCGACGGA	Gateway™ primer fwd. / BP reaction	Antibody production
COP1-attB2-915NT	GGGGACCACTTTGTACAAGAAAGCTGGG TCTAAATCATTGAACTGAGCATG	Gateway™ primer rev. / BP reaction	
SPA1-attB1	GGGGACAAGTTTGTACAAAAAAGCAGGC TTAATGCCTGTTATGGAAAGAGT	Gateway™ primer fwd. / BP reaction	
SPA1-570-R-attB2	GGGGACCACTTTGTACAAGAAAGCTGGG TACATTTGGACACCTTCACTGATC	Gateway™ primer rev. / BP reaction	
PAP1-352-attB1	GGGGACAAGTTTGTACAAAAAAGCAGGC TTCATAAAGATGAAAAAGAGAG	Gateway™ primer fwd. / BP reaction	
PAP1-attB2	GGGGACCACTTTGTACAAGAAAGCTGGG TACTAATCAAATTTCACAGTCTCTC	Gateway™ primer rev. / BP reaction	
SPA1-2917-F-RT	TCTTTACCGATGCCAATGACT	Realtime primer fwd.	Realtime analysis
SPA1-2998-R-RT	CAGACGCTCGACACAAACTG	Realtime primer rev.	

SPA2-RT-2932-F	TCAGGTAAGGAGATAGAGGAGGAC	Realtime primer fwd.	
SPA2-RT-3043-R1	TGTAGAACTTTGATTGACCCATTT	Realtime primer rev.	
PAP-attB2-F1	CAAAGTGGTGCCTAGGTGAG	Realtime primer fwd. *HA-PAP*	
OCS-R	AGGCGTCTCGCATATCTCAT	Realtime primer rev. *HA-PAP*	
UBQ10 F3	GGCCTTGTATAATCCCTGATGAATAAG	Realtime primer fwd.	
UBQ10 R3	AAAGAGATAACAGGAACGGAAACATAGT	Realtime primer rev.	
35S-F2	GTAAGGGATGACGCACAATCC	Colony PCR primer fwd.	**Cloning, transgenic plants**
PAP1-252-R	GAAGATCGACTTCATCAGAGC	Colony PCR primer rev.	

fwd.: forward; rev.: reverse

IV.1.5 Enzymes

IV.1.5.1 Restriction endonucleases

Restriction enzymes were purchased from Fermentas (St.Leon-Rot, Germany). Enzymes were supplied with 10 x reaction buffer, which was used for restriction digests.

IV.1.5.2 Nucleic acid modifying enzymes

Standard PCR reactions were performed using home-made Taq DNA polymerase. Pfu polymerase was used when PCR products were generated for cloning. Modifying enzymes and their suppliers are listed below:

Taq DNA polymerase	home made (K.Fittinghoff)
Pfu DNA polymerase (native)	Fermentas (St.Leon-Rot, Germany)

RevertAid™ H Minus M-MuLV Reverse transcriptase	Fermentas (St. Leon-Rot, Germany)
Gateway™ BP Clonase™ Enzyme mix	Invitrogen (Karlsruhe, Germany)
Gateway™ LR CLonase™ Enzyme mix	Invitrogen (Karlsruhe, Germany)

IV.1.5.3 Restriction proteases

Enterokinase	Roche (Mannheim, Germany)

IV.1.6 Chemicals

Laboratory grade chemicals and reagents were purchased from Applichem (Darmstadt, Germany), Applied Biosystems (Carlsbad, USA), Bio-Rad Laboratories (Hercules, USA), Clontech (Palo Alto, USA), Colgate-Palmolive (Hamburg, Germany), Difco (Detroit, USA), Duchefa (Haarlem, Netherlands), Gibco BRL (Neu Isenburg, Germany), Fermentas (St. Leon- Rot, Germany), Invitrogen (Karlsruhe, Germany), Merck (Darmstadt, Germany), Promega (Mannheim, Germany), Riedel-de-Haen (Seelze, Germany), Roche (Mannheim, Germany), Roth (Karlsruhe, Germany), Serva (Heidelberg, Germany), Sigma-Aldrich (Munich, Germany), Thermo Scientific (Rockford, USA), VWR (Darmstadt, Germany).

IV.1.7 Media

Media were sterilized by autoclaving at 121°C for 20 min. For the addition of antibiotics and heat label compounds the solution was cooled to 60°C. Antibiotics were sterilized using filter sterilization units prior to addition.

Escherichia coli media

LB (Luria-Bertani) broth

Tryptone	10.0	g/l
Yeast extract	5.0	g/l
NaCl	5.0	g/l

For LB agar plates 1.5% (w/v) agar was added to the broth above.

Agrobacterium tumefaciens media

YEB

Beef extract	5.0	g/l
Yeast extract	1.0	g/l
Peptone	5.0	g/l
Sucrose	5.0	g/l
1M $MgSO_4$	2.0	ml/l

pH 7.2

For YEB agar plates 1.5 % (w/v) agar was added to the broth above.

Saccharomyces cerviseae media

YAPD (Yeast Extract Adenine Peptone Dextrose Medium)

Peptone	20.0	g/l
Yeast extract	10.0	g/l
Glucose	20.0	g/l
Adenine hemisulfate	100	mg/l

pH 5.8

Synthetic “drop-out” medium

Nitrogen base	6.7	g/l
Glucose	20.0	g/l
Adenine hemisulfate	40	mg/l
Drop-out supplement	(0.64 g/l –Leu,-Trp/ or 0.6 g/l –Leu,-Trp,-His,-Ade)	

Plant MS media

Murashige and Skoog

MS salt 4.62 g/l

pH 5.7

For MS agar plates 1% (w/v) agar was added.

IV.1.8 Radioactivity

[^{35}S]-Methionin was purchased from GE Healthcare (Piscataway, USA) and Hartmann Analytic (Braunschweig, Germany).

IV.1.9 Antibiotics (stock solutions)

Ampicillin (Amp)	100 mg/ml in ddH2O
Gentamycin (Gent)	15 mg/ml in ddH2O
Kanamycin (Kan)	50 mg/ml in ddH2O
Rifampicin (Rif)	100 mg/ml in DMSO
Spectinomycin (Spec)	10 mg/ml in ddH2O
Tetracycline (Peng et al.)	10 mg/ml in 70 % ethanol
Chloramphenicol (Cm)	100 mg/ml in isopropyl alcohol

Stock solutions (1000x; 100x for Spectinomycin) stored at -20° C. Aqueous solutions were sterile filtrated.

IV.1.10 Antibodies

Listed below are primary and secondary commercially available antibodies used for immunoblot detection.

Primary antibodies

Antibody	Source	Dilution	Reference
anti-HA 3F10	rat monoclonal	1:4000	Roche (Mannheim, Germany)
anti-HA 3F10 (HRP conj.)	rat monoclonal	1:1000	Roche (Mannheim, Germany)
anti-HSC-70	mouse monoclonal	1:20000	Stressgen (Victoria, Canada)

Antibody	Source	Dilution	Reference
anti-Histone-H3	rabbit polyclonal	1:5000	Abcam (Cambridge, UK)
anti-GAL4-AD	mouse monoclonal	1:1000	Santa Cruz (Santa Cruz, USA)
anti-His_6	mouse monoclonal	1:1000	Roche (Mannheim, Germany)

Secondary antibodies

Antibody	Source	Dilution	Reference
goat anti-rat IgG-HRP	horseradish peroxidase conjugated	1:5000	Santa Cruz (Santa Cruz, USA)
goat anti-mouse IgG-HRP	horseradish peroxidase conjugated	1:10000	Sigma-Aldrich (Munich,Germany)
goat anti-rabbit IgG-HRP	horseradish peroxidase conjugated	1:80000	Sigma-Aldrich (Munich,Germany)

IV.1.11 Buffers and solutions

General buffers and solutions are displayed in the following listing. All buffers and solutions were prepared with Milli-Q® or TKA® water. Buffers and solutions for molecular biological experiments were autoclaved. Buffers and solutions not displayed in this listing are denoted within the corresponding methods.

DNA gel loading dye (10x)	Glycerol	30	%(v/v)
	Brome phenol blue	0,25	%(w/v)
PCR reaction buffer (10x)	Tris	100	mM
	KCl	500	mM
	$MgCl_2$	15	mM
	pH 9.0		
	Stock solution was filter-sterilized and used for home-made Taq DNA polymerase.		

Honda buffer	Ficoll 400	5	g
	Dextran T40	10	g
	Sucrose	27.38	g
	Tris	0.606	g
	$MgCl_2$	0.407	g
	dH_2O to 200 ml		
	pH 7.4		
	Prior to use 10 mM DTT and protease inhibitor cocktail for plant cell and tissue extracts (Sigma) were added.		
SDS-PAGE:			
Resolving gel buffer	Tris	1	M
	pH 8.8 (HCl)		
Stacking gel buffer	Tris	1	M
	pH 6.8 (HCl)		
Running buffer (10x)	Glycine	1.9	M
	Tris	240	mM
	SDS	34	mM
	ad 1l H_20		
Laemmli buffer (5x)	Tris (pH 6.8)	310	mM
	SDS	10	%(w/v)
	Glycerol	50	%(v/v)
	Bromephenol blue	0.5	%(w/v)
	DTT	500	mM
Immunoblot:			
Towbin Buffer	Glycine	96	mM
	Tris	10	mM
	Methanol	10	%(v/v)

Carbonate Buffer (1x)	Na_2CO_3	29	mM
	$NaHCO_3$	100	mM
	SDS	0.08	%(v/v)
TBS Buffer (10x)	NaCl	1.37	M
	Tris	100	mM
	pH 7.3 (HCl)		
TBS-T Buffer (1x)	NaCl	137	mM
	Tris	10	mM
	Tween® 20	0.1	% (v/v)
	pH 7.3 (HCl)		

IV.2. Methods

IV.2.1 Seed sterilization

In order to grow sterile *Arabidopsis* plants on MS-Plates, seeds were surface sterilized. Liquid sterilization was applied for anhocyanin measurements, protein preparation from seedlings and segregation analysis. The seeds were incubated with 20% (v/v) Klorix (Colgate- Palmolive, Hamburg, Germany) and 0.03% (v/v) Triton X-100 for 10 min. Afterwards, seeds were washed three times with sterile water, and plated on 1x MS with or without sucrose.
For segregation analysis seeds were sterilized by using chlorine gas. 80 ml of sodium hypochlorite was mixed with 2.5 ml concentrated hydrochloric acid in an exsiccator. Aliquots of seeds were incubated for approximately 3 h.

IV.2.2 Plant growth

Seeds of *Arabidopsis* were stratified at 4°C for minimum 3 up to 5 days. They were sown in a substrate mixture containing three parts soil and one part Vermiculit. In the greenhouse, plants were grown under long day conditions with 16 h light and 8 h darkness. The relative humidity was approximately 40%. A temperature of 21°C during light periods and 18°C during dark periods

was maintained. For seedling analysis on solid media plates samples were kept in the dark and stratified for 3 days at 4°C. Germination was induced by a 3 h white-light treatment (40 µmol $m^{-2}s^{-1}$, Fluora L58W/77, Osram, Berlin) at 21°C. The plates were kept for 21 h in darkness and then transferred to the certain light condition. For white light treatments seedlings were grown at 40 µmol $m^{-2}s^{-1}$. For far red light and red light treatment LED light sources (Quantum Devices, Barnevled, WI, USA) were employed. Seedlings were grown at 0.35 µmol $m^{-2}s^{-1}$ far-red or 30 µmol $m^{-2}s^{-1}$ red light.

IV.2.3 Measurement of Anthocyanin content

Seedlings were transferred to reaction tubes containing 300 µl of anthocyanin extraction buffer [18% (v/v) isopropyl alcohol; 1% (v/v) HCl]. The samples were boiled for 3 min at 100°C and incubated in darkness for 24 h. After 15 min of centrifugation 100 µl of the supernatants were transferred to a 96 well microtiterplate. The anthocyanin content was determined spectral-photometrically by the difference at the absorptions 535 nm and 650 nm (A_{535nm}-A_{650nm}) using a Tecan™ Infinite® 200 plate reader.

IV.3 Methods for molecular biology

IV.3.1 General methods in molecular biology

Standard methods of molecular biology like precipitation of nucleic acids, gel electrophoresis and staining of nucleic acids was performed after the protocols from Sambrook and Russell (2001). Purification of nucleic acids was carried out with the Qiagen Gel Extraction Kit or PCR Purification Kit (Qiagen GmbH, Hilden, Germany). Plasmid DNA from *E.coli* in miniprep scale was isolated using the Qia-prep Spin Miniprep Kit (Qiagen GmbH, Hilden, Germany). Larger amounts of plasmid were prepared with the Plasmid Midi (Qiagen GmbH, Hilden, Germany) or JetSorb-collumns (Genomed, Bad Oyenhausen) according to manufacturers protocols.

IV.3.2 Polymerase chain reaction (PCR)

Standard PCR was performed in a volume of 20 or 50 µl. Oligonucleotides (0.2 µM), dNTPs (0.5 mM) and 1x PCR reaction buffer (IV.1.11) were mixed. 1 µl of genomic DNA from plants or 1 µl from reverse transcription reaction were used as template. For a standard reaction 1 µl of home-made Taq was used. A Standard PCR cycle consisted of denaturing at 94°C for 30 sec, annealing at 55°C for 30 sec and elongation at 72°C for 30 sec per 1 kb. In case of proof reading Pfu polymerase (native) (Fermentas, St. Leon-Rot, Germany), the elongation was performed at 72°C for 60 sec per 1 kb. For Colony PCR a standard PCR reaction was carried out with a part of a *E.coli* colony directly added to the reaction. Denaturation in the beginning of the PCR run was prolonged to 5 min.

IV.3.3 Isolation of total RNA from seedling tissue

Total RNA from seedlings was isolated using the RNeasy Plant Mini Kits from Qiagen (Hilden, Germany) according to manufacturers protocol. RNA concentration was determined spectral-photometrically. The quality of the RNA was analyzed on a 2 % agarose gel.

IV.3.4 DNase treatment and reverse transcription of total RNA

1 µg of total RNA was incubated in a volume of 20 µl containing 2 µl DNase (RNase-free) and 2 µl of 10x DNase Buffer (Fermentas^{TM} (St. Leon-Rot, Germany) for 1 h at 37°C. 2 µl of EDTA (25mM) was added to the sample to prevent hydrolytic cleavage during the heat inactivation of the DNase. DNase was inactivated for 10 min at 65°C. 2 µl of the DNase-digested RNA were transferred to new reaction tubes to control the digest in a standard PCR (IV.3.2) using UBQ10 primers (Table 4.5).
For reverse transcription 20 µl of the digested RNA, together with Oligo-dT-nuleotides (25 mM) was denatured at 72°C in a volume of 26 µl for 10 min. The reaction tube was afterwards directly transferred to ice to prevent renaturation of the RNAs. 4 µl of 5 mM dNTPs, 8 µl of 5 x RT-buffer and 1 µl of RevertAID^{TM} H Minus M-MuLV reverse transcriptase (Fermentas, St. Leon-

Rot, Germany) was added. The sample was incubated for 5 min at 37°C and then 60 min at 42°C. Reverse Transcriptase was inactivated at 70°C for 10 min. The resulting cDNA was stored at -20°C until usage.

IV.3.5 Real time PCR

To determine transcript levels 1 µl of cDNA (resulting from IV.3.4) was analyzed in a 25 µl reaction containing POWER SYBR Green pre-mix (Applied Biosystems, Carlsbad, USA), and gene specific primers. The sample was analyzed in the Applied Biosystems 7300 real-time PCR system. Two biological replicates were used and each was analyzed in triplicate. The results were analyzed by the $\Delta\Delta C_t$ method. (www.appliedbiosystems.com).

IV.3.6 Gateway™ cloning

BP reaction and LR reaction were performed according to manufacturers protocol (Invitrogen, Karlsruhe, Germany). Empty Entry and Destination Gateway™ vectors were propagated in the *DB 3.1 E.coli* strain (see IV.1.2.1).

IV.3.7 DNA sequencing

All DNA sequences were determined by AGOWA (Berlin), GATC (Konstanz) or the University of Cologne (Department of Genetics).

IV.3.8 DNA sequence analysis

Sequence data were analyzed using Vector NTI®- (Invitrogen, Karlsruhe, Germany) and Lasergene®- (DNASTAR, Madison, USA) Software.

IV.3.9 Preparation of chemically competent *E.coli* cells

Chemically competent *E.coli* cells were prepared after Inoue et al. (1990). This protocol was performed for *DH5α, DB3.1* and *BL21-CodonPlus (DE3)-RIL* cells.

IV.3.10 Transformation of chemically competent *E.coli* cells

A 50 µl aliquot of chemically competent cells was thawed on ice. 10-100 ng of plasmid DNA was mixed with the aliquot and incubated on ice for 30 min. The mixture was heat-shocked for 90 sec at 42°C and immediately put on ice for 1 min. 500 µl of LB medium were added to the reaction tube and incubated at 37°C for 1 h on a shaker. The transformation mixture was centrifuged for 1 min at 13000 rpm, resuspended in 50 µl LB medium and plated onto selective media plates.

IV.3.11 Transformation of electro-competent *A.tumefaciens* cells

Electro-competent *Agrobacterium tumefaciens* cells of the strain GV3101 (pMK90RK) were transformed with the MicroPulser™ electroporator from Bio-Rad Laboratories (Hercules, USA) after manufacturers protocol. Transformed cells were resuspended in 50 µl YEB medium and plated onto selective media plates.

IV.3.12 *Agrobacterium*-mediated stable transformation of *Arabidopsis* (floral dip)

Agrobacteria transformation was performed after Clough and Bent (1998).

IV.3.13 Generation of transgenic *Arabidopsis* plants

PAP1 cDNA from PAP1-pENTR entry clone (see IV.1.3.1) was cloned by LR reaction into pEGATE100 and pEGATE204 (see IV.1.3.7) using Gateway® technology. Positive clones were selected by Colony PCR using primers listed in Table 4.5. PAP1-pEGATE201 and PAP2-pEGATE201 were obtained from Andrea Schrader (Huelskamp laboratory, Botanical Institute, Cologne, Germany). All destination vector constructs listed under point IV.1.3.7 were transformed into *Arabidopsis* wild-type (Col-0) plants by the floral dip method.

IV.3.13.1 Selection of *Arabidopsis* transformants

Stably transformed *Arabidopsis* Col-0 wild-type and *cop1-4* mutant plants with the constructs given under point IV.3.1.7 were selected with DL-Phosphinothricin (BASTA; Duchefa, Haarlem, Netherlands) spray [125 µg/ml BASTA; 0.04% (v/v) Silwet L-77] in T_1 generation. Segregation analysis in T_2- and T_3-generation was carried out on 1x MS plates containing 10 µg/ml BASTA.

IV.3.14 Crossings and selection of crosses

35S::HA-PAP1 L8/3, *35S::HA-PAP2* L8/8, *pap1-D, PAP1*RNAi and *Myb*RNAi plants were crossed into *cop1-4* mutant background (two independent crosses). Fine tweezers and a magnifying glass were used to emasculate an individual flower. To prevent self-pollination, only flowers that had a well-developed stigma but immature stamen were used for crossing. Pollen from donor stamens was dabbed onto each single stigma. Mature siliques containing F_1 seed were harvested and allowed to dry. Approximately five F_1 seeds per cross were grown as described above and allowed to self-pollinate. Produced F_2 seeds were collected and stored. F_2 seeds were grown in the greenhouse and in case of *35S::HA-PAP1*, *35S::HA-PAP2* and *pap1-D* crosses selected with BASTA (see IV.3.9.2). BASTA resistant *cop1-4* plants were selected to generate F_3 seeds. In case of *PAP1*RNAi and *Myb*RNAi crosses, 80 dwarf looking plants (homozygous for *cop1-4*) were selected and transferred to new pots. F_3 analysis was carried out on 1x MS plates containing BASTA and in case of *PAP1*RNAi and *Myb*RNAi crosses kanamycin to analyze segregation.

IV.4 Biochemical methods

IV.4.1 *Arabidopsis* total protein extraction for immunoblot analysis

For isolation of HA-tagged and non-tagged SPA1 protein and protein isolations performed for antibody production 100-300 mg of frozen tissue (in liquid nitrogen) from four-day-old seedlings were ground to a fine powder. The

powder was resuspended in protein extraction buffer [150 mM NaCl, 50 mM Tris, pH 7.5; 1 mM EDTA; 0.1 % (v/v) Nonidet-P20; 10 % (v/v) glycerol; 1 mM DTT; 1x Protease Inhibitor Cocktail P9599 (Sigma-Aldrich, Munich, Germany)]. The sample was clarified by 10 min (13000 rpm) centrifugation and total protein was determined using Bradford reagent (Bio-Rad Protein Assay, Bio-Rad, Hercules, USA). 20-40 µg of total protein were separated by SDS PAGE (see IV.4.5) and blotted onto polyvinylidene difluoride (PVDF) membranes (see IV.4.6).

For Isolation of PAP proteins 100 - 300mg from four-day-old seedlings, tissue were ground in liquid nitrogen. The powder was directly resuspended in 2x Laemmli buffer (IV.1.11) in a ration of 1:1.2. Total protein was determined by using the Amido Black staining method (IV.4.2). 50- 90 µg of total protein were separated by SDS-PAGE and blotted onto PVDF membranes.

IV.4.2 Amido Black assay

For determination of total protein from samples isolated in Laemmli buffer (IV.1.11) the Amido Black method was carried out. 5-7 µl of the sample were mixed with 500 µl of Amido Black dye solution [0.25 % (w/v) Napthol blue black, 45 % (v/v) methanol, 10 % (v/v) glacial acetic acid, ad H_2O]. Samples were mixed by vortexing and centrifuged at 14000 rpm for 10 min at room temperature to preticipate the proteins. After discarding the supernatant, pellets were washed with 1 ml wash solution [10% (v/v) glacial acetic acid, 90 % (v/v) methanol] and centrifuged again for 10 min at 14000 rpm. The supernatants were discarded again and the pellets air-dried for 10 min. The pellets were resupended in 1 ml 0.2N NaOH and 100 µl analyzed spectral-photometrically at the absorption 595 nm. The desired protein amount was calculated using a calibration curve.

IV.4.3 Nuclear fractionation for immunoblot analysis

Nuclear fractionation was performed according to the protocols of Kinkema et al. (2000) and Xia et al. (1997) with minor modifications. 1.5 g of four-day-old seedling tissue was homogenized in 3 ml Honda buffer (see IV.1.11) using a pre-cooled mortar and pestle. Samples were then filtered through a 62 µm

(pore size) nylon mesh by centrifugation at 400 *g* for 5 min. Triton X-100 (10% working solution) was added to a final concentration of 0.5 % and the solutions were incubated on ice for 15 min. The extracts were then centrifuged for 5 min at 1500 *g*. An aliquot of the nuclei-depleted fraction was saved and the pellets washed by gentle resuspension in 2.5 ml Honda buffer containing 0.1 % Triton X-100. The samples were centrifuged again at 1500 *g* for 5 min. Pellets were resuspended in 2.5 ml Honda buffer and 620 µl aliquots were transferred to 1.5 ml reaction tubes. Samples were centrifuged at 100 *g* for 5 min to pellet starch and cell debris. Supernatants were transferred to new reaction tubes and centrifuged at 2000 *g* for 5 min to pellet the nuclei. Nuclear pellets were resuspended in 200 µl 2x Laemmli buffer, boiled for 10 min and pooled. 200 µl of nuclei-depleted samples were added to 40 µl 5x Laemmli buffer and boiled for 10 min. The nuclear and nuclei-depleted fractions were resolved on 7.5 %, 12 % and 15 % SDS-gels. Anti-HSC70 and anti-histone-H3 antibodies (see IV.1.10) were used as cytosolic and nuclear markers, respectively.

IV.4.4 MG132 treatments

Four-day-old white light grown seedlings were transferred from solid to liquid 1x MS + 1% Suc medium containing 50µM MG132 or 0.5% DMSO, respectively, and vacuum-infiltrated for 10 min. Seedlings were kept in darkness for 4 h.

IV.4.5 Denaturing SDS-polyacrylamide gel electrophoresis (SDS-PAGE)

Denaturing SDS-PAGE was performed using Mini-PROTEAN® Tetra cell (Bio-Rad, Hercules, USA) and SE 250 Mighty Small II (Hoefer, Holliston, USA) electrophoresis systems. In case of antibody production large preparative gels were carried out using the PROTEAN® II xi Cell system (Bio-Rad, Hercules, USA). Protein samples were separated in a discontinuous gel system after Laemmli (Laemmli, 1970). Resolving gels with the concentrations of 7.5%, 10%, 12.5% and 15% polyacrylamide were used in this study. Resolving gels were overlayed with a 5% stacking gel. When protein samples were not directly extracted in 2x Laemmli buffer (see IV.4.1 and IV.1.11 for buffer)

proteins were denatured by adding 5x Laemmli buffer to the protein sample followed by an incubation at 90 °C for 8 min.

IV.4.6 Immunoblot analysis

Proteins that had been resolved by SDS-PAGE were transferred to polyvinylidene difluoride (PVDF) membrane (GE Healthcare, Piscataway, USA). Gels and membranes were incubated for 15 min in Towbin buffer prior to blotting (Towbin et al., 1979). Proteins were then transferred to the membranes using a semi-dry-blotter (LTF, Wasserburg, Germany). The transfer was carried out at 0.35 mA/cm^2 for 120 min. Blots from nuclear fractionation were blotted on PVDF membrane using Carbonate Buffer and the Mini Trans-Blot cell from Bio-Rad (Hercules, USA). The transfer was carried out for 1h at 45 V and 4°C. Membranes were blocked for 1 h at room temperature with 1x Roti®-Block (Roth, Karlsruhe) and primary antibodies were incubated over night on a rotary shaker in 3% (w/v) non-fat dried milkpowder solution (in 1x TBS) containing the primary antibody (see IV.1.10) at 4°C. Primary antibody solution was removed and membranes were washed for two times 10 min with 1x TBS-T at room temperature on a rotary shaker. Bound primary antibodies were detected using horseradish peroxidase (HRP)-conjugated goat anti-rabbit, goat anti-mouse or got anti-rat secondary antibodies (see IV.1.10) diluted in 1x TBS containing 3% (w/v) non-fat dried milkpowder. Membranes were incubated again for 1 h at room temperature slowly rotating and were washed afterwards two times 10 min with 1x TBS-T. The signal was detected using ECL Plus™ Western Blotting Reagents- (GE Healthcare, Piscataway, USA) or SuperSignal® West Femto Maximum Sensitivity-kits (Thermo Scientific, Rockford, USA) according to manufacturers protocol. The membranes were exposed in a LAS-4000 mini (GE Healthcare, Piscataway, USA) imaging system. Quantification of immunoblots was carried out using Multi Gauge vers. 3.0 software (Fujifilm, Japan) and the antibody anti-HSC70 (see IV.1.10) for normalization.

IV.4.7 Staining of SDS-PAGE gels and polyvinylidene difluoride (PVDF) membranes.

SDS-PAGE resolving gels were stained with Coomassie. The gels were incubated at room temperature over night with Coomassie staining solution [0,25% (w/v) Coomassie Brilliant Blue R250, 50% (w/v) methanol, 7% w/v acetic acid] on a rotary shaker. Gels were destained with destainig solution [50% (v/v) methanol, 7 % v/v acetic acid] on a rotary shaker. For antibody production Coomassie gels were destained over night with water.
PVDF-membranes were stained for 2 min with Coomassie staining solution and destained with destaining solution. All incubations were performed at room temperature.

IV.4.8 *In vivo* Co-immunoprecipitation (CoIP) from *Arabidopsis* seedling extracts

For *in vivo* CoIP studies protein was isolated from 4-day-old *SPA1::SPA1-HA*, RLD and *cop1-4* seedlings as described in IV.4.1. 500 µg of total protein (minimum 500 µl total volume) were incubated with 100 µl Anti-HA Affinity Matrix [Rat monoclonal antibody (Clone 3F10), immobilized, Roche, Germany] for 2 h on a rotator at 4°C. Reaction tubes were centrifuged for 10 sec at 200 rpm and the supernatants discarded. Pellets were washed three times with ice-cold extraction buffer (see IV.4.1) and resupended in one volume of 1x Laemmli buffer (see IV.1.11). The proteins from flow through and wash steps were also collected for the analysis. All samples were analyzed by SDS-PAGE and following Immunoblot analysis.

IV.4.9 *In vitro* Co-immunoprecipitation (*in vitro* CoIP) using radioactively labeled methionine

All vectors used for this assay were provided and are listed under point IV.1.3.2.

IV.4.9.1 Production of recombinant protein using the TnT®-system (Promega)

In order to produce small amounts of recombinant protein for *in vitro* CoIP the TnT® Quick Coupled Transcription/Translation system from Promega (Mannheim, Germany) was used. In this system cDNAs are transcribed under the control of a T7 promoter, and resulting mRNAs are translated. During the synthesis radioactively labeled [^{35}S]-methionine (see IV.1.8) is incorporated into the amino acid sequence. The labeling was performed partially for the bait proteins GAD-SPA1, GAD-SPA2, GAD-SPA3 and GAD-SPA4 in a ratio of 1:3 by mixing one part of radioactive [^{35}S]-methionine with three parts of non-labeled methionine. In case of the prey proteins only [^{35}S]-methionine was incorporated. The samples were incubated at 30°C for 90 min and stored on ice.

IV.4.9.2 *In vitro* Co-immunoprecipitation

For *in vitro* CoIP the labeled proteins synthesized by the TnT® system were required. The partially labeled bait proteins carry a GAL4-activation domain at the N-terminus, which allows pulldown of the protein with an anti-GAL4 antibody (Figure 4.1). Prey proteins were not fused to a tag. For CoIP, 11.5 µl of partially labeled bait- and 11.5 µl of fully labeled prey-protein were mixed in 200 µl of ice-cold CoIP buffer (20mM Tris; pH 7.5; 150mM NaCl, 1mM DTT; 0.1% (v/v) Tween®-20). The reaction was incubated for 2 h on a rotator at 4°C. As a negative control GAD protein was incubated with the prey proteins.
After incubation 2 µl of anti-GAD-antibody (Santa Cruz, Santa Cruz, USA) was added to each tube for additional 30 min at 4°C. 8 µl of previously in CoIP buffer washed magnetic protein A beads (Dynabeads® Protein A, Invitrogen, Karslruhe) were added, which bind the anti-GAD-antibody. After 30 min at 4°C the samples were treated with a magnet and the supernatants were transferred to new tubes. The pellets (beads) were washed three times with ice-cold CoIP buffer. Beads were resupended in 30 µl 1x Laemmli buffer. From the supernatants 30 µl were added to 30 µl of 2x Laemmli buffer. All Laemmli samples were boiled for 8 min at 90°C. Samples were analyzed by

SDS-PAGE. The resolved SDS gels were incubated for 30 min in destaining solution (see IV.4.5) and dried in a gel dryer system (Gel Dryer Model 583, Biorad, Hercules, USA). The dried gels were exposed to phosphoimager plates (type BAS MS, Fujifilm, Japan). Readout of the plates was carried out with the FLA-7000 (GE Healthcare, Piscataway, USA) imaging system. Data analysis and quantification were carried out using the Multi Gauge Ver. 3.0 Software package (Fuji Film, Japan).

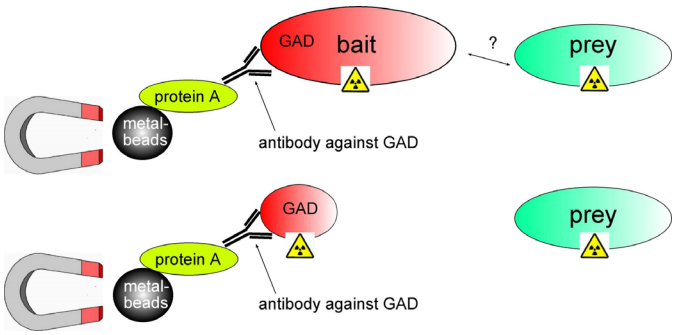

Figure 4.1: Principle of *in vitro* CoIP. Radioactively labeled bait- and prey-proteins were pulled down by using an anti-GAL4-activation domain- antibody and metal beads with protein A immobilized on the surface. GAD alone served as negative control.

IV.4.10 *In planta* interaction assays

Bimolecular Fluorescence Complementation experiments (Walter et al., 2004) in onion (*Allium cepa*) epidermal cells and co-localization studies in *Arabidopsis* leaf epidermal cells were carried out to verify the SPA-SPA interactions *in planta*.

IV.4.10.1 Bimolecular Fluorescence Complementation assay (BiFC)

In order to perform the BiFC assay, two YFP fusion proteins were required. One of those proteins carried the N-terminal part of YFP the other one the C-terminal part of YFP. Whenever those proteins are in a close proximity in the living cell a functional YFP is reconstituted, what can be detected by a fluorescent microscope. BiFC was carried out with N-terminally tagged YFP-SPA fusion proteins. For this purpose the four *SPA* cDNA sequences from the obtained Entry vectors (see IV.1.3.1) were cloned by LR reaction into the Destination vectors pCL112 and pCL113 (see IV.1.3.3) using the Gateway™

system. Expression was under the control of the *CaMV 35S* promoter. All clones were confirmed by restriction digest and sequencing. Besides the two YFP fusions the actin-binding protein CFP-talin (see IV.1.3.3) was co-transformed as a marker for transformation. CPRF1 fusion proteins were used as negative controls (see IV.1.3.3).

IV.4.10.2 Co-localization experiments in *Arabidopsis* leaf cells

N-terminal CFP- and YFP-fusions of the SPA proteins (see IV.1.3.4) were transiently introduced into *Arabidopsis* leaf epidermal cells. Four-day-old white-light-grown Col-0 wild-type seedlings grown on 1x MS plates were transfected by particle bombardment with the respective constructs (IV.4.10.5).

IV.4.10.3 Preparation of gold particles

30 mg of gold particles (1 µm, Bio-Rad, Hercules, USA) were incubated for 15 min with 1 ml of 70% (v/v) ethanol. The reaction tube was centrifuged for 15 sec at 400 rpm. After discarding the supernatant the particles were washed twice with 1 ml of sterile water and resupended in 1ml of sterile water. Particles were briefly sonificated for 3 sec in a sonificator (Branson Sonifier 250, USA). Afterwards aliquots of 50 µl were made while vortexing. The aliquots were frozen in liquid nitrogen and stored at -20 °C to keep the solution homogenous.

IV.4.10.4 Coating of gold particles

600 ng of each plasmid DNA were added to a reaction tube. Water was added to a final volume of 12 µl. While vortexing 20 µl of 2.5 M $CaCl_2$, 8 µl of 0.1 M spermidine and 10 µl of the gold particle solution were added. The reaction tubes were vortexed for another 10 min. Afterwards gold particles were pelleted by pulse-centrifugation (5 sec, 10000 rpm). The supernatants were carefully removed and the gold particles were washed with 100 µl of 70% (v/v) ethanol and 40 µl of 100% (v/v) ethanol. Finally, the gold particles were resupended in 24 µl of 100% (v/v) ethanol by sonification for 3 sec. Two times

10 µl were dropped on a macro carrier plate (Bio-Rad, Hercules, USA) and dried until the ethanol evaporated.

IV.4.10.5 Particle bombardment

Particle bombardment was carried out with a helium Helios gun (Bio-Rad, Hercules, USA) according to manufacturers instructions. All particle bombardment experiments in this study were carried out using Rupture disks breaking at 900 psi. Prior to analysis onion cells and *Arabidopsis* plants were kept in darkness for 24 h.

IV.4.10.6 Fluorescence microscopy

Fluorescence microscopy was performed using a Leica DMRE microscope equipped with a high-resolution KY-F70-3CCD JVC camera, differential interference contrast (Nomarski) optics, and epifluorescence optics.

IV.4.11 Yeast Two-Hybrid analysis

The vectors employed for Yeast Two-Hybrid analysis are listed under point IV.1.3.7. In addition, *SPA3* cDNA sequence was cloned into pAS2-attR vector by LR reaction using the Gateway™ system. Since PAP1 and PAP2 proteins are transcription factors and GAL4-binding domain fusions are highly autoactivating in the Yeast Two-Hybrid system, only SPA proteins fused to the GAL4-binding domain were employed in these experiments. The vectors containing *PAP* cDNA sequences fused to GAL4-activation domain were obtained from Andrea Schrader (Huelskamp laboratory, Cologne). Yeast Two-Hybrid analysis was performed using the *HIS3* reportergene (Synthesis of histidine) of the *Saccharomyces cerevisiae* strain *AH109* (see IV.1.2.3).

IV.4.11.1 Growth and harvesting of competent yeast cells

For transformation two yeast colonies of strain *AH109* were incubated for 15-16 h in 100 ml YAPD medium. The Erlenmeyer flask was incubated at 30°C on a rotary shaker until OD_{600} reached 0.6. Cells were harvested by

centrifugation (3000 rpm, 5 min) in a sterile 50 ml Falcon® tube. The supernatant was discarded and the pellet washed with 20 ml sterile water. After another centrifugation step (3000 rpm, 5 min) the cells were resupended in 1 ml sterile 1x TE (10mM Tris; 1mM EDTA; pH 7.5) / 100mM lithumacetate. Cells were immediately used for transformation.

IV.4.11.2 Co-transformation of yeast cells

For transformation of yeast cells 1 µg of bait- and prey-plasmids were mixed with 100 µg salmonsperm-DNA (denatured by 2 min boiling) and 50 µl competent *AH109* cell suspension (see IV.4.11.1). As a negative control one sample contained no plasmid DNA. 300 µl of PEG / lithiumacetate solution [40% (v/v) PEG; 10 mM Tris; 1 mM EDTA; 100 mM lithiumacetate; pH 7.5] was added and the samples were incubated for 30 min at 30°C. 35 µl DMSO were added and the cells were incubated at 42°C for 15 min. After centrifugation for 1 min at 10000 rpm the cells were resuspended in 100 µl sterile 1x TE [10 mM Tris; 1 mM EDTA; pH 7.5].

IV.4.11.3 Selection of co-transformed yeast cells

Half of the transformed cells were plated onto synthetic “drop-out“-plates (see IV.1.7) without leucin (-Leu) and tryptophane (-Trp), hereafter called nonselective media. The other half was plated onto “drop-out“ plates without leucin, tryptophane, and histidine (-His) hereafter called selective media. After plating, the samples were kept for 3 days at 30°C. –Leu –Trp plates indicated the sucess of co-transformation of the plasmids. –Leu –Trp –His plates were used for the verification of the interactions. Since adenine hemisulfate was added to media “drop out“ media (see IV.1.7), the mutation in the *ADE*- gene was of no importance in these experiments. To determine autoactivation of the system each construct was co-transformed with the empty vectors (pGADT7 = GAL4 activation domain and pGBKT7= GAL4 binding domain). To discriminate strong activation from weak using the *HIS3* reporter, 3-Amino-1, 2, 4-triazole (3-AT; Sigma) was added in different concentrations to “drop-out“ plates. 3-AT suppresses the autoactivation of the

HIS3 reporter. For serial yeast drop test single colonies from transformed yeast cells were grown over night in liquid –Leu –Trp medium until OD_{600} =0.6. 10 µl cell supspension was resupendend in 100 µl sterile ddH_2O. 10 µl were dropped on selective media, respectively.

IV.4.12 Antibody production

IV.4.12.1 Cloning

For antibody production of COP1 the first 915 bp of *COP1* cDNA were amplified in a PCR using COP1-pDONR201 (See IV.1.3.1) as a template and template specific Gateway^{Tm} primers listed in Table 4.5. The purified PCR product was cloned by BP reaction into pDONR221. After sequencing the cDNA was cloned by LR reaction from COP1-915-pDONR221 into pET-32b (+)-att destination vector (See IV.1.3.5).
In case of SPA1 antibody production the first 570 bp of *SPA1* cDNA were amplified in a PCR using SPA1-pENTR3C as a template and template specific Gateway^{TM} primers listed in Table 4.5. The purified PCR product was cloned into pDONR221 using BP reaction. SPA1-570-pDONR221 was employed to clone *SPA1-570* sequence into pDEST17 destination vector.
For PAP1 antibody production the last 396 bp of *PAP1* cDNA were amplified in a PCR using PAP1-pENTR as a template and template specific Gateway^{TM} primers (Table 4.5). The purified PCR product was cloned into pDONR221. PAP1-396-pDONR221 was used for LR reaction into pDEST17 (IV.1.3.5). All vectors were verified by restriction digest and sequencing.

IV.4.12.2 Expression of recombinant protein in *E.coli*.

All cloned constructs for expression (IV.1.3.5) were transformed each (see IV.3.10) into *BL21-CodonPlus (DE3)-RIL* cells for expression respectively. One single colony was grown in a 50 ml LB media overnight culture containing 100 µg/ml ampicillin at 37°C on a rotary shaker. On the next day a 500 l LB medium culture containing ampicillin was inoculated with 20 ml of the overnight culture (1:50) and grown until OD_{600} = 0.6. Protein expression was induced adding 1 mM Isopropyl-β-D-1-thiogalactopyranoside (IPTG). The

culture was incubated for additional 5 h and harvested afterwards by centrifugation at 4000 rpm in a GS3 rotor. The supernatant was discarded and the pellet stored overnight at -20°C.

IV.4.12.3 Purification of His_6-tagged protein from *E.coli*

Lysis and purification under denaturing conditions using Ni-NTA agarose resin was carried out after The QIAexpressionist™ protocols 8, 10 and 17 (Qiagen GmbH, Hilden, Germany) with a few modifications. For the flow trough sample, the 4 ml lysate solution dropping out of the column containing the unbound protein was collected. 36 µl of flow trough lysate were added to 9 µl 5x Laemmli buffer. For the wash sample the 8 ml washing buffer were collected and pooled. 36 µl of wash sample were added to 9 µl 5x Laemmli buffer. Purified His_6-SPA1-570 and His_6-PAP1-396 proteins were directly transferred to large preparative SDS-PAGE gels (IV.4.5), Coomassie stained and destained as described under point IV.4.7 and cut out for immunization.

IV.4.12.4 Dialysis and protease digestion

In case of the COP1-915 protein, which was tagged with multiple tags at the N-terminus, the tags were cleaved off using enterokinase protease (Roche, Mannheim, Germany). Therefore the protein eluted in 8 M Urea needed to be dialyzed in a buffer that maintained enterokinase activity.

For dialysis 30-40 cm of visking cellulose (20/32 inch, 0.025mm) tubes were employed (Carl Roth, Karlsruhe, Germany). The tube was boiled four times in the microwave in 2% $NaCO_3$ solution, two times with sterile water and three times in 1 mM EDTA. The solution was exchanged after every boiling. Prepared dialysis tubes were stored in 1 mM EDTA solution at 4°C.

Dialysis was carried out overnight at 4°C in a buffer containing 3 M Urea, 20 mM methylamine and 50 mM Tris pH 7.7. After the estimation of protein concentration using the Bradford assay (Bradford, 1976), the samples were directly used for protease digestion.

For digestion 1 mg of the dialyzed protein was processed with 93 µl (0.3mg/ml) enterokinase at 37°C for 24 h according to manufacturers

protocol. The digest was split into small aliquots for digestion and pooled afterwards.

IV.4.12.5 Protein immunization

After Coomassie staining SPA1-570-, PAP1-396- and processed COP1-915-protein were cut out from a large 12.5% preparative SDS-PAGE gel and sent for immunization. A total of 2 mg of each purified protein was sent for immunization. After screening 6 to 24 rabbit preimmune sera by immunoblot analysis, two rabbits were chosen for each immunization. 100 - 200 µg of recombinant protein were administered per boost. COP1-915 protein was immunized for nine months with a break of four weeks. SPA1-570 protein was immunized for seven months. SPA2 peptides were immunized for six months with a break of two months. PAP1-396 was immunized for nine months. All antibody productions were performed at Agrisera AB (www.agrisera.com, Sweden).

IV.4.12.6 Purification of polyclonal antibodies using polyvinylidene difluoride membranes (PVDF) membranes

100 µg of the purified proteins were resolved on SDS-PAGE gels. The gels were blotted onto PVDF membranes and the membranes were stained with Poncau S (ATX Ponceau S concentrate; Sigma-Aldrich, Munich, Germany). The region containing the protein was cut into small pieces fitting in a reaction tube. The membranes were blocked with 1% BSA, 0.05% (v/v) Tween®-20 in 1x TBS solution. 2 ml of antiserum were incubated with the membranes over night at 4°C on a rotator. On the next day the samples were washed four times with 1x TBS at 4°C. The antibodies were eluted by vortexing the membranes slices with 450 µl of 0.1 M glycine, 0.5 M NaCl and 0.05% (v/v) Tween®-20, pH 2.6 (with HCl) for 90 sec at 4°C. After 90 sec, 50 µl of 1 M Tris pH 8.0 were added immediately to the sample. The elution was repeated with another 450 µl. For long term-storage 0.05% (w/v) sodiumazide as 0.1% (w/v) BSA was added to 1ml antibody solution (2x 500 ml). The membranes were

washed with 1x TBS and long term stored in 1x TBS containing 5 % (w/v) sodiumazide and 0.1% (w/v) BSA at -80°C.

V Supplement

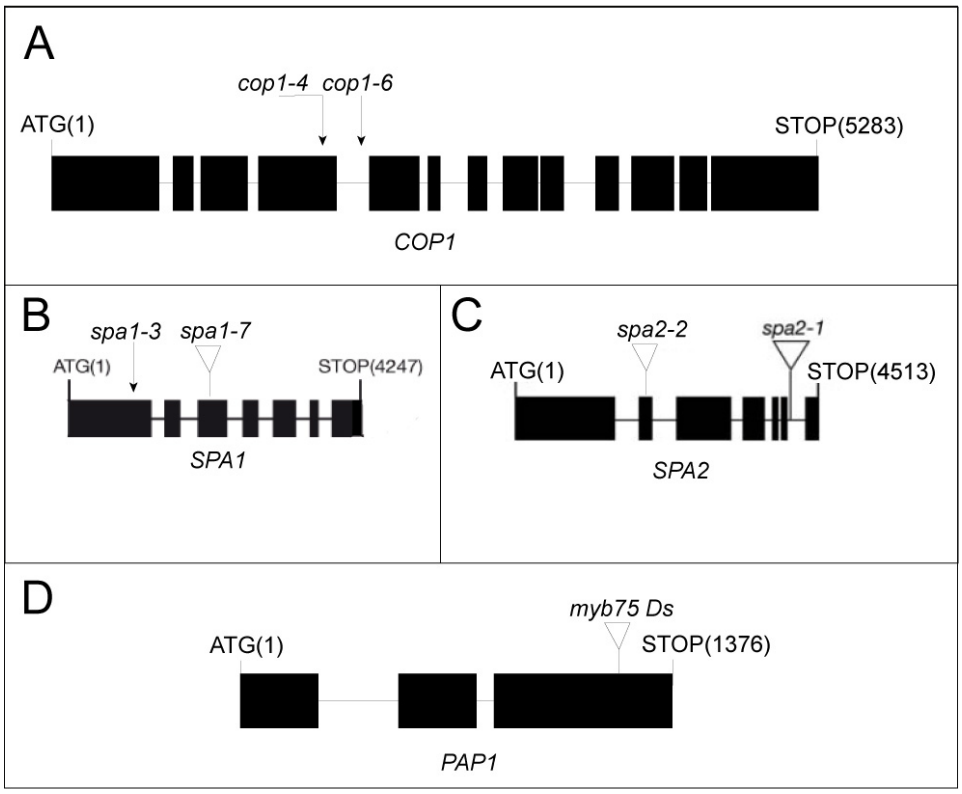

Supplemental figure 5.1: Mutants used with generated antibodies. Shown are intron-exon structures of the *COP1*, *SPA1*, *SPA2* and *PAP1* gene. Positions of the EMS mutations are indicated with an arrow. The positions of T-DNA insertion mutants are indicated with a triangle. The size of the coding region of the genes is given in brackets. (A) Intron-exon structure of the *COP1* gene (13 exons). The *cop1-4* mutation (EMS) represents a C-to-T mutation in exon 4 at postion 1581 bp, what changes Gln-283 CAA codon to a UAA stop codon. The early stop codon results in a truncated version of the COP1 protein with a size of about 33kDa. The *cop1-6* mutation (EMS) changes the splicing junction "AG" at the 3' end of intron 4 to "GG" and leads to three principal cryptically spliced mRNA transcripts and a transcript with an unspliced intron. (B) Intron-exon structure of the *SPA1* gene (7 exons; modified after Fittinghoff et al. 2006). The *spa1-3* mutation (EMS) represents a C-to-T mutation at position 1233 bp in the first exon of the *SPA1* gene. *spa1-7* is a T-DNA mutation. The T-DNA is inserted in exon 3 at position 2638 bp. (C) Intron-exon structure of the *SPA2* gene (7 exons; modified after Laubinger et al., 2004). *spa2-1* is a T-DNA insertion mutation. The T-DNA inserted in the last intron at position 4008 bp after the presumed start codon. *spa2-2* is also a T-DNA insertion mutation. The T-DNA inserted in exon 2 at postiion 1331 bp. (D) Intron-exon structure of the *PAP1* gene (3 exons). *myb75 Ds* is a T-DNA insertion mutant. The T-DNA inserted at position 1266 bp in the last exon.

VI References

Adrian, J. (2005). Untersuchung zur Funktion von SPA1-interagierenden Proteinen ei *Arabiopsis thaliana*. Diplomarbeit im Institut für Enwicklungs- und Molekularbiologie der Pflanzen (Düsseldorf: Heinrich-Heine Universität Düsseldorf).

Ahmad, M., and Cashmore, A.R. (1993). *HY4* gene of *A. thaliana* encodes a protein with characteristics of a blue-light photoreceptor. Nature **366,** 162-166.

Al-Sady, B., Ni, W., Kircher, S., Schafer, E., and Quail, P.H. (2006). Photoactivated phytochrome induces rapid PIF3 phosphorylation prior to proteasome-mediated degradation. Mol Cell **23,** 439-446.

Ang, L.-H., and Deng, X.-W. (1994). Regulatory hierarchy of photomorphogenic loci: Allele-specific and light-dependent interaction between the *HY5* and *COP1* loci. Plant Cell **6,** 613-628.

Ang, L.H., Chattopadhyay, S., Wei, N., Oyama, T., Okada, K., Batschauer, A., and Deng, X.W. (1998). Molecular interaction between COP1 and HY5 defines a regulatory switch for light control of Arabidopsis development. Mol Cell **1,** 213-222.

Balcerowicz, M., Fittinghoff, K., Wirthmueller, L., Maier, A., Fackendahl, P., Fiene, G., Koncz, C., and Hoecker, U. (2011). Light exposure of Arabidopsis seedlings causes rapid de-stabilization as well as selective post-translational inactivation of the repressor of photomorphogenesis SPA2. Plant J **65,** 712-723.

Ballesteros, M.L., Bolle, C., Lois, L.M., Moore, J.M., Vielle-Calzada, J.P., Grossniklaus, U., and Chua, N.H. (2001). LAF1, a MYB transcription activator for phytochrome A signaling. Genes Dev **15,** 2613-2625.

Baudry, A., Caboche, M., and Lepiniec, L. (2006). TT8 controls its own expression in a feedback regulation involving TTG1 and homologous MYB and bHLH factors, allowing a strong and cell-specific accumulation of flavonoids in Arabidopsis thaliana. Plant J **46,** 768-779.

Bauer, D., Viczian, A., Kircher, S., Nobis, T., Nitschke, R., Kunkel, T., Panigrahi, K.C., Adam, E., Fejes, E., Schafer, E., and Nagy, F. (2004). Constitutive photomorphogenesis 1 and multiple photoreceptors control degradation of phytochrome interacting factor 3, a transcription factor required for light signaling in Arabidopsis. Plant Cell **16,** 1433-1445.

Baumgardt, R.L., Oliverio, K.A., Casal, J.J., and Hoecker, U. (2002). SPA1, a component of phytochrome A signal transduction, regulates the light signaling current. Planta **215,** 745-753.

Bhargava, A., Mansfield, S.D., Hall, H.C., Douglas, C.J., and Ellis, B.E. (2010). MYB75 functions in regulation of secondary cell wall formation in the Arabidopsis inflorescence stem. Plant Physiol.

Borevitz, J.O., Xia, Y., Blount, J., Dixon, R.A., and Lamb, C. (2000). Activation tagging identifies a conserved MYB regulator of phenylpropanoid biosynthesis. Plant Cell **12,** 2383-2394.

Bradford, M.M. (1976). A rapid and sensitive method for the quantitation of microgram quantities of protein utilizing the principle of protein-dye binding. Anal Biochem **72,** 248-254.

Braun, E.L., and Grotewold, E. (1999). Newly discovered plant c-myb-like genes rewrite the evolution of the plant myb gene family. Plant Physiol **121,** 21-24.

Braun, H. (2005). Biochemische und genetische Untersuchungen zur Lichtsignaltransduktion bei Arabidopsis thaliana. Diplomarbeit im Institut für Entwicklungs- und Molekularbiologie der Pflanzen (Düsseldorf: Heinrich-Heine-Universität Düsseldorf).

Briggs, W.R., and Olney, M.A. (2001). Photoreceptors in plant photomorphogenesis to date. Five phytochromes, two cryptochromes, one phototropin, and one superchrome. Plant Physiol **125,** 85-88.

Broun, P. (2005). Transcriptional control of flavonoid biosynthesis: a complex network of conserved regulators involved in multiple aspects of differentiation in Arabidopsis. Current Opinion in Plant Biology **8,** 272-279.

Brown, B.A., Cloix, C., Jiang, G.H., Kaiserli, E., Herzyk, P., Kliebenstein, D.J., and Jenkins, G.I. (2005). A UV-B-specific signaling component orchestrates plant UV protection. Proc Natl Acad Sci U S A **102,** 18225-18230.

Casal, J.J., Sanchez, R.A., and Yanovsky, M.J. (1997). The function of phytochrome A. Plant Cell Environ **20,** 813-819.

Casal, J.J., Yanovsky, M.J., and Luppi, J.P. (2000). Two photobiological pathways of phytochrome A activity, only one of which shows dominant negative suppression by phytochrome B. Photochem Photobiol **71,** 481-486.

Cashmore, A.R., Jarillo, J.A., Wu, Y.J., and Liu, D.M. (1999). Cryptochromes: Blue light receptors for plants and animals. Science **284,** 760-765.

Castillon, A., Shen, H., and Huq, E. (2007). Phytochrome Interacting Factors: central players in phytochrome-mediated light signaling networks. Trends in Plant Science **12,** 514-521.

Chamovitz, D.A., Wei, N., Osterlund, M.T., von Arnim, A.G., Staub, J.M., Matsui, M., and Deng, X.W. (1996). The COP9 complex, a novel multisubunit nuclear regulator involved in light control of a plant developmental switch. Cell **86,** 115-121.

Chang, C.S., Li, Y.H., Chen, L.T., Chen, W.C., Hsieh, W.P., Shin, J., Jane, W.N., Chou, S.J., Choi, G., Hu, J.M., Somerville, S., and Wu, S.H. (2008). LZF1, a HY5-regulated transcriptional factor, functions in Arabidopsis de-etiolation. Plant J **54,** 205-219.

Chattopadhyay, S., Ang, L.H., Puente, P., Deng, X.W., and Wei, N. (1998). Arabidopsis bZIP protein HY5 directly interacts with light-responsive promoters in mediating light control of gene expression. Plant Cell **10,** 673-683.

Chen, H., Huang, X., Gusmaroli, G., Terzaghi, W., Lau, O.S., Yanagawa, Y., Zhang, Y., Li, J., Lee, J.H., Zhu, D., and Deng, X.W. (2010). Arabidopsis CULLIN4-damaged DNA binding protein 1 interacts with CONSTITUTIVELY PHOTOMORPHOGENIC1-SUPPRESSOR OF PHYA complexes to regulate photomorphogenesis and flowering time. Plant Cell **22,** 108-123.

Chory, J., Peto, C., Feinbaum, R., Pratt, L., and Ausubel, F. (1989). *Arabidopsis thaliana* mutant that develops as a light-grown plant in the absence of light. Cell **58,** 991-999.

Christie, J.M., Reymond, P., Powell, G.K., Bernasconi, P., Raibekas, A.A., Liscum, E., and Briggs, W.R. (1998). Arabidopsis NPH1: a flavoprotein with the properties of a photoreceptor for phototropism. Science **282,** 1698-1701.

Clough, S.J., and Bent, A.F. (1998). Floral dip: a simplified method for *Agrobacterium*-mediated transformation of *Arabidopsis thaliana*. Plant J **16,** 735-743.

Cominelli, E., Gusmaroli, G., Allegra, D., Galbiati, M., Wade, H.K., Jenkins, G.I., and Tonelli, C. (2008). Expression analysis of anthocyanin regulatory genes in response to different light qualities in Arabidopsis thaliana. J Plant Physiol **165,** 886-894.

Corbesier, L., Vincent, C., Jang, S., Fornara, F., Fan, Q., Searle, I., Giakountis, A., Farrona, S., Gissot, L., Turnbull, C., and Coupland, G. (2007). FT protein movement contributes to long-distance signaling in floral induction of Arabidopsis. Science **316,** 1030-1033.

Coupland, G., Igeno, M.I., Simon, R., Schaffer, R., Murtas, G., Reeves, P., Robson, F., Pineiro, M., Costa, M., Lee, K., and Suarez-Lopez, P. (1998).

The regulation of flowering time by daylength in Arabidopsis. Symp Soc Exp Biol **51,** 105-110.

Crocco, C.D., Holm, M., Yanovsky, M.J., and Botto, J.F. (2010). AtBBX21 and COP1 genetically interact in the regulation of shade avoidance. Plant J **64,** 551-562.

Deng, X.W., Caspar, T., and Quail, P.H. (1991). cop1: a regulatory locus involved in light-controlled development and gene expression in Arabidopsis. Genes Dev **5,** 1172-1182.

Deng, X.W., Matsui, M., Wei, N., Wagner, D., Chu, A.M., Feldmann, K.A., and Quail, P.H. (1992). COP1, an Arabidopsis regulatory gene, encodes a protein with both a zinc-binding motif and a G beta homologous domain. Cell **71,** 791-801.

Downes, B.P., Stupar, R.M., Gingerich, D.J., and Vierstra, R.D. (2003). The HECT ubiquitin-protein ligase (UPL) family in Arabidopsis: UPL3 has a specific role in trichome development. Plant J **35,** 729-742.

Dubos, C., Le Gourrierec, J., Baudry, A., Huep, G., Lanet, E., Debeaujon, I., Routaboul, J.M., Alboresi, A., Weisshaar, B., and Lepiniec, L. (2008). MYBL2 is a new regulator of flavonoid biosynthesis in Arabidopsis thaliana. Plant J **55,** 940-953.

Duek, P.D., and Fankhauser, C. (2003). HFR1, a putative bHLH transcription factor, mediates both phytochrome A and cryptochrome signalling. Plant J **34,** 827-836.

Duek, P.D., and Fankhauser, C. (2005). bHLH class transcription factors take centre stage in phytochrome signalling. Trends in Plant Science **10,** 51-54.

Duek, P.D., Elmer, M.V., van Oosten, V.R., and Fankhauser, C. (2004). The degradation of HFR1, a putative bHLH class transcription factor involved in light signaling, is regulated by phosphorylation and requires COP1. Curr Biol **14,** 2296-2301.

Earley, K.W., Haag, J.R., Pontes, O., Opper, K., Juehne, T., Song, K., and Pikaard, C.S. (2006). Gateway-compatible vectors for plant functional genomics and proteomics. Plant J **45,** 616-629.

El Refy, A., Perazza, D., Zekraoui, L., Valay, J.G., Bechtold, N., Brown, S., Hulskamp, M., Herzog, M., and Bonneville, J.M. (2003). The Arabidopsis KAKTUS gene encodes a HECT protein and controls the number of endoreduplication cycles. Mol Genet Genomics **270,** 403-414.

Fairchild, C.D., Schumaker, M.A., and Quail, P.H. (2000). HFR1 encodes an atypical bHLH protein that acts in phytochrome A signal transduction. Genes Dev **14,** 2377-2391.

Falke, C. (2008). Biochemische und histologische Untersuchungen zur Lichtsignaltransduktion bei Arabidopsis. In Botanical Insitute (Cologne: University of Cologne).

Fankhauser, C., and Chory, J. (1997). Light control of plant development. Annu Rev Cell Dev Biol **13,** 203-229.

Fankhauser, C., and Chory, J. (2000). RSF1, an Arabidopsis locus implicated in phytochrome A signaling. Plant Physiol **124,** 39-45.

Favory, J.J., Stec, A., Gruber, H., Rizzini, L., Oravecz, A., Funk, M., Albert, A., Cloix, C., Jenkins, G.I., Oakeley, E.J., Seidlitz, H.K., Nagy, F., and Ulm, R. (2009). Interaction of COP1 and UVR8 regulates UV-B-induced photomorphogenesis and stress acclimation in Arabidopsis. EMBO Journal **28,** 591-601.

Feldbrugge, M., Sprenger, M., Hahlbrock, K., and Weisshaar, B. (1997). PcMYB1, a novel plant protein containing a DNA-binding domain with one MYB repeat, interacts in vivo with a light-regulatory promoter unit. Plant J **11,** 1079-1093.

Feldbrugge, M., Sprenger, M., Dinkelbach, M., Yazaki, K., Harter, K., and Weisshaar, B. (1994). Functional analysis of a light-responsive plant bZIP transcriptional regulator. Plant Cell **6,** 1607-1621.

Fittinghoff, K. (2009). Functional Analysis of the SPA Gene Family in Arabidopsis thaliana. Inaugural Dissertation. Botanical Institute (Cologne: University of cologne).

Fittinghoff, K., Laubinger, S., Nixdorf, M., Fackendahl, P., Baumgardt, R.L., Batschauer, A., and Hoecker, U. (2006). Functional and expression analysis of Arabidopsis SPA genes during seedling photomorphogenesis and adult growth. Plant J.

Franklin, K.A., Larner, V.S., and Whitelam, G.C. (2005). The signal transducing photoreceptors of plants. Int J Dev Biol **49,** 653-664.

Fuglevand, G., Jackson, J.A., and Jenkins, G.I. (1996). UV-B, UV-A, and blue light signal transduction pathways interact synergistically to regulate chalcone synthase gene expression in Arabidopsis. Plant Cell **8,** 2347-2357.

Gonzalez, A., Zhao, M., Leavitt, J.M., and Lloyd, A.M. (2008). Regulation of the anthocyanin biosynthetic pathway by the TTG1/bHLH/Myb transcriptional complex in Arabidopsis seedlings. Plant J **53,** 814-827.

Gould Kevin, D.K., Winefield Chris. (2009). Anthocyanins: Biosynthesis, Functions, and Applications.

Gould, K.S. (2004). Nature's Swiss Army Knife: The Diverse Protective Roles of Anthocyanins in Leaves. J Biomed Biotechnol **2004,** 314-320.

Guo, H., Yang, H., Mockler, T.C., and Lin, C. (1998). Regulation of flowering time by Arabidopsis photoreceptors. Science **279,** 1360-1363.

Guo, H., Duong, H., Ma, N., and Lin, C. (1999). The Arabidopsis blue light receptor cryptochrome 2 is a nuclear protein regulated by a blue light-dependent post-transcriptional mechanism. Plant J **19,** 279-287.

Harborne, J.B., and Williams, C.A. (2000). Advances in flavonoid research since 1992. Phytochemistry **55,** 481-504.

Henriques, R., Jang, I.C., and Chua, N.H. (2009). Regulated proteolysis in light-related signaling pathways. Current Opinion in Plant Biology **12,** 49-56.

Hisada, A., Hanzawa, H., Weller, J.L., Nagatani, A., Reid, J.B., and Furuya, M. (2000). Light-induced nuclear translocation of endogenous pea phytochrome A visualized by immunocytochemical procedures. Plant Cell **12,** 1063-1078.

Hoecker, U. (2005). Regulated proteolysis in light signaling. Current Opinion in Plant Biology **8,** 469-476.

Hoecker, U., and Quail, P.H. (2001). The phytochrome A-specific signaling intermediate SPA1 interacts directly with COP1, a constitutive repressor of light signaling in Arabidopsis. J Biol Chem **276,** 38173-38178.

Hoecker, U., Xu, Y., and Quail, P.H. (1998). SPA1: A new genetic locus involved in phytochrome A - Specific signal transduction. Plant Cell **10,** 19-33.

Hoecker, U., Tepperman, J.M., and Quail, P.H. (1999). SPA1, a WD-repeat protein specific to phytochrome A signal transduction. Science **284,** 496-499.

Holm, M., Ma, L.G., Qu, L.J., and Deng, X.W. (2002). Two interacting bZIP proteins are direct targets of COP1-mediated control of light-dependent gene expression in Arabidopsis. Genes Dev **16,** 1247-1259.

Holton, T.A., and Cornish, E.C. (1995). Genetics and Biochemistry of Anthocyanin Biosynthesis. Plant Cell **7,** 1071-1083.

Huala, E., Oeller, P.W., Liscum, E., Han, I.S., Larsen, E., and Briggs, W.R. (1997). Arabidopsis NPH1: a protein kinase with a putative redox-sensing domain. Science **278,** 2120-2123.

Imaizumi, T., Tran, H.G., Swartz, T.E., Briggs, W.R., and Kay, S.A. (2003). FKF1 is essential for photoperiodic-specific light signalling in Arabidopsis. Nature **426,** 302-306.

Inoue, H., Nojima, H., and Okayama, H. (1990). High efficiency transformation of Escherichia coli with plasmids. Gene **96,** 23-28.

Ishikawa, M., Kiba, T., and Chua, N.H. (2006). The Arabidopsis SPA1 gene is required for circadian clock function and photoperiodic flowering. Plant J **46,** 736-746.

Jaeger, K.E., and Wigge, P.A. (2007). FT protein acts as a long-range signal in Arabidopsis. Curr Biol **17,** 1050-1054.

James, P., Halladay, J., and Craig, E.A. (1996). Genomic libraries and a host strain designed for highly efficient two-hybrid selection in yeast. Genetics **144,** 1425-1436.

Jang, I.C., Yang, J.Y., Seo, H.S., and Chua, N.H. (2005). HFR1 is targeted by COP1 E3 ligase for post-translational proteolysis during phytochrome A signaling. Genes Dev **19,** 593-602.

Jang, I.C., Yang, S.W., Yang, J.Y., and Chua, N.H. (2007). Independent and interdependent functions of LAF1 and HFR1 in phytochrome A signaling. Genes Dev **21,** 2100-2111.

Jang, I.C., Henriques, R., Seo, H.S., Nagatani, A., and Chua, N.H. (2010). Arabidopsis PHYTOCHROME INTERACTING FACTOR proteins promote phytochrome B polyubiquitination by COP1 E3 ligase in the nucleus. Plant Cell **22,** 2370-2383.

Jang, S., Marchal, V., Panigrahi, K.C., Wenkel, S., Soppe, W., Deng, X.W., Valverde, F., and Coupland, G. (2008). Arabidopsis COP1 shapes the temporal pattern of CO accumulation conferring a photoperiodic flowering response. EMBO Journal **27,** 1277-1288.

Jenkins, G.I. (1997). UV and blue light signal transduction in Arabidopsis. Plant Cell Environ **20,** 773-778.

Jeong, R.D., Kachroo, A., and Kachroo, P. (2010a). Blue light photoreceptors are required for the stability and function of a resistance protein mediating viral defense in Arabidopsis. Plant Signal Behav **5**.

Jeong, R.D., Chandra-Shekara, A.C., Barman, S.R., Navarre, D., Klessig, D.F., Kachroo, A., and Kachroo, P. (2010b). Cryptochrome 2 and phototropin 2 regulate resistance protein-mediated viral defense by negatively regulating an E3 ubiquitin ligase. Proc Natl Acad Sci U S A **107,** 13538-13543.

Kaiser, T., Emmler, K., Kretsch, T., Weisshaar, B., Schafer, E., and Batschauer, A. (1995). Promoter elements of the mustard CHS1 gene are sufficient for light regulation in transgenic plants. Plant Mol Biol **28,** 219-229.

Kang, C.Y., Lian, H.L., Wang, F.F., Huang, J.R., and Yang, H.Q. (2009). Cryptochromes, phytochromes, and COP1 regulate light-controlled stomatal development in Arabidopsis. Plant Cell **21,** 2624-2641.

Kim, J.Y., Yi, H.K., Choi, G., Shin, B., Song, P.S., and Choi, G.S. (2003). Functional characterization of phytochrome interacting factor 3 in phytochrorne-mediated light signal transduction. Plant Cell **15,** 2399-2407.

Kim, Y.M., Woo, J.C., Song, P.S., and Soh, M.S. (2002). HFR1, a phytochrome A-signalling component, acts in a separate pathway from HY5, downstream of COP1 in Arabidopsis thaliana. Plant J **30,** 711-719.

Kinkema, M., Fan, W., and Dong, X. (2000). Nuclear localization of NPR1 is required for activation of PR gene expression. Plant Cell **12,** 2339-2350.

Kircher, S., Kozma-Bognar, L., Kim, L., Adam, E., Harter, K., Schafer, E., and Nagy, F. (1999). Light quality-dependent nuclear import of the plant photoreceptors phytochrome A and B. Plant Cell **11,** 1445-1456.

Kleine, T., Lockhart, P., and Batschauer, A. (2003). An Arabidopsis protein closely related to Synechocystis cryptochrome is targeted to organelles. Plant J **35,** 93-103.

Koes, R., Verweij, W., and Quattrocchio, F. (2005). Flavonoids: a colorful model for the regulation and evolution of biochemical pathways. Trends in Plant Science **10,** 236-242.

Koncz, C., Martini, N., Szabados, L., Hrouda, M., Bachmair, A., and Schell, J. (1994). Specialized vectors for gene tagging and expression studies. In Plant Molecular Biology Manual, Vol. B2, S.B. Gelvin and R.A. Schilperoort, eds (Dordrecht: Kluwer Academic Publishers), pp. 1-22.

Koornneef, M., Hanhart, C.J., and van der Veen, J.H. (1991). A genetic and physiological analysis of late flowering mutants in Arabidopsis thaliana. Mol Gen Genet **229,** 57-66.

Kranz, H., Scholz, K., and Weisshaar, B. (2000). c-MYB oncogene-like genes encoding three MYB repeats occur in all major plant lineages. Plant J **21,** 231-235.

Kwok, S.F., Staub, J.M., and Deng, X.W. (1999). Characterization of two subunits of Arabidopsis 19S proteasome regulatory complex and its possible interaction with the COP9 complex. J Mol Biol **285,** 85-95.

Laemmli, U.K. (1970). Cleavage of structural proteins during the assembly of the head of bacteriophage T4. Nature **227,** 680-684.

Laubinger, S. (2006). Die Funktion der SPA Gene in der lichtgesteuerten Entwicklung von *Arabidopsis thaliana*.
Inaugural-Dissertation zur Erlangung des Doktorgrades der Mathematisch-Naturwissenschaftlichen Fakultät der Heinrich-Heine-Universität Düsseldorf.

Laubinger, S., and Hoecker, U. (2003). The SPA1-like proteins SPA3 and SPA4 repress photomorphogenesis in the light. Plant J **35,** 373-385.

Laubinger, S., Fittinghoff, K., and Hoecker, U. (2004). The SPA quartet: a family of WD-repeat proteins with a central role in suppression of photomorphogenesis in arabidopsis. Plant Cell **16,** 2293-2306.

Laubinger, S., Marchal, V., Le Gourrierec, J., Wenkel, S., Adrian, J., Jang, S., Kulajta, C., Braun, H., Coupland, G., and Hoecker, U. (2006). Arabidopsis SPA proteins regulate photoperiodic flowering and interact with the floral inducer CONSTANS to regulate its stability. Development **133,** 3213-3222.

Lee, J., He, K., Stolc, V., Lee, H., Figueroa, P., Gao, Y., Tongprasit, W., Zhao, H., Lee, I., and Deng, X.W. (2007). Analysis of transcription factor HY5 genomic binding sites revealed its hierarchical role in light regulation of development. Plant Cell **19,** 731-749.

Lepiniec, L., Debeaujon, I., Routaboul, J.M., Baudry, A., Pourcel, L., Nesi, N., and Caboche, M. (2006). Genetics and biochemistry of seed flavonoids. Annu Rev Plant Biol **57,** 405-430.

Lillo, C., Lea, U.S., and Ruoff, P. (2008). Nutrient depletion as a key factor for manipulating gene expression and product formation in different branches of the flavonoid pathway. Plant Cell Environ **31,** 587-601.

Lin, C., Ahmad, M., and Cashmore, A.R. (1996). Arabidopsis cryptochrome 1 is a soluble protein mediating blue light-dependent regulation of plant growth and development. Plant J **10,** 893-902.

Lin, C.T., Yang, H.Y., Guo, H.W., Mockler, T., Chen, J., and Cashmore, A.R. (1998). Enhancement of blue-light sensitivity of Arabidopsis seedlings by a blue light receptor cryptochrome 2. Proc Natl Acad Sci USA **95,** 2686-2690.

Lin, M.K., Belanger, H., Lee, Y.J., Varkonyi-Gasic, E., Taoka, K., Miura, E., Xoconostle-Cazares, B., Gendler, K., Jorgensen, R.A., Phinney, B., Lough, T.J., and Lucas, W.J. (2007). FLOWERING LOCUS T protein may act as the long-distance florigenic signal in the cucurbits. Plant Cell **19,** 1488-1506.

Liscum, E., and Briggs, W.R. (1995). Mutations in the NPH1 locus of Arabidopsis disrupt the perception of phototropic stimuli. Plant Cell **7,** 473-485.

Liu, L., Zhang, Y., Tang, S., Zhao, Q., Zhang, Z., Zhang, H., Dong, L., Guo, H., and Xie, Q. (2010). An efficient system to detect protein ubiquitination by agroinfiltration in Nicotiana benthamiana. Plant J **61,** 893-903.

Liu, L.J., Zhang, Y.C., Li, Q.H., Sang, Y., Mao, J., Lian, H.L., Wang, L., and Yang, H.Q. (2008). COP1-mediated ubiquitination of CONSTANS is implicated in cryptochrome regulation of flowering in Arabidopsis. Plant Cell **20,** 292-306.

Ma, L., Li, J., Qu, L., Hager, J., Chen, Z., Zhao, H., and Deng, X.W. (2001). Light control of Arabidopsis development entails coordinated regulation of genome expression and cellular pathways. Plant Cell **13,** 2589-2607.

Martinez-Garcia, J.F., Huq, E., and Quail, P.H. (2000). Direct targeting of light signals to a promoter element-bound transcription factor. Science **288,** 859-863.

Mathieu, J., Warthmann, N., Kuttner, F., and Schmid, M. (2007). Export of FT protein from phloem companion cells is sufficient for floral induction in Arabidopsis. Curr Biol **17,** 1055-1060.

Matsui, K., Umemura, Y., and Ohme-Takagi, M. (2008). AtMYBL2, a protein with a single MYB domain, acts as a negative regulator of anthocyanin biosynthesis in Arabidopsis. Plant J **55,** 954-967.

Mazzella, M.A., Cerdan, P.D., Staneloni, R.J., and Casal, J.J. (2001). Hierarchical coupling of phytochromes and cryptochromes reconciles stability and light modulation of Arabidopsis development. Development **128,** 2291-2299.

McNellis, T.W., and Deng, X.W. (1995). Light control of seedling morphogenetic pattern. Plant Cell **7,** 1749-1761.

McNellis, T.W., von Arnim, A.G., Araki, T., Komeda, Y., Misera, S., and Deng, X.W. (1994). Genetic and molecular analysis of an allelic series of cop1 mutants suggests functional roles for the multiple protein domains. Plant Cell **6,** 487-500.

Mockler, T., Yang, H., Yu, X., Parikh, D., Cheng, Y.C., Dolan, S., and Lin, C. (2003). Regulation of photoperiodic flowering by Arabidopsis photoreceptors. Proc Natl Acad Sci U S A **100,** 2140-2145.

Moon, J., Parry, G., and Estelle, M. (2004). The ubiquitin-proteasome pathway and plant development. Plant Cell **16,** 3181-3195.

Nagatani, A. (2004). Light-regulated nuclear localization of phytochromes. Current Opinion in Plant Biology **7,** 708-711.

Nagatani, A., Reed, J.W., and Chory, J. (1993). Isolation and Initial Characterization of Arabidopsis Mutants That Are Deficient in Phytochrome A. Plant Physiol **102,** 269-277.

Nesi, N., Debeaujon, I., Jond, C., Pelletier, G., Caboche, M., and Lepiniec, L. (2000). The TT8 gene encodes a basic helix-loop-helix domain protein required for expression of DFR and BAN genes in Arabidopsis siliques. Plant Cell **12,** 1863-1878.

Ni, M., Tepperman, J.M., and Quail, P.H. (1999). Binding of phytochrome B to its nuclear signalling partner PIF3 is reversibly induced by light. Nature **400,** 781-784.

Nixdorf, M., and Hoecker, U. (2010). SPA1 and DET1 act together to control photomorphogenesis throughout plant development. Planta **231,** 825-833.

Ogata, K., Morikawa, S., Nakamura, H., Sekikawa, A., Inoue, T., Kanai, H., Sarai, A., Ishii, S., and Nishimura, Y. (1994). Solution structure of a specific DNA complex of the Myb DNA-binding domain with cooperative recognition helices. Cell **79,** 639-648.

Ohgishi, M., Saji, K., Okada, K., and Sakai, T. (2004). Functional analysis of each blue light receptor, cry1, cry2, phot1, and phot2, by using combinatorial multiple mutants in Arabidopsis. Proc Natl Acad Sci U S A **101,** 2223-2228.

Olsen, K.M., Slimestad, R., Lea, U.S., Brede, C., Lovdal, T., Ruoff, P., Verheul, M., and Lillo, C. (2009). Temperature and nitrogen effects on regulators and

products of the flavonoid pathway: experimental and kinetic model studies. Plant Cell Environ **32,** 286-299.

Osterlund, M.T., Wei, N., and Deng, X.W. (2000a). The roles of photoreceptor systems and the COP1-targeted destabilization of HY5 in light control of Arabidopsis seedling development. Plant Physiol **124,** 1520-1524.

Osterlund, M.T., Hardtke, C.S., Wei, N., and Deng, X.W. (2000b). Targeted destabilization of HY5 during light-regulated development of *Arabidopsis*. Nature **405,** 462-466.

Oyama, T., Shimura, Y., and Okada, K. (1997). The *Arabidopsis HY5* gene encodes a bZIP protein that regulates stimulus-induced development of root and hypocotyl. Genes Dev **11,** 2983-2995.

Payne, C.T., Zhang, F., and Lloyd, A.M. (2000). GL3 encodes a bHLH protein that regulates trichome development in arabidopsis through interaction with GL1 and TTG1. Genetics **156,** 1349-1362.

Pelletier, M.K., Murrell, J.R., and Shirley, B.W. (1997). Characterization of flavonol synthase and leucoanthocyanidin dioxygenase genes in Arabidopsis. Further evidence for differential regulation of "early" and "late" genes. Plant Physiol **113,** 1437-1445.

Peng, Z., Shen, Y., Feng, S., Wang, X., Chitteti, B.N., Vierstra, R.D., and Deng, X.W. (2003). Evidence for a physical association of the COP9 signalosome, the proteasome, and specific SCF E3 ligases in vivo. Curr Biol **13,** R504-505.

Pepper, A.E., and Chory, J. (1997). Extragenic suppressors of the Arabidopsis *det1* mutant identify elements of flowering-time and light-Response regulatory pathways. Genetics **145,** 1125-1137.

Putterill, J., Robson, F., Lee, K., Simon, R., and Coupland, G. (1995). The CONSTANS gene of Arabidopsis promotes flowering and encodes a protein showing similarities to zinc finger transcription factors. Cell **80,** 847-857.

Quail, P.H. (1997). The phytochromes: a biochemical mechanism of signaling in sight? Bioessays **19,** 571-579.

Quail, P.H. (2002). Phytochrome photosensory signalling networks. Nature Reviews Molecular Cell Biology **3,** 85-93.

Ranjan, A. (2010). The role of COP1/SPA in light signaling:
Growth control, cell-cell communication and
functional conservation in plants. Inaugural Dissertation (Cologne: University of Cologne).

Rockwell, N.C., Su, Y.S., and Lagarias, J.C. (2006). Phytochrome Structure and Signaling Mechanisms. Annu Rev Plant Biol.

Rowan, D.D., Cao, M., Lin-Wang, K., Cooney, J.M., Jensen, D.J., Austin, P.T., Hunt, M.B., Norling, C., Hellens, R.P., Schaffer, R.J., and Allan, A.C. (2009). Environmental regulation of leaf colour in red 35S:PAP1 Arabidopsis thaliana. New Phytol **182,** 102-115.

Saijo, Y., Sullivan, J.A., Wang, H.Y., Yang, J.P., Shen, Y.P., Rubio, V., Ma, L.G., Hoecker, U., and Deng, X.W. (2003). The COP1-SPA1 interaction defines a critical step in phytochrome A-mediated regulation of HY5 activity. Genes & Development **17,** 2642-2647.

Saijo, Y., Zhu, D., Li, J., Rubio, V., Zhou, Z., Shen, Y., Hoecker, U., Wang, H., and Deng, X.W. (2008). Arabidopsis COP1/SPA1 complex and FHY1/FHY3 associate with distinct phosphorylated forms of phytochrome A in balancing light signaling. Mol Cell **31,** 607-613.

Sakamoto, K., and Nagatani, A. (1996). Nuclear localization activity of phytochrome B. Plant J **10,** 859-868.

Sakamoto, K., and Briggs, W.R. (2002). Cellular and subcellular localization of phototropin 1. Plant Cell **14,** 1723-1735.

Sambrook, J., Fritsch, E.F., and Maniatis, T. (1989). Molecular Cloning. A Laboratory Manual. (Cold Spring Harbor: Cold Spring Harbor Laboratory Press).

Sambrook, J., Russell, D. (2001). Molecular Cloning: A Laboratory Manual.

Schepens, I., Duek, P., and Fankhauser, C. (2004). Phytochrome-mediated light signalling in Arabidopsis. Current Opinion in Plant Biology **7,** 564-569.

Schmid, M., Davison, T.S., Henz, S.R., Pape, U.J., Demar, M., Vingron, M., Scholkopf, B., Weigel, D., and Lohmann, J.U. (2005). A gene expression map of Arabidopsis thaliana development. Nat Genet **37,** 501-506.

Schultz, T.F., Kiyosue, T., Yanovsky, M., Wada, M., and Kay, S.A. (2001). A role for LKP2 in the circadian clock of Arabidopsis. Plant Cell **13,** 2659-2670.

Schulze-Lefert, P., Dangl, J.L., Becker-Andre, M., Hahlbrock, K., and Schulz, W. (1989). Inducible in vivo DNA footprints define sequences necessary for UV light activation of the parsley chalcone synthase gene. EMBO Journal **8,** 651-656.

Seo, H.S., Watanabe, E., Tokutomi, S., Nagatani, A., and Chua, N.H. (2004). Photoreceptor ubiquitination by COP1 E3 ligase desensitizes phytochrome A signaling. Genes Dev **18,** 617-622.

Seo, H.S., Yang, J.Y., Ishikawa, M., Bolle, C., Ballesteros, M.L., and Chua, N.H. (2003). LAF1 ubiquitination by COP1 controls photomorphogenesis and is stimulated by SPA1. Nature **423,** 995-999.

Serino, G., and Deng, X.W. (2003). THE COP9 signalosome: Regulating plant development through the control of proteolysis. Annu Rev Plant Biol **54,** 165-182.

Sessa, G., Carabelli, M., Sassi, M., Ciolfi, A., Possenti, M., Mittempergher, F., Becker, J., Morelli, G., and Ruberti, I. (2005). A dynamic balance between gene activation and repression regulates the shade avoidance response in Arabidopsis. Genes Dev **19,** 2811-2815.

Shalitin, D., Yang, H.Y., Mockler, T.C., Maymon, M., Guo, H.W., Whitelam, G.C., and Lin, C.T. (2002). Regulation of Arabidopsis cryptochrome 2 by blue-light-dependent phosphorylation. Nature **417,** 763-767.

Sharrock, R.A., and Quail, P.H. (1989). Novel phytochrome sequences in *Arabidopsis thaliana*: Structure, evolution, and differential expression of a plant regulatory photoreceptor family. Genes Dev **3,** 1745-1757.

Shen, H., Zhu, L., Castillon, A., Majee, M., Downie, B., and Huq, E. (2008). Light-induced phosphorylation and degradation of the negative regulator PHYTOCHROME-INTERACTING FACTOR1 from Arabidopsis depend upon its direct physical interactions with photoactivated phytochromes. Plant Cell **20,** 1586-1602.

Shen, Y., Khanna, R., Carle, C.M., and Quail, P.H. (2007). Phytochrome induces rapid PIF5 phosphorylation and degradation in response to red-light activation. Plant Physiol **145,** 1043-1051.

Shen, Y., Feng, S., Ma, L., Lin, R., Qu, L.J., Chen, Z., Wang, H., and Deng, X.W. (2005). Arabidopsis FHY1 protein stability is regulated by light via phytochrome A and 26S proteasome. Plant Physiol **139,** 1234-1243.

Shi, M.Z., and Xie, D.Y. (2010). Features of anthocyanin biosynthesis in pap1-D and wild-type Arabidopsis thaliana plants grown in different light intensity and culture media conditions. Planta **231,** 1385-1400.

Shin, J., Park, E., and Choi, G. (2007). PIF3 regulates anthocyanin biosynthesis in an HY5-dependent manner with both factors directly binding anthocyanin biosynthetic gene promoters in Arabidopsis. Plant J **49,** 981-994.

Simillion, C., Vandepoele, K., Van Montagu, M.C., Zabeau, M., and Van de Peer, Y. (2002). The hidden duplication past of Arabidopsis thaliana. Proc Natl Acad Sci U S A **99,** 13627-13632.

Somers, D.E., Kim, W.Y., and Geng, R. (2004). The F-box protein ZEITLUPE confers dosage-dependent control on the circadian clock, photomorphogenesis, and flowering time. Plant Cell **16,** 769-782.

Stracke, R., Ishihara, H., Huep, G., Barsch, A., Mehrtens, F., Niehaus, K., and Weisshaar, B. (2007). Differential regulation of closely related R2R3-MYB transcription factors controls flavonol accumulation in different parts of the Arabidopsis thaliana seedling. Plant J **50,** 660-677.

Subramanian, C., Kim, B.H., Lyssenko, N.N., Xu, X.D., Johnson, C.H., and von Arnim, A.G. (2004). The Arabidopsis repressor of light signaling, COP1, is regulated by nuclear exclusion: Mutational analysis by bioluminescence resonance energy transfer. Proceedings of the National Academy of Sciences of the United States of America **101,** 6798-6802.

Suzuki, G., Yanagawa, Y., Kwok, S.F., Matsui, M., and Deng, X.W. (2002). Arabidopsis COP10 is a ubiquitin-conjugating enzyme variant that acts together with COP1 and the COP9 signalosome in repressing photomorphogenesis. Genes Dev **16,** 554-559.

Takemiya, A., Inoue, S., Doi, M., Kinoshita, T., and Shimazaki, K. (2005). Phototropins promote plant growth in response to blue light in low light environments. Plant Cell **17,** 1120-1127.

Tanaka, Y., and Ohmiya, A. (2008). Seeing is believing: engineering anthocyanin and carotenoid biosynthetic pathways. Curr Opin Biotechnol **19,** 190-197.

Teng, S., Keurentjes, J., Bentsink, L., Koornneef, M., and Smeekens, S. (2005). Sucrose-specific induction of anthocyanin biosynthesis in Arabidopsis requires the MYB75/PAP1 gene. Plant Physiol **139,** 1840-1852.

Tepperman, J.M., Zhu, T., Chang, H.S., Wang, X., and Quail, P.H. (2001). Multiple transcription-factor genes are early targets of phytochrome A signaling. Proc Natl Acad Sci U S A **98,** 9437-9442.

Tohge, T., Matsui, K., Ohme-Takagi, M., Yamazaki, M., and Saito, K. (2005a). Enhanced radical scavenging activity of genetically modified Arabidopsis seeds. Biotechnol Lett **27,** 297-303.

Tohge, T., Nishiyama, Y., Hirai, M.Y., Yano, M., Nakajima, J., Awazuhara, M., Inoue, E., Takahashi, H., Goodenowe, D.B., Kitayama, M., Noji, M., Yamazaki, M., and Saito, K. (2005b). Functional genomics by integrated analysis of metabolome and transcriptome of Arabidopsis plants over-expressing an MYB transcription factor. Plant J **42,** 218-235.

Towbin, H., Staehelin, T., and Gordon, J. (1979). Electrophoretic transfer of proteins from polyacrylamide gels to nitrocellulose sheets: procedure and some applications. Proc Natl Acad Sci USA **76,** 4350-4354.

Ulm, R., Baumann, A., Oravecz, A., Mate, Z., Adam, E., Oakeley, E.J., Schafer, E., and Nagy, F. (2004). Genome-wide analysis of gene expression reveals function of the bZIP transcription factor HY5 in the UV-B response of Arabidopsis. Proc Natl Acad Sci U S A **101,** 1397-1402.

Von Arnim, A., and Deng, X.W. (1996). Light Control of Seedling Development. Annu Rev Plant Physiol Plant Mol Biol **47,** 215-243.

von Arnim, A.G. (2003). On again-off again: COP9 signalosome turns the key on protein degradation. Current Opinion in Plant Biology **6,** 520-529.

von Arnim, A.G., and Deng, X.W. (1994). Light inactivation of Arabidopsis photomorphogenic repressor COP1 involves a cell-specific regulation of its nucleocytoplasmic partitioning. Cell **79,** 1035-1045.

von Arnim, A.G., Osterlund, M.T., Kwok, S.F., and Deng, X.W. (1997). Genetic and developmental control of nuclear accumulation of COP1, a repressor of photomorphogenesis in Arabidopsis. Plant Physiol **114,** 779-788.

Wade, H.K., Bibikova, T.N., Valentine, W.J., and Jenkins, G.I. (2001). Interactions within a network of phytochrome, cryptochrome and UV-B phototransduction

pathways regulate chalcone synthase gene expression in Arabidopsis leaf tissue. Plant J **25,** 675-685.

Walter, M., Chaban, C., Schutze, K., Batistic, O., Weckermann, K., Nake, C., Blazevic, D., Grefen, C., Schumacher, K., Oecking, C., Harter, K., and Kudla, J. (2004). Visualization of protein interactions in living plant cells using bimolecular fluorescence complementation. Plant J **40,** 428-438.

Wang, H., Kang, D., Deng, X.W., and Wei, N. (1999). Evidence for functional conservation of a mammalian homologue of the light-responsive plant protein COP1. Curr Biol **9,** 711-714.

Wang, H., Ma, L.G., Li, J.M., Zhao, H.Y., and Deng, X.W. (2001). Direct interaction of Arabidopsis cryptochromes with COP1 in light control development. Science **294,** 154-158.

Weigel, D., Ahn, J.H., Blazquez, M.A., Borevitz, J.O., Christensen, S.K., Fankhauser, C., Ferrandiz, C., Kardailsky, I., Malancharuvil, E.J., Neff, M.M., Nguyen, J.T., Sato, S., Wang, Z.Y., Xia, Y., Dixon, R.A., Harrison, M.J., Lamb, C.J., Yanofsky, M.F., and Chory, J. (2000). Activation tagging in Arabidopsis. Plant Physiol **122,** 1003-1013.

Wertz, I.E., O'Rourke, K.M., Zhang, Z., Dornan, D., Arnott, D., Deshaies, R.J., and Dixit, V.M. (2004). Human De-etiolated-1 regulates c-Jun by assembling a CUL4A ubiquitin ligase. Science **303,** 1371-1374.

Whitelam, G.C., Johnson, E., Peng, J., Carol, P., Anderson, M.L., Cowl, J.S., and Harberd, N.P. (1993). Phytochrome A null mutants of arabidopsis display a wild-type phenotype in white light. Plant Cell **5,** 757-768.

Winkel-Shirley, B. (2001a). Flavonoid biosynthesis. A colorful model for genetics, biochemistry, cell biology, and biotechnology. Plant Physiol **126,** 485-493.

Winkel-Shirley, B. (2001b). It takes a garden. How work on diverse plant species has contributed to an understanding of flavonoid metabolism. Plant Physiol **127,** 1399-1404.

Wu, G., and Spalding, E.P. (2007). Separate functions for nuclear and cytoplasmic cryptochrome 1 during photomorphogenesis of Arabidopsis seedlings. Proc Natl Acad Sci U S A **104,** 18813-18818.

Xia, Y., Nikolau, B.J., and Schnable, P.S. (1997). Developmental and hormonal regulation of the arabidopsis CER2 gene that codes for a nuclear-localized protein required for the normal accumulation of cuticular waxes. Plant Physiol **115,** 925-937.

Yamaguchi, A., Kobayashi, Y., Goto, K., Abe, M., and Araki, T. (2005). TWIN SISTER OF FT (TSF) acts as a floral pathway integrator redundantly with FT. Plant Cell Physiol **46,** 1175-1189.

Yanagawa, Y., Sullivan, J.A., Komatsu, S., Gusmaroli, G., Suzuki, G., Yin, J., Ishibashi, T., Saijo, Y., Rubio, V., Kimura, S., Wang, J., and Deng, X.W. (2004). Arabidopsis COP10 forms a complex with DDB1 and DET1 in vivo and enhances the activity of ubiquitin conjugating enzymes. Genes Dev **18,** 2172-2181.

Yang, H.Q., Tang, R.H., and Cashmore, A.R. (2001). The signaling mechanism of Arabidopsis CRY1 involves direct interaction with COP1. Plant Cell **13,** 2573-2587.

Yang, J., and Wang, H. (2006). The central coiled-coil domain and carboxyl-terminal WD-repeat domain of Arabidopsis SPA1 are responsible for mediating repression of light signaling. Plant J **47,** 564-576.

Yang, J., Lin, R., Hoecker, U., Liu, B., Xu, L., and Wang, H. (2005). Repression of light signaling by Arabidopsis SPA1 involves post-translational regulation of HFR1 protein accumulation. Plant J **43,** 131-141.

Yi, C., and Deng, X.W. (2005). COP1 - from plant photomorphogenesis to mammalian tumorigenesis. Trends Cell Biol **15,** 618-625.

Yu, J.W., Rubio, V., Lee, N.Y., Bai, S., Lee, S.Y., Kim, S.S., Liu, L., Zhang, Y., Irigoyen, M.L., Sullivan, J.A., Lee, I., Xie, Q., Paek, N.C., and Deng, X.W. (2008). COP1 and ELF3 control circadian function and photoperiodic flowering by regulating GI stability. Mol Cell **32,** 617-630.

Yu, X., Klejnot, J., Zhao, X., Shalitin, D., Maymon, M., Yang, H., Lee, J., Liu, X., Lopez, J., and Lin, C. (2007). Arabidopsis cryptochrome 2 completes its posttranslational life cycle in the nucleus. Plant Cell **19,** 3146-3156.

Zhang, F., Gonzalez, A., Zhao, M., Payne, C.T., and Lloyd, A. (2003). A network of redundant bHLH proteins functions in all TTG1-dependent pathways of Arabidopsis. Development **130,** 4859-4869.

Zhu, D., Maier, A., Lee, J.H., Laubinger, S., Saijo, Y., Wang, H., Qu, L.J., Hoecker, U., and Deng, X.W. (2008). Biochemical characterization of Arabidopsis complexes containing CONSTITUTIVELY PHOTOMORPHOGENIC1 and SUPPRESSOR OF PHYA proteins in light control of plant development. Plant Cell **20,** 2307-2323.

Zhu, H.F., Fitzsimmons, K., Khandelwal, A., and Kranz, R.G. (2009). CPC, a single-repeat R3 MYB, is a negative regulator of anthocyanin biosynthesis in Arabidopsis. Mol Plant **2,** 790-802.

Zimmermann, I.M., Heim, M.A., Weisshaar, B., and Uhrig, J.F. (2004a). Comprehensive identification of Arabidopsis thaliana MYB transcription factors interacting with R/B-like BHLH proteins. Plant J **40,** 22-34.

Zimmermann, P., Hirsch-Hoffmann, M., Hennig, L., and Gruissem, W. (2004b). GENEVESTIGATOR. Arabidopsis microarray database and analysis toolbox. Plant Physiol **136,** 2621-2632.

Zuluaga DL, G.S., Loreti E, Pucciariello C, Degl'Innocenti E. (2008). Arabidopsis thaliana MYB75/PAP1 transcription factor induces anthocyanin production in transgenic tomato plants. Functional Plant Biology **35,** 606-618.

VII Danksagung

Ich möchte mich herzlich bei all jenen Personen bedanken, die mich auf unterschiedliche Weise unterstützt und somit zu dieser Dissertation beigetragen haben.
An erster Stelle richtet sich mein Dank an Frau Prof. Dr. Ute Höcker, die mir für die Dauer der Erstellung dieser Dissertation stets mit Ratschlägen, Kritik und viel Geduld zur Seite stand. Herrn Prof. Dr. Hülskamp danke ich für die Übernahme des Zweitgutachtens. Ich danke Herrn Prof. Dr. Werr für die Übernahme des Prüfungsvorsitzes.

Des Weiteren möchte ich den Gärtnern des Gewächshauses, sowie dem technischen Personal des Biozentrums, bzw. des alten Botanischen Instituts danken, die ich aufgrund ihrer Anzahl nicht alle namentlich erwähnen kann. Auch möchte ich den Mitarbeitern der AG Bucher, AG Flügge und AG Hülskamp danken mit denen ich viel Zeit in Seminaren und auf sonstigen Festivitäten verbringen durfte. Hier möchte ich besonders Andrea Schrader, Simona Digiuni und Alban Jacques danken.

Da ich bereits meine Diplomarbeit in der AG Höcker verfasst habe möchte ich auch „alten“ Kollegen des Institutes in Düsseldorf danken, die mir stets ihr offenes Ohr liehen. Namentlich zu erwähnen sind hier Udo Gowik und Sascha Laubinger.

Ich danke allen Mitarbeiter der AG Höcker, besonders Kirsten Fittinghoff und Petra Fackendahl, mit denen ich während der ersten Zeit viel Lustiges zusammen erlebt habe. Aashish Ranjan möchte ich danken für seine starke Besonnenheit und Trinkfestigkeit. Gabi Fiene und Sebastian Rolauffs möchte ich danken für ihre kölsche Attitüde und seine unglaubliche Menschlichkeit. Ich danke allen Hiwis, die ich jemals mit meiner Arbeit quälen durfte. Im Besonderen Martin Balcerowicz, der mir auch bei der Korrektur dieser Arbeit geholfen hat.

Ein großer Dank geht an meine Familie: meine Eltern Gabriele Polenthon-Maier und Alexius Maier sowie meinen Bruder Maximilian Maier, die mich stets unterstützt haben.

Der größte Dank jedoch geht an meine Lebenspartnerin Dagmar Lyska, die mir während all dieser Jahre, besonders in schwierigen Zeiten, zur Seite stand.

VIII Erklärung

Ich versichere, dass ich die von mir vorgelegte Dissertation selbständig angefertigt, die benutzten Quellen und Hilfsmittel vollständig angegeben und die Stellen der Arbeit –einschließlich Tabellen, Karten und Abbildungen -, die anderen Werken im Wortlaut oder dem Sinn nach entnommen sind, in jedem Einzelfall als Entlehnung kenntlich gemacht habe; dass diese Dissertation noch keiner anderen Fakultät oder Universität zur Prüfung vorgelegen hat; dass sie – abgesehen von unten angegebenen Teilpublikationen – noch nicht veröffentlicht worden ist sowie, daß ich eine solche Veröffentlichung vor Abschluß des Promotionsverfahrens nicht vornehmen werde. Die von mir vorgelegte Dissertation ist von Prof. Dr. Ute Höcker betreut worden.

Alexander Maier

Veröffentlichungen:

Zhu, D., Maier, A., Lee, J.H., Laubinger, S., Saijo, Y., Wang, H., Qu, L.J., Hoecker, U., and Deng, X.W. (2008). Biochemical characterization of Arabidopsis complexes containing CONSTITUTIVELY PHOTOMORPHOGENIC1 and SUPPRESSOR OF PHYA proteins in light control of plant development. Plant Cell **20**, 2307-2323.

Balcerowicz, M., Fittinghoff, K., Wirthmueller, L., Maier, A., Fackendahl, P., Fiene, G., Koncz, C., and Hoecker, U. (2011). Light exposure of Arabidopsis seedlings causes rapid de-stabilization as well as selective post-translational inactivation of the repressor of photomorphogenesis SPA2. Plant J **65,** 712-723.

Lebenslauf

Alexander Maier

Botanisches Institut, Zülpicher Str.47B
D50674, Köln
Geburtdatum: 13.05.1981
Geburtsort: Krefeld-Hüls
Staatsangehoerigkeit: Deutsch

Schulbildung

-von August 1987 bis 1991 Gemeinschaftsgrundschule St. Hubert.
-von August 1990 bis Juni 2000 Bischöfliche- Maria-Montessori-Gesamtschule. Abschluss: Allgemeine Hochschulreife.

Hochschulbildung

-von Oktober 2001 bis Oktober 2006 Diplomstudiengang Biologie an der Heinrich-Heine-Universität Düsseldorf. Titel der Arbeit: „Biochemische und molekulare Analyse von SPA1-Interaktionspartnern".Betreuerin: Prof Dr. Ute Höcker
-von November 2006 bis Mai 2011 Promotionsstudium Biologie an der Universität zu Köln. Titel der Arbeit: "Genetic and Biochemical Characterization of COP1/SPA Function in *Arabidopsis* Photomorphogenesis" Betreuerin: Prof. Dr. Ute Höcker

Teilnahme an wissenschaftlichen Konferenzen

06/2009 — 15th International Congress of Photobiology, Duesseldorf, Deutschland.
Vortrag und Poster Präsentation: Genetic and biochemical analysis of SPA/COP1 function in *Arabidopsis thaliana* light signaling.

02/2009 — 21st Conference of Molecular Biology of Plants, Dabringhausen, Germany.
Poster Präsentation: Biochemical characterisation of COP1-SPA complexes.

08/2007 — EPS Summer school, Utrecht, The Netherlands.
Poster Präsentation: The four SPA genes have overlapping but also disctinct functions in regulating plant development.

Publikationen

Zhu, D., Maier, A., Lee, J.H., Laubinger, S., Saijo, Y., Wang, H., Qu, L.J., Hoecker, U., and Deng, X.W. (2008). Biochemical characterization of Arabidopsis complexes containing CONSTITUTIVELY PHOTOMORPHOGENIC1 and SUPPRESSOR OF PHYA proteins in light control of plant development. Plant Cell **20**, 2307-2323.

Balcerowicz, M., Fittinghoff, K., Wirthmueller, L., Maier, A., Fackendahl, P., Fiene, G., Koncz, C., and Hoecker, U. (2011). Light exposure of Arabidopsis seedlings causes rapid de-stabilization as well as selective post-translational inactivation of the repressor of photomorphogenesis SPA2. Plant J **65,** 712-723.